The Evolution of Magmatic-Hydrothermal Fluids as Recorded by Stable Cl Isotopes and Cl/Br Elemental Ratios in Geothermal Systems, Porphyry Copper and Iron-Oxide-Copper-Gold Deposits

by

Nelson Ferney Bernal

A thesis submitted in partial fulfillment of the requirements for the degree of

Doctor of Philosophy

Department of Earth and Atmospheric Sciences

University of Alberta

Abstract

This research was conducted with the purpose of identifying the processes that affect the halogen distribution and the Cl isotope composition of hydrothermal fluids under different pressure and temperature conditions in the crust. In order to attain this goal, three different geological settings were investigated; active geothermal systems in the Taupo Volcanic Zone (TVZ), North Island, New Zealand, the Porphyry Copper Gold Deposit (PCD) at Butte, Montana, USA, and selected Iron Oxide Copper Gold Deposits (IOCG) in Norrbotten, Sweden. This research also focussed on identifying analytical issues related to sample preparation procedures and stable Cl isotope analysis.

Deep geothermal fluids representing 14 active geothermal systems in the TVZ, North Island New Zealand, were analyzed in this study to identify changes in the halogen (Cl and Br) and isotope compositions ($\delta^{37}Cl$, $\delta^{7}Li$, $\delta^{18}O$ and δD) of hydrothermal fluids associated with rhyolitic and andesitic magmas. Low $\delta^{7}Li$ values were measured in geothermal water samples indicating that most water-rock interactions occur with rhyolitic host rocks. Two different halogen compositions were identified in the geothermal waters, one related to andesitic magmas in the east and the other associated with predominantly rhyolitic magmatism in the west.

Comparisons of the Cl and Br concentrations of geothermal waters from the andesitic geothermal systems and MORB samples from Macquarie Island, located some 1,200 km south of New Zealand, indicate a common origin for these two sets of samples; a high-alumina basalt, which evolved to andesitic and rhyolitic compositions. The

geothermal samples related to rhyolitic magmatism have Cl and Br compositions comparable to acidic volcanic rocks reported in previous studies.

This study contributes the first data on the effect of magmatic segregation on the δ^{37}Cl composition of geothermal fluids, forming different, and characteristic, isotopic signatures for rhyolitic and andesitic sources. This work concludes that Cl/Br molar ratios and stable Cl isotopes have the potential to identify andesitic and rhyolitic magmatic sources of halogens in geothermal systems.

The Butte Porphyry Copper Deposit (PCD) is arguable the deepest PCD in the world, formed at depths around 9 km and maximum temperatures of 600 °C. Data obtained from Cl/Br molar ratios measured in fluid inclusion leachates in the deep pre-Main Stage veins have high Cl/Br molar ratios, which could be derived from the interaction between felsic and mafic magmas. At shallower levels in the deposit the precipitation of Cl-bearing minerals results in distinctive Cl/Br molar ratios, lower than those measured in the deepest veins. The stable Cl isotopes appear affected by kinetic fractionation, the result of phase separation, brine condensation, vapor formation and remixing, occurring locally in cracks and fractures. However, similar δ^{37}Cl values and comparable chemical compositions of the deep pre-Main Stage and the shallower and economically important Main Stage (MS) mineralisations, indicate a common magmatic-hydrothermal source that persisted during the formation of the Butte PCD.

The IOCG-type deposits of the Norrbotten County, Sweden, were formed during the Paleoproterozoic by Ca-rich salinity brines at temperature above 500 °C and depths of 8 to10 km. Scapolites were formed during an earlier regional metasomatic event (RM), and during a later IOCG mineralization. These scapolites were found to be of marialitic

composition and most of them had Cl/Br molar ratios that reflect mixed sources related to halite dissolution, seawater and/or magmatic contributions. However, some scapolites from the Pahtohavare and Sarkivaara deposits had Cl/Br molar ratios that were lower than seawater, which suggests the chlorinity in these samples may have been derived from evaporative brines.

Measured δ^{37}Cl values in fluid inclusions (Gleeson and Smith, 2009) and spatially related scapolite in one of the samples allowed the calculation of an empiric isotope fractionation of +1.9‰ between the mineral and the fluid. This value contradicts predictions for isotope fractionation between a silicate mineral such as scapolite and a monovalent hydrothermal fluid with high NaCl activities. This research shows that the Cl/Br molar ratios and δ^{37}Cl values are decoupled, possibly owing to the presence of recycled Br in IOCG scapolites and different fluid-rock interaction histories.

Preface

This thesis is comprised of three research papers corresponding to chapters 3, 4 and 5. Chapter 3 has been published as Bernal, N. F., Gleeson, S. A., Dean S. A., Liu X. M., Hoskin P. "The sources of halogens in geothermal fluids from the taupo Volcanic Zone, North Island, New Zealand". Geochimica et Cosmochimica Acta. 126, 265-283. I was responsible for the sample preparation, analysis, data interpretation and manuscript composition. S.A. Gleeson was the supervisory author and was involved with the concept, formation and editing of the manuscript. A. S. Dean collected the samples in the field. X. M. Liu and A. S. Dean conducted the δ^7Li analysis. P. Hoskin supplied the samples and mediated access to the sampling sites.

Chapters 4 is to be submitted as Bernal, N. F., Gleeson, S. A., Rusk, B., The origin and the effects of phase separation on the halogen compositions of magmatic-hydrothermal fluids from the Butte Porphyry-Copper Deposit: constraints from Cl/Br molar ratios and the δ^{37}Cl values of fluid inclusion leachates. I was responsible for sample preparation, analysis, data interpretation and manuscript composition. S.A. Gleeson was the supervisory author and was involved with the concept, formation and editing of the manuscript. B. Rusk provided the samples I analyzed for this research. B. Rusk also contributed to the editing of the manuscript.

Chapter 5 is still to be submitted as Bernal, N. F., Gleeson, S. A., Smith, M. P., Barnes, J. D. and Pan, Y., The stable chlorine isotope composition of scapolites from iron oxide-copper-gold (IOCG) deposits and regional Na-Cl metasomatic alteration, Norrbotten County, Sweden. I was responsible for the construction of a pyrohydrolysis apparatus, the preparation and analysis of the samples, data interpretation and manuscript composition. S.A. Gleeson was the supervisory author and was involved with the concept, formation and editing of the manuscript. M. P. Smith provided EPMA analysis of scapolites and contributed with the editing of the manuscript. J. D. Barnes, conducted the stable chlorine isotope analysis of the pyrohydrolysis solutions. Y. Pan contributed with micro-XRF analysis in scapolite samples.

Acknowledgements

This study was funded with a NSERC Discovery grant to S. A. Gleeson. The Li isotope work was supported by an NSF grant to R.L. Rudnick and W.F. McDonough (EAR 0948549). Thanks to Leonard Wassenaar and Geoff Koehler for their assistance with the analysis of the Cl isotopes. Andres Arcila Rivera is gratefully acknowledged for establishing the connections with the School of the Environment at the University of Auckland. Thanks to my supervisor, Sarah Gleeson, for giving me the opportunity to freely work my ideas, holding my feet to the ground at the same time, a very challenging task at times. But in particular, I want to recognize Sarah's patient and encouragement troughout the most difficult episodes of this journey. Thanks to Tom Chacko for his feedback and comments, which made this work more consistent. I thank the Department of Earth and Atmospheric Sciences at the University of Alberta, for their laboratory support and finantial assistance.

On a personal note, I would like to thank my parents Horacio Bernal and Maria Helena Cortes for their love and support and also for their example of hard work and persistence. Thanks to my sister Diana and my brother Mauricio for their motivation and permanent encouragement despite the distance. To my dear friends Francisco Castrillon, Marilise Turnbull, Mariana and Isabella, thanks for your company, motivation and sincere friedship. Thanks to Dirk, Blanca, Natalia, Kira and Amelie Seidel for being our family in Edmonton. Also, I would like to thank Gideon Lambiv, Osbaldo Zamora, Andreas Enggis, Ali Imer, Mary Borrero, Guadalupe Maldonado, Rares Bistran and my dear friend Pedro Acosta for the good times we enjoyed together, you guys made life more enjoyable.

Finally, I would like to dedicate this work to my wife Gloria Patricia Cepeda and to my daughter Allison Bernal-Cepeda. Thanks Pekas for following me without hesitation sacrificing your family, personal goals and career. But above all, thanks for your love and patient, I can not ask for a better life partner. To my little Allison, thanks Chiquilinis for your understanding and for being my endless source of joy and inspiration.

Table of Contents

List of Tables

List of Figures

List of Symbols and Abbreviations

‰	Parts per thousand or per mille
Br	Bromine or bromide
°C	Celsius degrees
Cl	Chlorine or chloride
CO_3	Carbonate
$\delta^{37}Cl$	Stable chlorine isotopes relative to Ocean Scientific International, Atlantic Seawater.
δD	Hydrogen isotopes relative to V-SMOW
$\delta^{7}Li$	Lithium isotopes relative to L-SVEC lithium carbonate
$\delta^{18}O$	Oxygen isotopes relative to V-SMOW
e.g.	For example
EPMA	Electron microprobe
Ga	Giga annum, Billions of years
i.e.	That is
IOCG	Iron-oxide-copper-gold deposits
IOCG-M	Iron oxide-copper-gold deposits altered metabasic rocks
IOCG-PS	Iron oxide-copper-gold deposits proximal alteration/Na-

	skarns
IRMS	Isotope ratio mass spectrometry
kbar	Kilobar
K_D	Distribution coefficient
km	Kilometers
LA-ICPMS	Laser ablation inductively coupled plasma mass spectrometry
Ma	Mega Annum, Millions of years
MC-ICP-MS	Nu Plasma Multi Collector-inductively coupled Plasma-Mass Spectrometry
Micro-XRF	Micro-X-ray fluorescence
Na	Sodium
psi	Pressure per square inch
ppm	Parts per million
RM	Regional Na-Cl metasomatic assemblages
SO_4	Sulfate
TVZ	Taupo Volcanic Zone
Wt.%	Weight percent

1 Introduction

1.1 Crust and Mantle reservoirs

Halogen elemental ratios, especially Cl/Br, have been successfully used to identify the source(s) of salinity in some near surface fluids, and rarely, fluids associated with igneous and metamorphic systems. However, most of these studies have focused on the origin of formation waters and on low temperature hydrothermal systems and as a result, on a global scale, the Cl cycle is not well understood (Jambon et al. 1995, Magenheim et al. 1995, Sharp et al. 2004, Barnes and Sharp 2005, Barnes et al. 2008, Bonifacie et al. 2007a, Bonifacie et al. 2008a, Bonifacie et al. 2008b, Layne et al. 2009). Chlorine has two stable isotopes (^{37}Cl and ^{35}Cl) and thus, it has been suggested that the Cl isotopic composition of fluids and minerals may help to identify the main Cl reservoirs and may contribute significantly to understanding the current and ancient global cycle of Cl (Bonifacie et al. 2007a).

The crustal Cl reservoir is dominated by the huge amount of Cl in the oceans and evaporitic deposits (Sharp and Barnes, 2004). In general, evaporitic deposits have δ^{37}Cl values in the range 0.0 ± 0.5‰ (Eastoe et al. 2007). The stable Cl isotopic compositions of brines and formation waters are more variable but in most cases are similar to evaporitic systems (e.g. Eggenkamp 1994, Kaufmann et al. 1998; Eastoe et al. 2001; Stotler et al. 2010).

The distribution of Cl in the Earth and the identification of its different isotopic reservoirs is still a matter of discussion. Sharp et al. (2007) analyzed chondrites and mantle samples as represented by mid-ocean ridge basalts (MORB) and halite nodules in kimberlite and found that these samples had a total range of δ^{37}Cl values from -2.09 to 0.30‰. The δ^{37}Cl value of the crustal material they analyzed was around 0‰ and they concluded the mantle, crust and chondrites have a similar stable Cl isotopic composition, and therefore, there was no isotopic fractionation of Cl during the differentiation of the planet.

Several recent studies have examined the Cl isotope composition of the oceanic crust (MORB) and subduction zones (serpentinites) in order to constrain the Cl cycle (Magenheim et al. 1995, Sharp et al. 2004, Barnes et al. 2005, Barnes et al. 2008, Bonifacie et al. 2007a, Bonifacie et al. 2008a, Bonifacie et al. 2008b, Layne et al. 2009; John et al. 2010; John et al. 2011). A study on 22 MORB samples suggested that δ^{37}Cl values in the mantle are ≤ -1.6‰ (Bonifacie et al 2008b). Using Secondary Ion Mass spectrometry (SIMS), Layne et al. (2009) analyzed glasses and melt inclusions from back-arc basin basalts, and confirmed the δ^{37}Cl values found by Bonifacie et al. (2008b) and identified even lower δ^{37}Cl values (≤-3.0‰) in very low Cl MORBs. Sharp et al., (2013), published a set of analysis on mantle-derived material and reasserted that the upper mantle must have a δ^{37}Cl value of -0.2±0.3‰. Based on their conclusion that there is no significant Cl isotope fractionation between the crust and the mantle, this study attributed the previously reported negative δ^{37}Cl values to analytical errors.

1.2 Magmatic – hydrothermal fluids

Despite the relatively narrow range of data cited by Sharp et al. (2007), the Cl isotope composition of crustal minerals and fluids range from -8 to +12‰ (summarized by Gleeson and Smith, 2009; Barnes et al., 2009), suggesting that there are processes occurring in the crust that may fractionate the Cl isotopes. Previous workers have suggested that hydrothermal systems may be responsible for significant mass transfer of Cl in the crust and that Br/Cl ratios may also be used as tracers to track a mantle source for volatiles in crustal systems (e.g. Bölhke and Irwin 1992, Kesler et al. 1995, Yardley et al. 2000; Nahnybida et al. 2009). Chlorine in particular has the potential to be an effective tracer in magmatic-hydrothermal systems. Chlorine is an incompatible element mobilized as consequence of degassing, partial melting, water-rock interaction and metasomatism (Bonifacie et al. 2007b). During magmatic fractionation, Cl is preferentially concentrated into the liquid phase and it is retained by a few minerals e.g. biotite, amphibole, scapolite, sodalite and nepheline (Webster et al. 2009). Therefore, due to its incompatibility, solubility and volatility, Cl can potentially elucidate physicochemical processes like phase separation and mixing during the ascent of hydrothermal fluids to the surface. At present, there is no comprehensive study aimed to understanding the isotopic fractionation of Cl in the magmatic-hydrothermal environment. In other environments, Cl can be fractionated during ion filtration, diffusion and advective mixing (Kaufmann et al. 1987, 1988 in Eastoe et al. 1989), but little is known about the effects of magmatic segregation, phase separation and mineral precipitation on the stable Cl isotopic composition of hydrothermal fluids.

1.3 Techniques for the measurement of Cl isotopes in minerals

One of the major issues with constraining the Cl isotopic composition of the crust and mantle has been the difficulty of accurately measuring the Cl isotopic composition of minerals. Many of the initial studies (Xiao and Zhang, 1992, Ransom et al. 1995, Numata et al. 2001 and Wei et al. 2007) analyzed samples using Thermal Ionization Mass spectrometry (TIMS). The δ^{37}Cl values acquired by TIMS in these earlier studies are more positive compared to data obtained with other techniques, due to potential isotope fractionation and contamination during the analysis (e.g. Bonifacie et al. 2007b; Sharp et al. 2007). These authors, therefore, have suggested that the early TIMS data are inaccurate and that this has resulted in a misinterpretation of the Cl cycle. Currently, it is accepted that the extraction of Cl from a mineral sample by pyrohydrolysis, followed by analyses by an isotope ratio mass spectrometer (IRMS) is the most accurate way to measure Cl isotopic data in minerals. There have been a few studies that suggest that it may be possible to measure Cl isotopes with SIMS (Layne et al. 2009, Sharp et al. 2007) but the full potential of this technique has not yet been realized. These two techniques therefore, can potentially produce data to further constrain the cycle of Cl and to allow the experimental determination of fractionation factors between fluids and minerals.

This research is focused on understanding the behaviour of stable Cl isotopes in hydrothermal fluids present in active geothermal systems in New Zealand, fluid inclusions from the Butte PCD, Montana, USA, and scapolites associated with IOCG mineralization in Norrbotten County in Sweden. Each of these geologic environments occurs in a particular temperature and pressure regime with the potential to fractionate the stable Cl isotopes as the hydrothermal systems evolve, providing a characteristic isotopic and halogen signature. The geothermal waters of the Taupo Volcanic Zone (TVZ) are heated in geothermal reservoirs 2 to 3 km deep in the crust at temperatures from 200 to 300 °C (Wilson and Rowland, 2011). The Butte PCD is thought to be formed at a depth of 9 km at temperatures from 600 to 350 °C (Rusk et al. 2008), the IOCG deposits in Norrbotten Sweden were formed at a range of depths between 10 and 8 km and temperatures from 500 to 350 °C (Lindblom et al., 1996; Gleeson and Martin, 2009). Based on the current knowledge of the isotopic composition of crust and mantle reservoirs, the origin of the salinity in these geological environments is also investigated.

Chapter 3, elaborates on the chemical and isotopic differences of 14 geothermal systems located in the Taupo Volcanic Zone (TVZ), North Island, New Zealand. Rifting and thinning of the TVZ, produced by the Kermadec subduction system, offers a great opportunity to study the interaction between the upper mantle and the crust. This interaction is reflected by the intense volcanic activity responsible for the occurrence of high enthalpy geothermal systems, associated with andesitic and rhyolitic magmas intruding the crust. The sources of halogens (Cl and Br) were evaluated in this study on the basis of the chemistry of geothermal waters and their stable isotope compositions (δ^{18}O, δ^{2}H, δ^{37}Cl and δ^{7}Li). Several fundamental questions were addressed in this study, including: what is the main source of salinity in the geothermal waters, water-rock interaction or magmatic fluids? Also we wanted to know if Cl stable isotopes and halogens in these geothermal waters were different enough to help in the identification of the two main magmatic sources in the TVZ (andesitic and rhyolitic). Considering the particular geology of the TVZ with a thin continental crust, we also wanted to know if the geothermal fluids preserve the isotopic signature of the mantle, and if possible, get an idea of the extent of the isotopic fractionation Cl experience during its transition from the upper mantle to the crust. Using δ^{18}O, δ^{2}H and δ^{7}Li values it was possible to identify the importance of the contribution of magmatic hydrothermal fluids to the salinity of the geothermal waters (relative to water-rock interaction processes). The origin of the salinity was constrained by using halogen compositions in combination with δ^{37}Cl values of the geothermal waters.

Chapter 4 presents the halogen (Cl and Br) and δ^{37}Cl composition of Pre-main stage and MS mineralization at the Butte Cu-Mo deposit, Montana. This deposit is arguably the deepest Porphyry Copper Deposit (PCD) in the world (Roberts 1975 and Rusk et al., 2008), allowing access to geochemical and isotopic data preserved in fluid inclusions contained in alteration veins. The halogens were extracted using the crush and leach technique (Gleeson, 2003) followed by IC analysis. Previous studies have concluded that a single magmatic- hydrothermal fluid evolved to generate the alteration assemblages characteristic of the Butte deposit (Rusk et al., 2008, Reed et al., 2013). Therefore, the main question we wanted to answer was if phase separation and mixing had a measurable effect on the Cl stable isotope composition and Cl/Br molar ratios as this original fluid evolved into Pre-main stage and MS mineralization. In addition, based on the characteristics of the hydrothermal fluid, indicating a magmatic origin, we wanted to know if the δ^{37}Cl values and Cl/Br molar ratios of the original hydrothermal fluid were reflected by the fluid inclusion leachates. Fluid inclusions in veins at different structural levels were analyzed by the crush and leach technique, in order to obtain a solution containing the chemical composition of the mineralizing fluid. Chloride and bromide concentrations were analyzed by IC and δ^{37}Cl values by CF-IRMS.

Chapter 5 is the study of Cl-bearing scapolites associated with the IOCG mineralization of Norrbotten County, Sweden, and the halogen and δ^{37}Cl compositions of scapolites from three alteration types. Magmatic intrusions, volcanism and regional metamorphism formed these IOCG deposits dated between 1.9 to 1.8 Ga. The main purpose of this study was to identify the isotopic enrichment or depletion of the Cl stable isotopes in the scapolites with respect to the hydrothermal fluid and compare it with published theoretical values for Cl-bearing silicates (Schauble et al., 2003). In the literature of IOCG deposits, the origin of salinity and metals has been associated with several sources, we aimed to identify these sources using Cl stable isotopes and Cl/Br molar ratios. In order to extract the Cl from the scapolite specimens, a pyrohydrolysis apparatus was constructed as part of this research, its construction itself offered several challenges. The Cl extraction had to be above 80% efficiency and isotopic fractionation in the reaction tube was to be avoided as the carrier steam cooled down from 1200 °C to 20 °C. In addition, the pyrohydrolysis solution containing the Cl extracted, had to be suitable for direct IC analysis to prevent contamination. The δ^{37}Cl values measured in the scapolites were predominantly positive or very close to zero. We compared our results with fluid inclusion data available from previous work (Gleeson and Smith, 2009). We analysed one scapolite sample, for which isotopic composition of the hydrothermal fluid was reported by Gleeson and Smith (2009), to determine the isotopic fractionation in the mineral with respect to the fluid. This was attempted by assuming full equilibrium between the fluid and the mineral at the temperature of formation (~500 °C). The Cl isotopic fractionation between fluid andscapolite obtained (+1.9‰) was found to be very high and in contradiction with the theoretical values proposed by Schauble et al. (2003) for Cl-bearing amphiboles and biotites in equilibrium with monovalent brines. However, a Rayleigh distillation process simulated using the measured isotope fractionation coefficient, reproduced the low isotopic values found in fluid inclusions by Gleeson and Smith (2009).

1.4 References

Barnes J. D and Sharp Z. D., 2005. A chlorine isotope study of DSDP/ODP serpentinazed ultramafic rocks: Insights into serpentinization process. Chem. Geol. 1413, 1-20.

Barnes J. D., Sharp Z. D. and Fischer T. P., 2008. Chlorine Isotope variations across the Izu-bonin-Mariana arc. The Geological Society of America. 36, 883-886.

Bonifacie M., Monnin C., Jendrzejewski N., Agrinier P. and Javoy M., 2007a. Chlorine stable isotopic composition of basement fluid of the eastern flank of the Juan de Fuca Ridge (ODP Leg 168). Earth Planet. Sci. Lett. 260, 10-22.

Bonifacie M., Jendrzejewski N., Agrinier P., Coleman M., Pineau F. and Javoy M., 2007b. Pyrohydrolysis-IRMS determination of silicate chlorine stable isotope compositions. Application to oceanic crust and meteorite samples. Chem. Geol. 242, 187-201.

Bonifacie, M., Busigny, V., Mevel, C., Philippot, P., Agrinier, P., Jendrzejewski, N., Scambelluri, M., and Javoy, M., 2008a. Chlorine isotopic composition in seafloor serpentinites and high-pressure metaperidotites: Insights into oceanic serpentinization and subduction processes: Geochim. Cosmochim. Acta. 72, 126–139.

Bonifacie, M., Jendrzejewski, N., Agrinier, P., Humler, E., Coleman, M., and Javoy, M., 2008b. The chlorine isotope composition of Earth's mantle: Science. 359, 1518–1520.

Böhlke J. and Irwin J., 1992. Laser microprobe analyses of Cl, Br, I, and K in fluid inclusions: implications of sources in some ancient hydrothermal fluids. Geochim. Cosmochim. Acta. 56, 203-225.

Eastoe C., Guilbert J. and Kaufmann R., 1989. Preliminary evidence for fractionation of stable chlorine isotopes in ore-forming hydrothermal systems. Geology 17, 285-288.

Eastoe, C.J., Long, A., Land, L.S., Kyle, J.R., 2001. Stable chlorine isotopes in halite and brine from the Gulf Coast Basin: brine genesis. Chem. Geol. 176, 343–360.

Eastoe C. Peryt T. Oleh Y. Petrychenko and Geisler-Cussey D., 2007. Stable chlorine isotopes in phanerozoic evaporates. Appl. Geochem. 22, 575-588.

Eggenkamp, H.G.M., 1994. δ^{37}Cl: The geochemistry of chlorine isotopes. Geol. Ultraiectina 16, 150 p.

Gleeson S.A., 2003. Bulk analysis of electrolytes in fluid inclusions. Fluid inclusions: Analysis and interpretation, Short Course Series 32, 233-246.

Gleeson S. A. and Smith M. P., 2009. The sources and evolution of mineralizing fluids in iron oxide-copper-gold systems, Norrbotten, Sweden: Constraints from Br/Cl ratios and stable Cl isotopes of fluid inclusion leachates. Geochim. Cosmochim. Acta. 73, 5658-5672.

Jambon A., Deruelle B., Dreibus G. and Pineau F., 1995. Chlorine and bromine abundance in MORB: the contrasting behavior of the Middle-Atlantic ridge and East Pacific Rise and implications for chlorine geodynamic cycle. Chem. Geol. 126: 101 – 117.

John, T., Layne, G. D., Haase, K. M., Barnes, J. D., 2010. Chlorine isotope evidence for crustal recycling into the Earth’s mantle. Earth Planet. Sci. Lett. 298, 175–182.

John, T., Scambelluri, M., Frische, M., Barnes, J. D. & Bach, W., 2011. Dehydration of subducting serpentinite: Implications for halogen mobility in subduction zones and the deep halogen cycle. Earth Planet. Sci. Lett. 308, 65–76.

Kaufmann, R.S., Long, A., Campbell, D.J., 1998. Chlorine isotope distribution in formation waters, Texas and Louisiana. AAPG Bull. 72, 839–844.

Kesler S. E., Appold M. S., Martini A. M., Walter L. M., Huston T. J. and Kyle J. R. 1995. Na–Cl–Br systematics of mineralizing brines in Mississippi Valley-type deposits. Geology 23, 641–644.

Layne G. D., Kent A. J. R. and Bach W., 2009. δ^{37}Cl systematic of back-arc spreading: the Lau Basin. Geology 37, 427–430.

Lindblom, S., Broman, C. & Martinsson, O.,1996. Magmatic-hydrothermal fluids in the Pahtohavare Cu-Au deposit in greenstone at Kiruna, Sweden. Mineral. Dep. 31, 307-318.

Magenheim A., Spivack A. Michael P. and Gieskes J., 1995. Chlorine stable isotope composition of the oceanic crust: implications for earth's distribution of chlorine. Earth Planet. Sci. Lett. 131, 427-432.

Nahnybida T., Gleeson S.A, Rusk B. and Wassennar L., 2009. Cl/Br ratios and stable chlorine isotope analysis of magmatic-hydrothermal fluid inclusions from Butte, Montana and Bingham Canyon, Utha. Doi:10.1007/s00126-009-0248-0.

Numata M., Nakamura N. and Gamo T., 2001. Precise measurement of chlorine stable isotopic ratios by thermal ionization mass spectrometry. Geochem. Jour. 35, 89-100.

Ransom B., Spivack A. and Kastner M., 1995. Stable Cl isotopes in subduction-zones pore waters: implications for fluid-rock reactions and the cycling of chlorine. Geology 23, 715-718.

Reed M., Rusk B. and Palandri J., 2013. The Butte magmatic-hydrothermal system: One fluid yields all alteration and veins. Econ. Geol. 108, 1379-1396.

Roberts S. A. 1975. Early hydrothermal alteration and mineralization in the Butte district, Montana: Unpublished Ph.D. dissertation, Harvard University, 157 p.

Rusk B., Reed M., and Dilles J., 2008. Fluid inclusion evidence of magmatic-hydrothermal fluid evolution in the porphyry copper-molybdenum deposite at Butte, Montana. Econ. Geol. 103, 307-334.

Schauble E., Rossman G. and Taylor H., 2003. Theoretical estimates of equilibrium chlorine-isotope fractionations. Geochim. Cosmochim. Acta. 67, 3267-3281.

Sharp Z. D. and Barnes J. D., 2004. Water-soluble chlorides in massive seafloor serpentinites: a source of chloride in subduction zones. Earth Planet. Sci. Lett. 226, 243 -254.

Sharp Z., Barnes J., Brearley A., Chaussidon M., Fischer T. and Kamenetsky V., 2007. Chlorine isotope homogeneity of the mantle, crust and carbonaceous chondrites. Nature Lett. 446, nature05748.

Sharp Z. D., Mercer J.A., Jones R. H., Brearley A. J., Selverstone J., Bekker A. and Stachel T., 2013. The chlorine isotope composition of chondrites and Earth. Geochim. Cosmochim. Acta. 107, 189-204.

Stotler, R.L., Frape, S.K., Shouakar-Stash, O., 2010. An isotopic survey of δ^{81}Br and δ^{37}Cl of dissolved halides in the Canadian and Fennoscandian Shields. Chem. Geol. 274, 38-55.

Webster J. Tappen C. and Mandeville C., 2009. Partitioning behavior of chlorine and fluorine in the system apatite-melt-fluid. II: Felsic silicate system at 200 MPa. Geochim. Cosmochim. Acta. 73, 559-581.

Wei, W., Kastner, M., Spivack, A., 2007. Chlorine stable isotope and halogen concentrations in convergent margins with implications for the Cl isotopes cycle in the ocean. Earth Planet. Sci. Lett. 266, 90–104.

Xiao and Zhang, 1992. High precision isotopic measurement of chlorine by thermal ionization mass spectrometry of the Cs_2Cl^+ ion. Intern. Jour. Mass Spec. Ion Proc. 116,183-192.

Yardley BWD, Gleeson S. A., Bruce S., Banks D. A., 2000. Origin of retrograde fluids in metamorphic rocks. Jour. Geochem. Exp. 69, 281-285.

Wilson C. J. N. and Rowland J. V., 2011. Volcanological and tectonic insights into geothermal systema in the central Taupo Volcanic Zone, New Zealand. New Zealand Geothermal Workshop 2011.

2 Analytical protocols

Early work on the behaviour of stable Cl isotopes was undertaken by Bartholomew et al. (1954) and showed that there were different rates of reaction for ^{35}Cl and ^{37}Cl. The light isotope (^{35}Cl) had a tendency to react faster than the heavy one (^{37}Cl). Later, Hoering et al. (1961) analyzed 81 naturally occurring samples and concluded that within the precision of the analyses (±1‰) there was no significant variation in the ratio of the stable Cl isotopes in natural environments. The extraction techniques were not very efficient at the time and the analytical precision was ±1‰, resulting in serious concerns about isotopic fractionation during sample preparation and memory effects. During the next decades these problems were addressed and Taylor and Grimsrud (1969) who developed the Cl extraction technique currently used, the precipitation of Cl from an aqueous solution as AgCl and its conversion to CH_3Cl, the analytical gas for mass spectrometry. Nevertheless, two important aspects, the precision of the mass spectrometry method and the definition of an international standard were not achieved until the work by Kaufmann et al., (1984). In this contribution, analytical precisions of ±0.2‰ were reported and the Standard Mean Ocean Chloride (SMOC) was established as the international standard for stable Cl isotopes analysis. Chlorine isotopic variations are reported as a per mille (‰) difference ($\delta^{37}Cl$) in a measured $^{37}Cl/^{35}Cl$ Ratio relative to SMOC:

$\delta^{37}Cl=[R_{sample}/R_{seawater} - 1]*1000$. (Godon et al. 2004) (1)

Both extraction and analytical techniques have been slightly modified allowing for better reproducibility and precision, expanding the application of these isotopes to more diverse geologic environments.

The present thesis work includes the extraction, preparation and analysis of Cl and stable Cl isotopes from different matrices: geothermal waters, fluid inclusion leachates and pyrohydrolysis solutions of scapolite. Chloride concentrations were measured in aqueous solutions by Ion Chromatography (IC) at the University of Alberta. As part of this research, a pyrohydrolysis apparatus was constructed at the University of Alberta to extract Cl from scapolite specimens. Samples prepared for isotope analysis were run at the National Water Research Institute, Environment Canada, Saskatoon

(NWRI-EC) and the department of Geological Sciences, University of Texas at Austin. The following section describes the analytical protocols used in these two laboratories and their main differences. The schematics of the different procedures to extract Cl from aqueous solutions and minerals is illustrated in Figure 2.1.

2.1 Ion chromatography

Chloride and bromide determinations were conducted at the University of Alberta in the Department of Earth and Atmospheric Sciences using Ion Chromatography (IC). In this technique the sample is injected into the flow of an eluent which carries the sample to an ion exchange column. Each of the ions within the sample has different affinities for the ion exchange resins and is retained for different lengths of time prior to being eluted off the column. The instrument used was a Dionex DX600 ion chromatograph with an AS-14A analytical column. In addition to Cl^- and Br^-, NO_3^-, NO_2^-, PO_4^{3-} and SO_4^- were also analyzed by IC. A seven ion standard was run along with the samples for accuracy purposes, also blanks and an internal quality control standard were used. The data are reported with an uncertainty of 5%. Solids present in the samples with sizes above 0.45 μm were retained in PTFE filters in order to obtain a fluid suitable for the IC analysis. The samples were analyzed in 7 mL vials with pierceable septums. Analyses of the Cl concentrations of all solutions were carried out before the samples were processed for Cl isotope analyses.

2.2 Chlorine Extraction from Minerals (Pyrohydrolysis)

The most reliable method to extract Cl from mineral samples, considering yields and minimization of possible fractionation effects, is pyrohydrolysis (Bonifacie et al. 2007). A pyrohydrolysis apparatus was built at the University of Alberta in order to extract the Cl contained in scapolite mineral separates (Figure 2.2). The purpose of this technique is to remove the Cl present in the molecular structure of a mineral by melting a small mass of sample (100 to 150 mg). The volatiles released during the reaction are carried by a steam flow to a distillation tube obtaining an aqueous solution. The pyrohydrolysis set up used was modified from the one described by Bonifacie et al., (2007) in order to allow for the direct analysis of the Cl concentration in the recovered solution by Ion chromatography (IC). In order to measure as pure a pyrohydrolysis solution as possible, we avoided the use of a NaOH collecting solution (e.g. Bonifacie et al., 2007). The use of a boiling reservoir and a condensation tube in the present set up, was modified from the pyrohydrolysis apparatus used at the University of New Mexico (Barnes and Sharp, 2006).

The system consist of three main parts: a Vecstar conductivity furnace able to operate at 1,200 °C, a boiling water reservoir used to produce steam (the carrier fluid) and a condensation tube where the volatiles are collected (Figure 2.2). A 55 cm borosilicate reaction tube with an internal diameter of 12 mm was selected in order to produce an effective water steam flow of 1.5 to 2.5 mL/minute, enough to transport the volatiles efficiently to the condensation tube (Whitehead and Tomas, 1985). The length of the section of the reaction tube between the furnace and the condensation tube (13 cm), was critical in order to quench the pyrohydrolysis solution down to 90 °C before the condensation tube, preventing excessive condensation, and the overheating and cracking of the condensation tube.

Between 98 and 226 mg of scapolite sample were used for pyrohydrolysis to obtain 1 to 5 mg of Cl. The amounts were based on the Cl wt% measured in the scapolite samples by Electron Microprobe Analysis (EMPA) and the amount of sample available. After determining the weight and Cl content of the sample, it was mixed with five parts V_2O_5 (Whitehead and Tomas, 1985), then the mix was transferred to the reaction tube, which was placed in a position coincident with the central area of the heating element inside the furnace, this to ensure the homogeneous heating and melting of the sample. The boiling reservoir, a 500 mL flask filled to the mark with deionized water, is attached to one end of the reaction tube using a Swagelok elbow (SS-810-9). The condensation tube is connected to the other end in the same way. A heating coil wrapped around a 10 cm section of the reaction tube end connected to the boiling water reservoir was set at 200 °C to prevent condensation before the furnace. A stream of water steam carries the volatiles from the furnace to the condensation tube where the solution containing Cl from the mineral sample is recovered. The final volume of pyrohydrolysis solution was between 90 and 161 mL.

With a view to conducting the Cl extractions under the same conditions for each sample, a heating sequence was implemented making sure the time under melting temperature (1200 °C) was enough for the successful recovery of all the Cl in the sample. But also, the steam flow had to be optimized in order to make sure the volatiles were evacuated fast enough as they were released from the melting sample in order to prevent isotopic fractionation. Therefore, the steam generation and sample melting processes had to be synchronized. This was achieved after several trials at different pre-heating temperatures and melting temperature durations. Also, the temperature of the mantle heating the deionize water reservoir was optimized to prevent excessive flow that could produce a burst of steam during extraction, displacing the sample in the furnace towards the condensation tube. It was found that the flow of steam was efficient to evacuate quickly the volatiles in the reaction tube when the temperature of the mantle was kept at 100 °C during sample melting at 1200 °C. During the entire process the borosilicate tube preserved its integrity, no cracks or other deformation features were noticed.

The description of the heating process used follows. The first step was the heating of the water reservoir to 100 °C (eighth mark on the mantle controller) and the activation of the heating coil wrapped around the reaction tube before the furnace to heat this portion to 200 °C. At the same time, the furnace was turned to heat at 400 °C, it took 10 minutes for the furnace to reach this temperature. This pre-heating stage was important to allow high temperature in the reaction tube and prevent condensation of the steam flow. Once the furnace reaches 400 °C, it was turned to 1200 °C. After 30 minutes, the water reservoir boiled gently and a steam flow was observed moving in the reaction tube, by this time the furnace was actively melting the sample. The scapolite samples were totally melted after 30 minutes at 1200 °C.

Deionized water from the boiling reservoir was analyzed by IC between runs to assess if any Cl had flowed back from the reaction tube, however Cl was not detected in any of the conducted tests. The maximum temperature recorded in the upper portion of the condensation tube was 70 °C, allowing for a final collection temperature of 20 °C. The total duration of each extraction was 1 hour, excluding a pre-heating stage to 400 °C of 15 minutes. The efficiency of the process was measured by using a well characterized biotite internal standard with a Cl concentration of 1900 ppm. The standard was mixed with V_2O_5 in the same proportion as with the scapolite samples and melted at 1200 °C following the same procedure described above. The biotite sample was run three times in the pyrohydrolysis apparatus. Then, the extraction solutions were measured by IC, obtaining Cl yields between 89 and 95%.

This pyrohydrolysis set up is simple but efficient, it allows for the direct measurement of the pyrohydrolysis solution by IC without further treatment, and by using water steam as carrier media, the injection of He or air in the system is not required. A factor that could have influenced the efficiency of the extraction, is the potential mass loss of the mix sample-flux during its transfer to the reaction tube. Using a clean plastic funnel the mix was transferred to the reaction tube, but some very fine material adhered to the walls. The use of a reaction boat, which is a recommended procedure (Whitehead and Tomas, 1985 and Bonifacie et al. 2007), was not practical in our case as the diameter of the reaction tube used was just 12 mm. A reaction boat to fit inside this tube would be too small to contain the mix to be melted.

2.3 Chlorine extraction from aqueous solutions

2.3.1 Silver chloride precipitation (University of Alberta)

Chlorine was extracted at the University of Alberta from aqueous samples using an extraction method introduced by Taylor and Grimsrud (1969). The main purpose of this method is to obtain an AgCl precipitate of enough quality to convert the Cl to CH_3Cl (the analytical gas) by reacting AgCl with CH_3I. This technique allows CH_3Cl yields of 99% thanks to the production of AgCl microcrystals with the addition of 0.4 M KNO_3. These microcrystals offer a bigger reaction surface allowing the most efficient conversion of AgCl to CH_3Cl. The method was slightly modified by Wassenaar and Koehler (2004) to adapt it to the work with small size samples (100 µmol of Cl^-). Following Wassenaar and Koehler (2004), an adjusted volume of the sample solution was prepared to 100 mL. Then 4 mL of 1 M KNO_3 was added, followed by 2 mL of 5% HNO_3 to prevent any chloride from precipitating (Figure 2.1). Significant amounts of S were detected in the fluid inclusion leachate samples from the Butte deposit in Montana. If S was detected by IC the procedure described in Sharp et al., (2009) was used to remove it from the solution and prevent the formation of Ag_2S. This procedure consists of the addition of 10 mL 50%

HNO_3 to the solution, which is then gently heated for 3 to 4 hours to allow the S to escape to the atmosphere. After that, the regular procedure to precipitate AgCl described by Wassenaar and Koehler (2004), was followed. This involves heating the solution in a beaker, wrapped with aluminum foil, to 85 °C. At this temperature 1 mL of 0.5 M $AgNO_3$ was added to samples above 100 µmol Cl^-. Right after that, the beaker with the solution was tightly sealed with more aluminum foil to prevent photodecomposition, and then put aside for cooling.

The AgCl precipitate formed was filtered through a previously weighed 0.7 µm Whatman glass fiber filter (GF/F) by using a vacuum filtration system. In order to recover as much AgCl as possible, the funnel in the filtration system was rinsed with a solution 0.2 vol % HNO_3, which was also passed through the filter. All of this procedure was conducted in the dark, the filter with the AgCl precipitate was then placed on a watch glass and left in the oven to dry overnight at 60 °C. Once dried, the filter contained the precipitate was weighted again and carefully rolled and put inside a 10 mL glass vial. The vial was sealed with butyl blue pierceable stoppers, and crimped with aluminum rings. The vials containing the AgCl precipitate were wrapped in aluminum foil and packed to be transported to NWRI-EC.

Seawater standard concentrations were prepared in order to bracket the concentrations and Cl mass of the samples to be analyzed. For instance, in the case of the geothermal reservoir water samples, given their high Cl concentrations (from 200 to more than 3000 ppm), the Cl masses recovered were well above 50µmol and four sets of seawater standards were prepared to include the most common concentrations detected in these samples (200, 500, 1000, 2000 and 3000 ppm). The Cl extraction, and CH_3Cl conversion for the standards were done in the same way as for the actual samples.

2.3.2 Silver Chloride precipitation (University of Texas)

The procedure used at the University of Texas varies slightly from the one described above. The concentration of the $AgNO_3$ solution is 0.5 M instead of the 0.4 M solution used at the University of Alberta. Also, the acid added to prevent the precipitation of Ag_2S is Na_2HPO_4 – citric acid buffer solution at the University of Texas (Barnes and Sharp, 2006 and Sharp et al. 2007), different to the 5% HNO_3 solution used at the University of Alberta.

2.4 Mass spectrometry

2.4.1 Production of the analyte gas and mass spectrometry (NWRI-EC)

Once in the mass spectrometry laboratory, the air in the vials was evacuated inserting a needle through the vial's septum, this needle was connected to a vacuum system run by a rotary pump. A volume of CH_3I equivalent to approximately 8 times the stoichiometric amount required for CH_3Cl conversion was injected in every sample (~150 µL) to ensure the full conversion of AgCl to CH_3Cl. The reaction to convert AgCl to CH_3Cl took place at 80 °C, so the vials were placed in an oven at this temperature for 48 hours, which is the recommended reaction time for the highest CH_3Cl yield.

Continuous flow IRMS allows for the analyses of smaller sample sizes, necessary for $\delta^{37}Cl$ value determinations in low concentration samples. Some available techniques allow for the analysis of very small Cl masses as low as 1.4 µmol (Shouakar-Stash et al. 2005). However, in this study, the method and instrumentation used by NWRI-EC was adopted. The detection limit of this method is 0.2 µmol Cl (Wassenaar and Koehler, 2004), quite suitable for fluid inclusion leachates and other dilute samples. This method also has the advantage of a rapid and more reliable sample preparation compared to other methods. For comparison, some samples were analysed in the Department of Geological Sciences at the University of Texas at Austin.

The mass spectrometer at NWRI-EC a GV Instruments Isoprime CF-IRMS, ran in continuous flow mode. The MS was modified to measure masses 52 and 50 of CH_3Cl gas (Wassenaar and Koehler, 2004). The reference gas was pure CH_3Cl introduced automatically to the MS from the dual-inlet bellows. A GC column located before the MS was dedicated to separate CH_3Cl from air and excess CH_3I using He as the carrier gas. Between 50 and 200 µL of sample CH_3Cl, extracted from the reaction vials with a gastight syringe, were injected in a sampling port placed in the GC column for the analysis. With this method up to 7µg Cl can be measured with a precision of ±0.2‰.

Once the IRMS is set up for Cl stable isotope analysis, a calibration process is performed injecting the analytical gas to the MS, in order to obtain the reference gas calibration curve. A plot peak area (PA) vs. raw $\delta^{37}Cl$ values is generated with five reference gas measurements, the slope of a best fit line is calculated in order to be used later to calibrate the delta values of the standards. Next, the standards are run in groups according to their concentrations, which should bracket the sample concentrations. The raw delta values are adjusted according to the equation:

$$\delta^{37}Cl_{adj} = \delta^{37}Cl_{raw} - (PA*m) \quad (2)$$

Where, $\delta^{37}Cl_{adj}$ is the delta value adjusted, $\delta^{37}Cl_{raw}$ is the raw delta value, PA is the peak area, and m is the slope of the reference gas calibration curve. The adjusted delta values are then averaged and their standard deviation calculated. The adjusted delta values is used in the following equation to calculate the delta SMOC of the standard ($\delta^{37}Cl\ SMOC_{std}$), which should be close to 0‰ ±0.2‰:

$$\delta^{37}Cl\ SMOC_{std} = \delta^{37}Cl_{adj} - \delta^{37}Cl_{avg} \quad (3)$$

Once the reproducibility of the standards is confirmed, the samples can be run. After obtaining the raw delta for the sample, it is adjusted using equation (2) for the respective values, and then equation (3) to obtain the actual $\delta^{37}Cl$ SMOC value of the sample, subtracting the $\delta^{37}Cl_{avg}$ of the standard from the $\delta^{37}Cl_{adj}$ of the sample.

2.4.2 Production of the analytic gas and mass spectrometry (University of Texas)

As described above, Wassenaar and Koehler (2004), injected CH_3I to react with AgCl in a vial, which after the reaction is complete allows for multiple determinations of a single sample, extracting small CH_3Cl gas volumes with a syringe to be analysed in the MS. The method used at the University of Texas doesn't allow for multiple determinations of a single sample, as the filter with AgCl is introduced in a Pyrex tube, then air is evacuated and CH_3I is added, after that the tube is fused at the top to retain the gas. The tubes are placed in the oven and kept there at 80 °C during 48 hours. As there is no other way to extract the gas from the tube other than breaking it, the sample can be analysed only once. Another important difference has to do with the concentration of the seawater standard. At the University of Texas, the Cl extractions of the seawater standard are not adjusted to resemble the Cl mass of the samples to be analysed.

At the University of Texas the isotopic analyses were conducted on a ThermoElectron MAT 253 in continuous flow mode. The sample, contained in a sealed Pyrex tube, is broken under vacuum inside a sleeve. The CH_3Cl gas and excess CH_3I are separated in a gas chromatographic system and carried by a He stream. The CH_3Cl gas sample is retained frozen in a series of steps to purify the sample before being presented to the ion source. This method requires the conversion of at least 0.08 mg AgCl (20µg Cl) to CH_3Cl gas in order to obtain reliable delta values with a precision of ±0.2‰.

2.5 Discussion of the analytical methods

Eggenkamp et al. (1995) suggested that the mass of Cl in a sample was of major importance for the isotopic analysis and the reproducibility of the data. In this research, samples below 4.5 µmol Cl, using the IRMS at NWRI-EC, showed inconsistent delta values when several runs with different volumes of CH_3Cl gas, extracted from a single vial, were performed. However, reproducible values were obtained adjusting the sample volume injected in the MS, so the sample CH_3Cl signal peak was between 80 and 95% of the reference gas signal peak. Also, anomalous delta values were obtained when the signal of the sample was higher than the signal in the reference gas. To obtain reproducible delta values, most of the samples from geothermal waters required the injection in the MS of volumes between 20 to 150 µL of CH_3Cl, but samples from fluid inclusion leachates required injections from 175 to 250 µL. Figure 2.3 depicts the increase in the volume of sample injected, in order to conserve a signal peak high enough to obtain reproducible delta values. Masses below 50 µmol Cl required more CH_3Cl gas injected to obtain reproducible delta values. Also, more seawater standards were used to control any variation in the $\delta^{37}Cl$ values.

At NWRI-EC, several runs with our seawater standard prepared at different Cl concentrations were performed in order to identify any changes in its delta value. It was concluded that at masses between 1.4 and 4.2 µmol Cl, the delta values were around 2.5‰ lower than samples prepared with seawater standard with higher Cl masses (Figure 2.4). For this reason, the seawater standards were prepared encompassing the ranges of Cl masses present in fluid inclusion leachates, in an effort to make the comparison between sample and standard representative.

As shown in Figure 2.4, samples around 20 µmol Cl can be more than 0.2‰ lower than the standard, which is the precision of the two methods discussed. The use of standards bracketing these small concentrations can be helpful to some extent. The MS methods for the stable Cl isotope analysis available can in fact measure small Cl masses (up to 0.2 µmol Cl), but the most important question at this point is: how representative the AgCl extraction really is when dealing with small Cl masses?

Eggenkamp et al., (1995), determined that during Cl extraction, both the mass of $AgNO_3$ added and the solubility of AgCl influence the amount of AgCl recovered. Low mass samples, under 3.5 mg Cl (Eggenkamp et al., 1995, and references therein), are more affected by low AgCl yields than samples with higher amounts of Cl. In the case of fluid inclusion leachates, the addition of large amounts of $AgNO_3$ to obtain higher AgCl yields becomes impractical, as low masses of Cl were recovered (0.11 to 3.28 µmol). Therefore, to recover most of the Cl in the sample solution the general preparation procedure for AgCl precipitation was slightly modified: 4 mL of KNO_3 solution 1M were mixed with the sample to produce small AgCl crystals with high ionic strength (Taylor and Grimsrud, 1969), and 40 mL of $AgNO_3$ solution 0.5M (0.02 moles) were added in excess to increase the probability of AgCl formation. Our seawater standards were prepared the same way as explained before (Section 2.3.1.) for the inclusion leachates to prevent anomalous deviations from SMOC in the delta values obtained.

In the inclusion leachate samples, the amount of AgCl recovered was too small to be weighed in a scientific scale and actual yields were not measured. Nevertheless, the AgCl precipitate was observed in some samples during reaction and confirmed during the IRMS runs, as measurable signal peaks were observed in the chromatogram, which confirmed the presence of CH_3Cl gas in these samples.

To confirm if different sample preparation methodologies and MS analytical techniques had an effect on the $\delta^{37}Cl$ values of low Cl concentration samples, fluid inclusion leachate samples from the Butte PCD deposit were sent to NWRI-EC and the University of Texas for comparison. Hydrothermal fluids at the Butte PCD are characterized by negative $\delta^{37}Cl$ values; however, in the set of isotope values reported by the University of Texas only two were close to 0‰ and the remaining eleven were between 0.9 and 1.3‰ (Table 2-1).

The method at the University of Texas uses seawater standards with fixed Cl masses. This can potentially mask variations in the isotopic composition of low Cl samples. One of the biggest advantages of the method at NWRI-EC is the possibility of obtaining several measurable volumes of CH_3Cl gas from a single vial, which is very convenient to adjust the signal peak size to obtain reliable isotopic ratios and run several duplicates of a single sample. The δ^{37}Cl values reported by NWRI-EC were within the expected ranges for this deposit. For this reason, we considered the method at NWRI-EC the most suitable to work with low Cl concentration samples like fluid inclusion leachates. The NWRI-EC MS laboratory was also selected to run the geothermal waters from the TVZ, New Zealand. However, considering the very high Cl concentration of the scapolite samples from Norrbotten, Sweden, (> 3.0 mg Cl) these samples were run at the University of Texas.

2.6 References

Barholomew R., Brown F. and Lounsbury M., 1954. Chlorine isotope effect. Nature 4420, 133.

Barnes J. D. and Sharp Z.D., 2006. A chlorine isotope study of DSDP/ODP serpentinized ultramafic rocks: Insights into the serpentinization process. Chem. Geol. 228, 246-265.

Bonifacie M., Jendrzejewski N., Agrinier P., Coleman M., Pineau F. and Javoy M., 2007. Pyrohydrolysis-IRMS determination of silicate chlorine stable isotope compositions. Application to oceanic crust and meteorite samples. Chem. Geol. 242, 187-201.

Eggenkamp H. and Kreulen R., 1995. Chlorine stable isotope variations in volcanic gasses, volcanic springs and crater lakes from Indonesia. The geochemistry of chlorine isotopes. Doctoral, Universiteit Utrecht.

Godon A., Jendrzejewski N., Eggenkamp H. G. M., Banks D. A., Ader M., Coleman M. L. and Pineau F., 2004. A crosscalibration of chlorine isotopic measurements and suitability of seawater as the international reference material. Chem. Geol. 207, 1–12.

Hoering T. and Parker P., 1961. The geochemistry of stable isotopes of chloride. Geochimica Cosmochimica Acta. 23, 186-199.

Kaufmann, R., Long, A., Bentley, H., Davis, S., 1984. Natural chlorine isotope variations. Nature 309, 338–341.

Sharp, Z.D., Barnes, J.D., Brearley, A.J., Chaussidon, M., Fischer, T.P., Kamenetsky, V.S., 2007. Chlorine isotope homogeneity of the mantle, crust and carbonaceous chondrites. Nature 446, 1062–1065.

Shouakar-Stash O. Drimmie R. J. and Frape S. K., 2005. Determination of inorganic chlorine stable isotopes by continuous flow isotope ratio mass spectrometry. RDM 19, 121-127.

Taylor J. W. and Grimsrud E. P., 1969. Chlorine isotopic ratios by negative ion mass spectrometry. Anal. Chem. 41, 805-810.

Wassenaar L. I. and Koehler G., 2004. On-Line technique for the determination of the δ^{37}Cl of inorganic and total organic in environmental samples. Anal. Chem. 76, 6384 – 6388.

Whitehead, D., Thomas, J.E., 1985. Use of a nebulizer in pyrohydrolytic decomposition of silicate materials for determination of fluorine and chlorine. Anal. Chem. 57, 2421–2423.

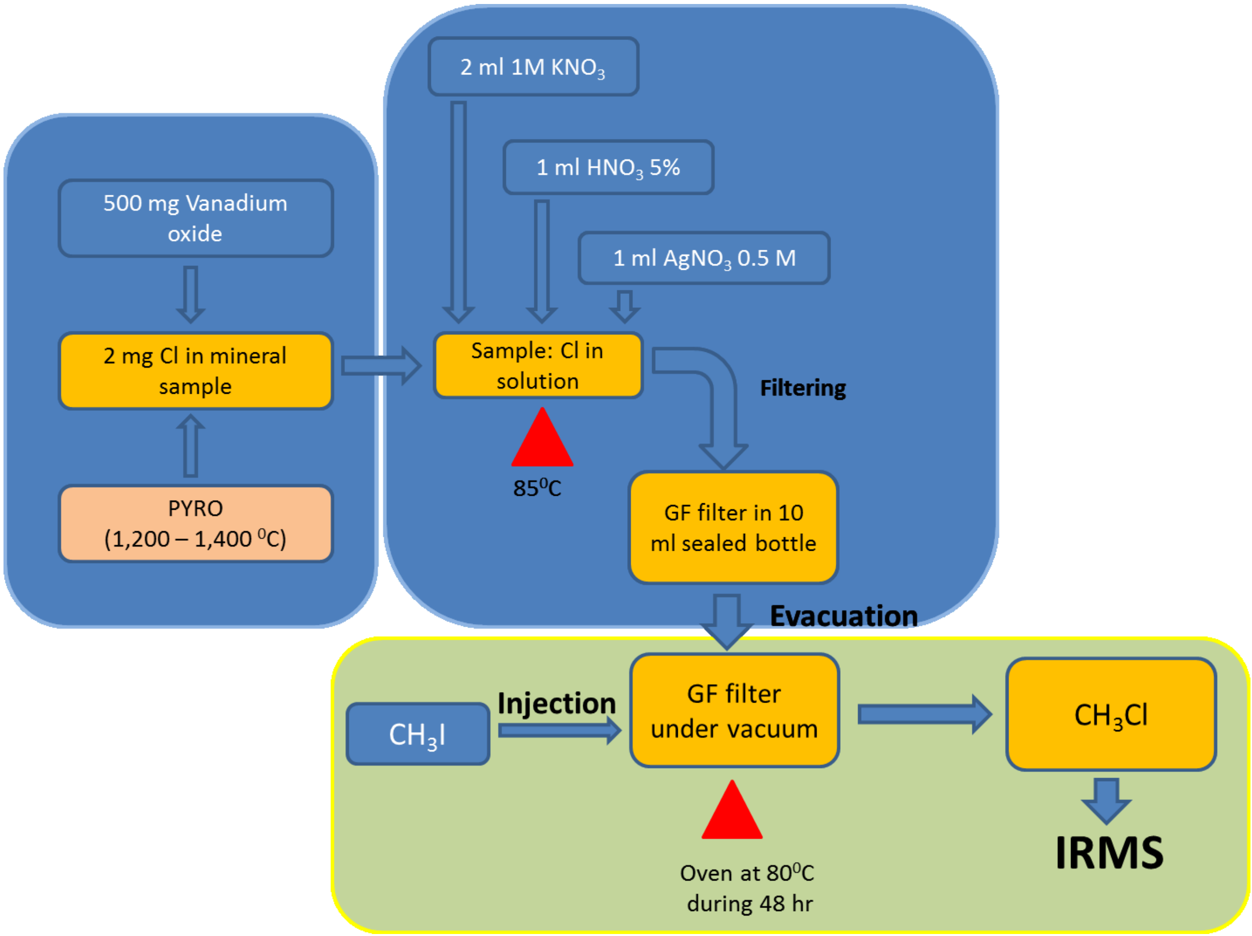

Figure 2-1 Chlorine extraction process.

Diagram representing the process to extract Cl from mineral samples and aqueous solutions. Chlorine extraction and precipitation as AgCl conducted at the University of Alberta. Reaction with CH_3I, conversion to CH_3Cl and IRMS analysis conducted at NWRI-EC and the University of Texas.

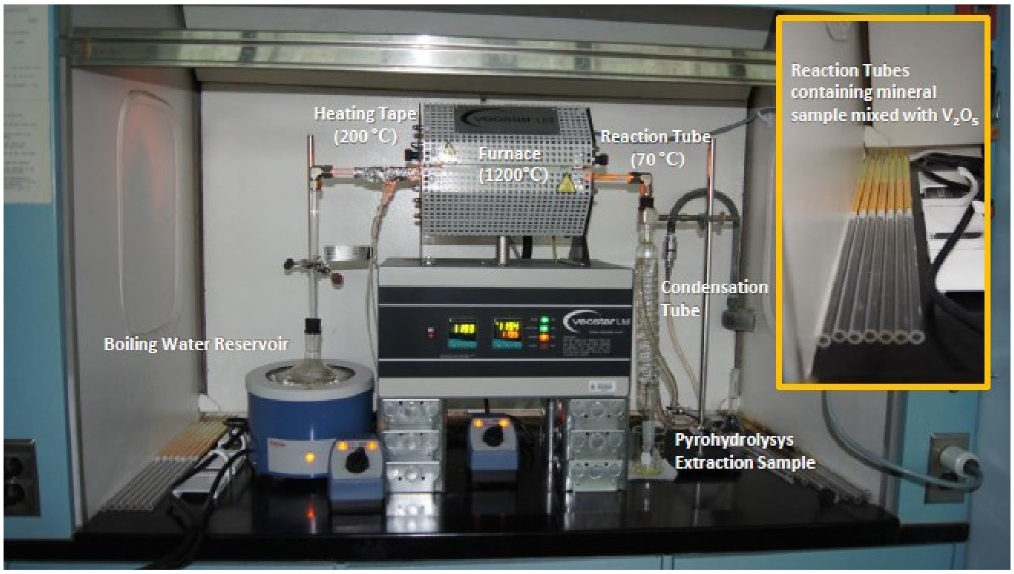

Figure 2-2 Pyrohydrolysis setup used for Cl extraction in scapolite samples.
The inset is a detail of the reaction tubes containing a mix of scapolite powder and vanadium pentoxide (V_2O_5).

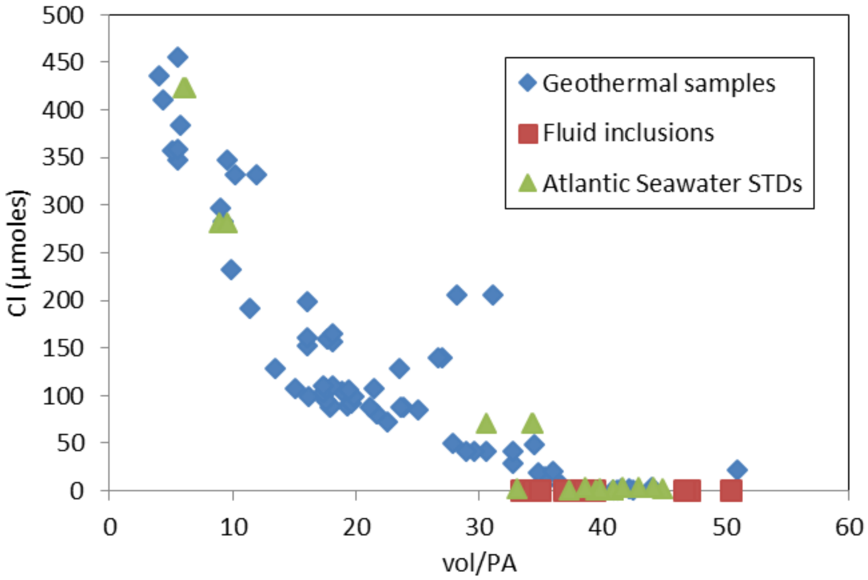

Figure 2-3 Volume of sample injected over peak area signal vs. mass of Cl analyzed. Note the steep fall in the general trend for samples below 50 µmol Cl.

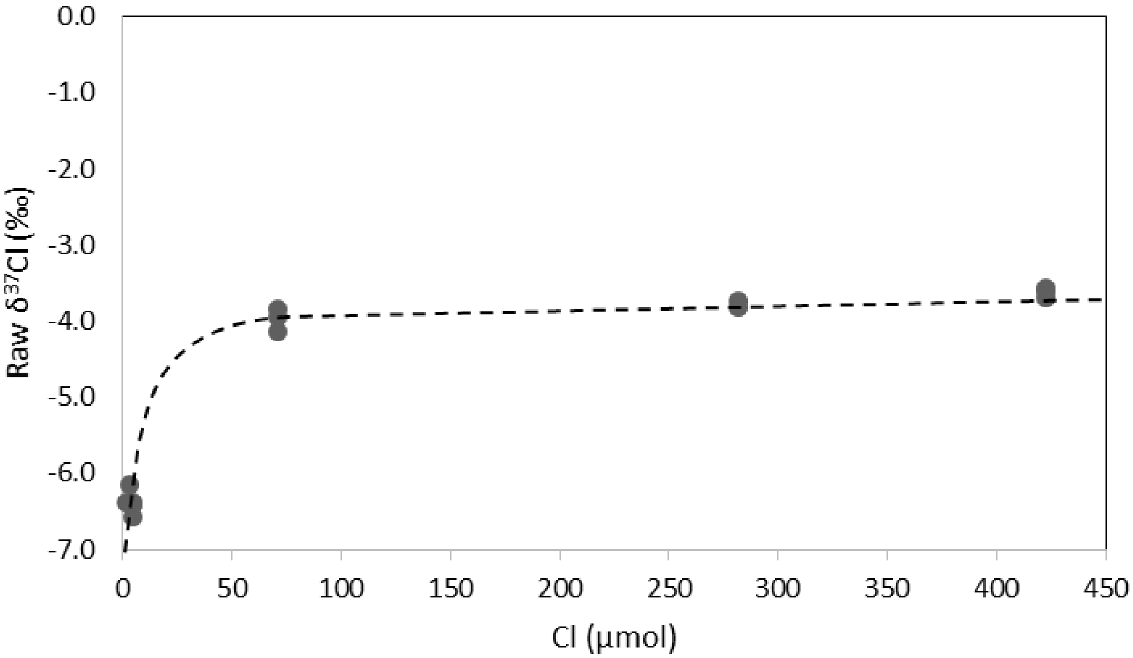

Figure 2-4 Variation in raw δ^{37}Cl values in Atlantic seawater standards. Analysis conducted at the MS laboratory, NWRI-EC.

Table 2-1 Comparison of Stable Cl isotope ratios in low Cl fluid inclusion leachates. Data reported by NWRI-EC and the University of Texas IRMS laboratories on samples from the Butte PCD. Due to small sample volumes and low Cl concentrations duplicates of the same sample were not available for comparison. However, overall the dataset, the data from samples analysed at the University of Texas tend to have higher δ^{37}Cl values.

Sample	Cl (ppm)	δ^{37}Cl (‰)	Laboratory
MS01QZ	8.07	-0.9	SK
MS01EN	2.63	-1.5	SK
MS03PY	14.88	0.9	UT
MS04QZ	5.38	-0.7	SK
MS05QZ	2.54	-0.2	SK
MS08PY	0.80	-1.4	SK
MS08CV	0.58	-0.4	SK
MS09PY	2.94	-0.2	SK
MS10FL	5.82	-0.7	SK
MS11QZ	2.96	-1.5	SK
MS11RC	2.07	-0.8	SK
MS11SL	5.23	0.5	UT
MS12QZ	9.75	-1.0	SK
PS14QZ	20.34	1.3	UT
PS16PY	3.13	-0.4	SK
PS19QZ	3.35	0.1	SK
PS18QZ	20.81	0.9	UT
D24QZ	13.18	1.2	UT
D25QZ	8.28	1.2	UT
D26QZ	9.27	-0.8	SK
D27QZ	6.38	1.1	UT
MD29QZ	14.58	1.3	UT
MD32QZ	5.77	1.3	UT
MD33QZ	37.24	1.0	UT
MD36QZ	15.39	0.4	UT
MD37QZ	6.44	1.3	UT
MD38QZ	18.72	0.9	UT
MD39QZ	3.71	0.5	SK
MD40QZ	8.38	0.1	SK
C42PY	16.63	0.4	SK
C44MT	8.26	-0.3	SK
C47MT	7.34	-0.4	SK

SK: Environment Canada Saskatoon

UT: University of Texas

3 The Source of Halogens in Geothermal Fluids from the Taupo Volcanic Zone, North Island, New Zealand.

3.1 Introduction

The North Island, New Zealand, is in a region of active plate convergence and contains the Taupo Volcanic Zone (TVZ), one of the most active geothermal areas in the world. In the TVZ, part of the heat transfer in the crust is attributed to geothermal activity, (estimated at about 2600 MW/100 km by Hochstein, 1995), and in the area from Tokaanu to Kawerau, 23 geothermal systems with temperatures above 250 °C (Hochstein, 1995), are found (Wilson and Rowland, 2011). Two different groups of fluids linked to either arc-type or rift-type magmas have been previously identified in the TVZ (Giggenbach, 1995).

The origin of the chlorinity in geothermal fluids has been rarely studied. In other systems, elemental ratios of Cl and Br have been successfully used to identify the source of salinity to constrain the origin of marine and non-marine brines in sedimentary basins (Rittenhouse, 1967; Carpenter, 1978; McCaffrey et al., 1987; Walter et al., 1990; Fontes and Matray, 1993; Kesler et al., 1995) but more recently, they have been used to constrain the origin of salinity in the magmatic, metamorphic, ore forming and geothermal environments (e.g. Sanjuan et al., 1990, Böhlke and Irwin, 1992; Gleeson and Turner, 2007; Nahnybida et al., 2009; Kendrick et al., 2012). Chlorine in particular, has potential to be an effective tracer in magmatic-hydrothermal systems. Chlorine is an incompatible element mobilized as a consequence of degassing, partial melting, water-rock interaction and metasomatism (Liebscher et al., 2006, Bonifacie et al., 2007, Sharp et al., 2009). During magmatic fractionation, Cl is preferentially concentrated into the liquid phase and it is retained by a few minerals e.g. biotite, amphibole, scapolite, sodalite and nepheline (Webster et al., 2009). Therefore, due to its incompatibility, solubility and volatility, Cl can potentially elucidate physicochemical processes like phase separation and mixing during the ascent of hydrothermal fluids to the surface.

There have been several studies that have analysed Cl in geothermal systems (e.g. Arnórsson and Andrésdóttir, 1995, Reyes and Trompetter, 2012, Millot et al. 2012). Chlorine has also been used with other elements such as B to identify water-rock interactions and magmatic inputs in geothermal areas of Iceland and Mexico (Sanjuan et al., 1990, Arnórsson and Andrésdóttir, 1995, Bernard et al., 2011). However, there have been relatively few studies that have applied coupled Cl and Br elemental analyses to geothermal systems. Ellis and Mahon (1964) measured Cl/Br ratios in samples from geothermal sites in the TVZ in order to investigate the effect of water-rock interactions on the chemical composition of these fluids. Recently, Millot et al. (2012), analyzed Cl and Br concentrations in samples from the TVZ but didn't calculate or interpret molar Cl/Br ratios.

Despite the potential of Cl isotopes as natural tracers, very few studies have been published on the Cl isotopic composition of geothermal fluids. Kaufmann (1986) studied the Cl isotopic compositions of the geothermal waters in Iceland, and identified both magmatic and seawater chlorine in the system. Eggenkamp and Kreulen (1995) analyzed waters from hot springs and crater lakes from Indonesia, and concluded that the source of Cl in geothermal fluids was volcanic HCl gas. Zhang and Nordstrom (2004) analyzed hot spring waters from Yellowstone National Park; here a magmatic fluid or leaching of the wall rocks were postulated as the sources of Cl. In other environments, Cl can be fractionated during ion filtration, diffusion and advective mixing (Kaufmann et al., 1987, 1988). However, little is known about the effects of phase separation and fluid mixing on the stable Cl isotopic values of geothermal fluids.

In this study, for the first time, the sources of Cl and Br in the geothermal systems of the TVZ are assessed using elemental Cl and Br and Cl stable isotopic data with additional isotopic tracers like oxygen, hydrogen and lithium isotopes. In the case of $\delta^{18}O$ and δD values, they have been used successfully in the past to infer the contribution of meteoric water to the geothermal reservoir and to identify evaporation in hot springs (Hedenquist et al., 1990; Giggenbach et al., 1994; Giggenbach, 1995, and Giggenbach, 1996). The potential of the lithium isotopes to identify water-rock interactions has been recognized since the first experiments with these isotopes were carried out (Chan and Edmond, 1988; Chan et al., 1993; Chan et al., 2002; Tomascak, 2004) and have been recently used in geothermal systems in the Taupo Volcanic Zone (TVZ) (Millot et al., 2012). The main goal of this study was to identify the source of the chlorinity in the fluids of the TVZ and to assess the extent and nature of the chlorine isotope fractionation in some of the most important geothermal systems in the North Island.

3.2 Geology of the Taupo Volcanic Zone (TVZ)

3.2.1 General overview

The TVZ is situated in a zone of active convergence where the Pacific plate is subducted under the Australian plate (Bibbly et al., 1995). In the last 2 m.y., intense volcanic activity has dominated the geological record of the North Island and has resulted in the formation of andesitic units, and since 1.6 Ma, extensive rhyolitic volcanic products have been deposited (Wilson et al., 1995). In total, the minimum amount of volcanic rocks accumulated in the TVZ is calculated to be 10,000 km^3 (Rowland et al., 2010). The boundaries of the TVZ are defined by the calderas and individual vent sites associated with the Kermadec subduction system of NNE-SSW direction (Figure 3.1). The eastern margin has been in the same position for the last 0.34 Ma, but the western margin has moved 15 km to the east. The current limits of the TVZ have been in the same location for the past 0.7 Ma (Wilson et al., 1995). The Modern TVZ includes the volcanic activity of the last 61 Ka (Wilson and Rowland, 2011).

Compositionally, the TVZ can be divided into three sections; north, central and south. The northern and southern sections are identified by the occurrence of andesites, while the central part is characterized by rhyolitic magmatism and associated caldera structures; most of the geothermal systems are located here. The spatial distribution of the andesites and rhyolites in the TVZ has been explained in terms of the tectonic setting of the North Island. The Pacific and Australian plates converge at 20° along the NE-SW-trending subduction interface; this interaction produces the rotation of the eastern side of the North Island in clockwise direction, resulting in the active rifting and thinning of the sub-arc crust of the TVZ. Geodetic and geophysical studies have demonstrated that the extension in the south is about 7 mm a^{-1} and around 15 mm a^{-1} in the north (Wallace et al., 2004).

The basement to the TVZ is composed of Mesozoic sandstones (greywacke) and argillite from the Torlesse Terrane (Mortimer, 1994). There are some differences in the basement found in deep drilling: to the east side of the TVZ, the geothermal systems have their reservoirs in the Mesozoic greywacke and the Torlesse Terrane; to the west these units are thought to be deeper and are cut by dykes and intrusions of granitic composition. Under the Whakamaru caldera (Figure 3.1), the basement is cut by dykes and plutons mainly of granitic composition (Wood, 1996). The basement is intersected by deep wells at Rotokawa, Ohaaki, Kawerau and Ngatamariki. Wells at Mokai, Tauhara and Wairakei have not intercepted the basement as it is deeper than 4000 m. The basement units are characterized by low rock permeability and fluid flow in these lithologies is controlled by secondary permeability (Wood, 1996). The heat source for the geothermal systems in the TVZ are magmatic bodies emplaced in the crust; volcanic studies have found that the shallower magma bodies are located at 4 ± 1 km (Wilson and Rowland, 2011). It has been observed that geothermal systems associated with volcanism younger than 65 Ka are the most productive in terms of steam generation (Wilson and Rowland, 2011).

Direct measurements of temperatures from deep geothermal wells were not available for this study. However, Kissling and Weir (2005) compiled reservoir temperatures in some of the most important geothermal reservoir in the TVZ, concluding that the highest reservoir temperatures are found in the eastern geothermal fields (arc-type), where temperatures around 310 °C are common. Whilst in the west (rift-type), the reservoir temperatures are around 265 °C, with the exception of Mokai (326 °C).

3.2.2 Sampling of the different geothermal systems

Hot springs and reservoir fluids were sampled from the andesitic hosted geothermal systems of: Kawerau, Rotokawa, Ohaaki, Ngatamariki, Waiotapu and Tokaanu. Also, samples were collected from the rhyolite hosted systems of: Wairakei, Tauhara, Mokai, Rotorua, Orakei Korako, Waikite and Waimangu (Figure 3.1).

3.2.2.1 Andesite hosted geothermal systems

The geology of Rotokawa has been well defined by cores and cuttings recovered from several deep geothermal wells. According to Browne et al. (1992), the upper sequence is composed of silicic volcanic rocks, overlying 1,100 m of andesitic lavas which were intercepted by wells at a depth of 1,400 m. The andesite sequence lies on the metasedimentary rocks of the Torlesse Terrane. It has been estimated that the geothermal activity at Rotokawa is no older than 20,000 yrs and is characterized by extensive hydrothermal explosion breccias (Krupp and Seward, 1987). Ten samples were collected from deep wells in the Rotokawa geothermal field.

Ngatamariki shares the same geology with the Rotokawa geothermal field, as they are located some 10 km apart. The first plutonic rock reached by deep drilling in the TVZ was found in Ngatamariki at a depth of 2,200 m; this rock was reported to be a diorite (Browne et al., 1992). One well sample was analysed for this study from Ngatamariki.

The Ohaaki and Kawerau geothermal systems have similar geological settings, and together with Rotokawa, are located on the east margin of the TVZ. Ohaaki and Kawerau are the only 2 productive geothermal systems not related to major rhyolitic calderas in the TVZ (Wood and Brathwaite, 1999). The most important difference between these two geothermal systems is perhaps their basement compositions. Following Wood and Brathwaite (1999), at Ohaaki, quartz is more abundant (32.8 %) than at Kawerau (8.8 to 13.2%) and the ductile-brittle transition is thought to occur at lower temperatures. This prevents the propagation of fractures in the basement and makes the reservoir at Ohaaki less permeable compared with the one at Kawerau (Wood and Brathwaite, 1999). Eight samples from deep geothermal wells were sampled and analysed from Kawerau and only one well sample from Ohaaki.

Although, Waiotapu and Waimangu are both located between the Haroharo and Reporoa Calderas, they differ in their lithology. Waiotapu is characterized by the occurrence of lavas identified as the Ngakoro Andesite, probably originated in the Reporoa caldera where evidence of an andesitic volcano were found preceding a recorded ignimbrite eruption (Nair et al., 2005). Other lithologies include the Waiotapu ignimbrite and the Whakamaru-group ignimbrites, which are the most important rhyolitic deposit in the TVZ (Wood, 1994). Three hot springs samples were analyzed from this geothermal field.

The Tokaanu geothermal system is located at the southern end of Lake Taupo, the hot springs in the area emanate from alluvial deposits. Tokaanu is located on the boundary between rhyolitic and andesitic volcanism. The geothermal features at Tokaanu are found close to the Kakaramea and Pihanga andesite massif (Robinson and Sheppard 1986). Three hot spring samples from this area were analyzed.

3.2.2.2 Rhyolite hosted geothermal systems

The Wairakei and Tauhara geothermal systems are located North of Lake Taupo. The geology in this area has been extensively studied due in part to the importance of the Wairakei geothermal field and to the volcanic activity of Lake Taupo. According to Rosenberg et al. (2009), the geology in the area is characterized by the occurrence of the Torlesse Terrane, volcanic deposits of rhyolitic composition, and the Waiora Valley Andesite, found at Tauhara. At Wairakei and Tauhara, one sample from a deep geothermal well was analyzed from each location and a hot spring by the shore of Lake Taupo.

Mokai is located to the SW of the Maroa volcanic center, very close to two main rhyolite domes associated with the Whakamaru caldera (Wilson et al., 1995). These domes are covered by ignimbrite deposits erupted by nearby volcanic centers; the hydrothermal activity in this area has been proposed to be persistent for over 300,000 yrs (Supri, 2000). As Mokai, the Wairakei and Tauhara geothermal systems are located in the Whakamaru caldera and the basement of the Torlesse Terrane has not been reached by deep drilling (down to 2,768 m) in any of these locations. A group of volcanic, volcaniclastic and sedimentary units on top of the basement named Tahorakuri Formation (Gravley et al., 2007) predates the Whakamaru Group ignimbrites. The Tahorakuri Formation has not been found in wells at Tauhara (Rosenberg et al., 2009). Six samples from the deep geothermal wells in Mokai were analyzed.

The Rotorua geothermal system is located on the southern margin of the Rotorua caldera, and is characterized by rhyolitic volcanism and massive ignimbrite deposits. Two main aquifers (so called due to their shallow depth and size) have been identified, one located in the Mamaku Ignimbrite and other in the Rotorua City domes. A cap of lacustrine deposits with low permeability confines the fluids in the aquifers (Wood, 1992). Three samples from the hot springs at Rotorua were analysed.

Orakei Korako is part of the SE margin of the Maroa caldera. The geology of the geothermal system was defined by examining material from 4 boreholes. In general, the stratigraphy of the area is characterized by the occurrence of pyroclastic deposits, calc-alkaline lavas and alluvial and lacustrine sediments. The Paeroa fault can be identified in Orakei Korako; it is expressed as three NE trending faults of NE direction (Clark and Browne, 2000). Four hot springs samples from Orakei Korako were analysed.

The Waikite geothermal system is related to the Paeroa Fault scarp, the east boundary of the Taupo Fault Belt; its heat source has been related to a lateral geothermal plume common to Waiotapu. Two hot springs from Waikite were analyzed.

Waimangu is located between the Haroharo caldera to the NE and the Reporoa caldera to the SW, in the central TVZ. In the area, rhyolite lava domes, ignimbrites and pyroclastic deposits are the common lithologies, filling the depressions produced by caldera collapses and regional downfaulting (Wood, 1994). Hydrothermal and phreatomagmatic activity was recorded in Waimangu during the 1886 eruption of the Tarawera volcano. This eruption was characterized by the extrusion of a basaltic magma along the summit of Tarawera. It has been postulated that the heat source for the Waimangu geothermal system is a rhyolitic magma chamber associated with Tarawera (Wood, 1994). Three hot spring samples were analysed from Waimangu.

3.3 Sampling methods and analytical techniques

3.3.1 Field sampling methods

The fluid from the hot springs was sampled in 1000 mL high density polyethelene (HDPE) bottles taken directly from the spring. The samples obtained from geothermal wells were collected at the wellhead by using a mini-separator, which is a device able to separate steam and water from the geothermal fluid for sampling. The mini-separator has a gauge to measure sampling pressures. In order to evaluate the geochemical relationships between hot spring samples and samples from deep geothermal wells, the sampling pressures and temperatures measured in the field were used to re-calculate the compositions determined at the wellhead (sampling point) to 1 atmosphere and 100 °C (weirbox conditions), according to the methodology described by Henley et al. (1984). Physico-chemical measurements in hot springs and geothermal well samples including pH, conductivity, and temperature were performed at the time of their collection.

3.3.2 Cl and Br analyses

The Cl and Br analyses were performed at the University of Alberta in the Department of Earth and Atmospheric Sciences using a Dionex DX600 ion chromatograph (IC). Previous to the analysis, all the samples were passed through 0.45 µm PTFE filters and then transferred to 7 mL vials with pierceable septums. In the IC, the ion-exchange resin in the AS-14A analytical column separated the ions according to their characteristic retention times. In order to ensure the accuracy of the determinations, a seven ion standard undiluted and diluted to several concentrations, as well as blanks and an internal quality control solution, were included in every run. Only the results within 5% error, calculated from 3 runs of each sample, were considered for this study. The detection limit was 0.005 ppm.

3.3.3 Cl extraction and δ^{37}Cl analyses

Samples with detected unoxidized sulphur were treated with nitric acid and heated according to the procedure described by Sharp et al. (2009). Chlorine was extracted from the geothermal fluids by reacting the sample with silver nitrate in order to precipitate silver chloride (Taylor and Grimsrud, 1969). Then, the silver chloride was reacted with methyl iodide to produce methyl chloride gas. The gas samples were analysed using a multicollector VG Isoprime CF-IRMS at Environment Canada, National Water Institute in Saskatoon, Saskatchewan (Wassenaar and Koehler, 2004). The gas samples were manually injected in the instrument and compared against the reference, a research grade CH_3Cl gas injected from the bellows in the IRMS. Each sample was run at least 3 times using gas from the same vial. Several standards were prepared with Ocean Scientific International, Atlantic Sea Water 35 wt % (± 0.2%) diluted to Cl concentrations bracketing 3 concentration ranges in the samples (500, 2,000 and 3,000 ppm). The detection limit of this method is 0.2 µmol Cl with a precision of 0.2‰ (Wassenaar and Koehler, 2004).

3.3.4 Determination of δ^{18}O and δD values

Also at the University of Alberta, the δ^{18}O and δD values were obtained in a LGR LWIA (Los Gatos Research Liquid Water Isotopes Analyzer). This instrument is capable of measuring both isotopes simultaneously in small water samples (2 mL vials) by using cavity enhanced absorption spectroscopy methods. With this technique, every sample is measured 6 times in order to eliminate memory effects. The precision of this instrument is 1‰ for δD and 0.3‰ for $\delta^{18}O$.

3.3.5 Li concentrations and isotope analyses

Li elemental concentrations were obtained by quadrupole inductively coupled plasma mass spectrometry (ICP-MS) at R.J. Hill Laboratories, Hamilton, New Zealand, with a detection limit of 0.0002 kg/L (Dean, 2011). Li isotope analyses were performed at the University of Maryland. The method of Li isotope analyses was previously described in Liu et al. (2010; 2013), which was modified from that originally described by Moriguti and Nakamura (1998). Between ~0.1 to 5 g of sample waters were weighted and evaporated to dryness. Then, these samples were dissolved using a ~ 3:1(v/v) mixture of HF and HNO_3 in Savillex® screw-top beakers on a hot plate ($T \approx 120$ °C), followed by twice HNO_3 and once HCl addition until all powder was dissolved and the final solution was clear. Sample solutions were then purified using four-step cation exchange columns (BioRad AG50W-x12, 200-400 mesh). Then, Li solutions (~ 50 ppb Li in ~2% HNO_3) were analyzed using a Nu Plasma Multi Collector-Inductively Coupled Plasma-Mass Spectrometer (MC-ICP-MS). Background signals for ^7Li (<10-4 V) were negligible compared to the typical sample signals (1-3 V). Standard bracketing, using L-SVEC (Flesch et al. 1973), was performed for all analyses. The Li isotopic composition is reported as δ^7Li values, where $\delta^7Li= [(^7Li/^6Li)\ sample/(^7Li/^6Li)L\text{-}SVEC -1]x1000$. The external precision of δ^7Li, based on 2σ of repeated runs of pure Li standard solutions, is ≤ ± 1.0‰. For example, repeat analyses of two pure Li solutions, analyzed during the course of this study (08/2010 to 10/2010) yield the following results: IRMM-016 (Qi et al., 1997) $\delta^7Li = -0.1 \pm 1.1$‰ (2 σ, n = 11); and the in-house standard, UMD-1, a purified Li solution from Alfa Aesar®, gives $\delta^7Li = +54.4 \pm 0.8$‰ (2 σ, n = 15). In addition, two USGS rock standards were analyzed. One analysis of BHVO-1 yielded a δ^7Li value of 4.6‰ cf. 4.0‰ to 5.6‰ in the literature (GeoReM database: http://georem.mpch-mainz.gwdg.de/), and one analysis of AGV-1 yielded a δ^7Li value of 4.4‰ cf. 4.6‰ and 6.7‰ for AGV-1 in Liu et al. (2013) and Magna et al. (2004), respectively.

3.4 Results

3.4.1 Cl, Br and Li concentrations

3.4.1.1 Cl, Br and Li concentrations in hot springs

The results of the analyses are presented in Table 3-1. The bulk of the Hot Spring samples have Cl and Br values in the range of 27 to 3,233 ppm and 0.23 to 6.34 ppm respectively (Figure 3.2A).

Orakei Korako, Waikite and Lake Taupo have the lowest concentrations of these two elements and Waiotapu has the highest variation in Br content (0.72 to 1.45 ppm). Tokaanu has much higher concentrations of Cl (2,908 and 3,233 ppm) and Br (5.70 to 6.34 ppm) and thus, is plotted separately on Figure 3.2B. Figure 3.2A shows a linear distribution of Cl and Br in the hot springs; after Tokaanu, Waimangu has the highest concentrations of Cl and Br: 570 to 727 ppm and 1.31 to 1.46 ppm respectively. The lowest concentrations found in samples from Lake Taupo and Waikite are in the range of 134 to 151 ppm Cl and 0.27 to 0.33 ppm Br. Intermediate Cl and Br concentrations were measured in the samples from Orakei Korako, Waiotapu and Rotorua.

A trendline with slope 0.0021 (R^2=0.99) and a constant Cl/Br ratio of 1,072 was defined using the hot springs shown in Figure 3.2A; this line also intersects the Tokaanu hot springs (Figure 3.2B) suggesting there is a correlation between the Cl and Br contents in the hot spring samples. On the other hand, there is no linear relationship between Li and Cl concentrations in hot springs (Figure 3.2C). Lake Taupo has the lowest Li concentration (1 ppm), the highest concentrations are found in Tokaanu (23 to 28 ppm) (Figure 3.2D) followed by Rotorua (2.4 to 4.1 ppm). Waiotapu has a variation of almost 4 ppm in Li concentrations (Table 3-1).

3.4.1.2 Cl, Br and Li concentrations in geothermal wells

The highest Cl and Br concentrations in the well samples (Figure 3.2B and D) come from Mokai (2,465 to 3,508 ppm Cl and 3.44 to 6.28 ppm Br); these values are comparable with the Tokaanu hot springs. The lowest concentrations of 207 to 781 ppm Cl and 0.47 to 1.56 ppm Br are found in Rotokawa. The samples from the Kawerau geothermal field have 635 to 915 ppm Cl and 1.47 to 2.19 ppm Br which are similar to those from Rotokawa. Between these two main compositional groups, are the geothermal fields Wairakei, Tauhara, Ohaaki and Ngatamariki. The 0.0021 trendline defined by the hot springs is also shown in Figure 3.2B; only the Rotokawa samples sit on this line. The data from Kawerau and Ohaaki have higher Br contents and plot above the trendline, while the rest of the well samples (Ngatamariki, Tauhara, Wairakei and Mokai) plot slightly below the trendline. A few steam condensate samples were available for Cl and Br analysis. These samples were collected from the Rotokawa, Mokai and Kawerau geothermal fields. In the steam condensates Cl concentrations ranged from 0.33 to 61.91 ppm and Br ranged from below the detection limit to 0.11 ppm.

In the geothermal wells, there is a correlation between Cl and Li concentrations, unlike in the hot spring data (Figure 3.2D). A trendline defined by using the well data has a slope of 0.0089 (R^2=0.93). Two samples from Rotokawa (RK03 and NAP06) plot off the trendline and have Li enrichments of around 5 ppm. One sample from Kawerau (KA08) had no detectable Li. Rotokawa is characterized by low Li (4.1 ppm) and Mokai has the highest (32.5 ppm) Li concentration.

3.4.2 Cl/Br molar ratios

3.4.2.1 Cl/Br molar ratios in hot springs

The Cl/Br molar ratios for sites with more than one sample analyzed (Figure 3.3A) are in the following ranges: Waikite from 1,039 to 1,299, Orakei Korako from 1,312 to 1,611, Waiotapu from 858 to 1,194, Waimangu from 980 to 1,249 and Rotorua from 977 to 1,019.

3.4.2.2 Cl/Br molar ratios in geothermal wells

Figure 3.3B suggests that two groups of waters can be defined on the basis of their Li concentrations; a group with low Li (0 to 11 ppm) and Cl/Br molar ratios of 659 to 1,478 (this includes the Rotokawa, Kawerau and Ohaaki geothermal fields) and a group with higher Li concentrations (15 to 33) and Cl/Br molar ratios (1,149 to 1,664) from the Wairakei, Tauhara, Ngatamariki and Mokai geothermal fields. The Tokaanu hot spring data plot with the latter group.

3.4.3 Stable isotope results

3.4.3.1 δ^{18}O and δD values

3.4.3.1.1 δ^{18}O and δD values of hot spring waters

The hot springs from Lake Taupo and Waikite, located to the SW of the TVZ plot on, or very close to, the meteoric water line (MWL) as defined for this area by Robinson and Sheppard (1986). The approximate average $\delta^{18}O$ and δD values of the recharge in this area were found to be -6.7‰ and -43‰ respectively (Table 3-1; Figure 3.4A). An evaporation line, obtained by connecting the isotopic values of the three Tokaanu hot springs is represented in Figure 3.4A. The horizontal shift in the $\delta^{18}O$ values (3.2 ‰) of well samples and other hot springs at Tokaanu was obtained based on data from Giggenbach (1996) in Figure 3.4A.

The hot springs data analyzed from the NE do not plot on the MWL but an estimation of the isotopic composition of the recharge in this area can be made. If an evaporation line connecting the Waiotapu hot springs is constructed, the first data point in this line projected to the MWL indicates a $\delta^{18}O$ value shift of 1.8 ‰. The hot springs with the lowest fluid-rock interaction, according to the $\delta^{18}O$ shift, are found in Orakei Korako; these waters have a positive shift in the $\delta^{18}O$ value of 1.5 ‰. The data from hot springs at Orakei Korako, Waimangu, and Rotorua suggest that recharge in this part of the TVZ has a $\delta^{18}O$ value of -5.5 ‰ and a δD value of -35 ‰, very close to the average $\delta^{18}O$ and δD values determined by Giggenbach (1995).

3.4.3.1.2 $\delta^{18}O$ and δD values in geothermal well fluids

The isotopic signatures of meteoric water recharge identified in the hot springs were also detected in the geothermal wells (Figure 3.4B). The fluids from the geothermal fields of Mokai and Rotokawa in the SW have isotopic values similar to the hot springs from Lake Taupo and Waikite. The δD values of the recharge for the Wairakei, Tauhara and Ngatamariki geothermal systems range from -35‰ to -39‰, and $\delta^{18}O$ values from -4.1‰ to -3.0‰. In the NE, Kawerau has the highest $\delta^{18}O$ and δD values of -2.2‰ and -29‰ respectively. Most of the geothermal well data are located to the right of the MWL suggesting there has been an increase in the $\delta^{18}O$ values by water-rock interaction. Waters from Rotokawa are shifted to higher values by 2‰, Tauhara by 2‰, Wairakei by 1.8‰, Ohaaki by 2.5‰ and Kawerau by 3‰. The well sample data from Mokai are quite intriguing; samples MK02 and MK01 collected at depths of 2,593 and 1,679 m respectively, plot near the MWL, but the rest of the data plot to the right with a 1‰ total increase in $\delta^{18}O$ with no change in δD values.

3.4.3.2 Stable Cl isotopes

3.4.3.2.1 Stable Cl isotopes in hot springs

In terms of chlorine isotopes, there are 2 broad groups of data represented in Figure 3.5: positive δ^{37}Cl values related to rhyolitic magmatism and negative values related to andesitic magmatism (see also Table 3-1). The samples related to the SW recharge zone, Waikite, Lake Taupo and Tokaanu, have δ^{37}Cl values that range from 0.2 to 0.7‰. In Figure 3.6, the grey box represents the geothermal systems included or near the Taupo-Whakamaru caldera complex, while the black box outlines the Rotorua-Haroharo caldera complex. The δ^{18}O and δD values of these two meteoric recharge areas are described above. Other hot springs located geographically in the limits of the SW and NE recharge zones (like Orakei Korako and Waimangu) have δ^{37}Cl values ranging from -0.3 to 0.2‰ and 0.0 to 0.2‰ respectively. All the samples from Rotokawa and two from Waiotapu have δ^{37}Cl values that range from -0.7 to -0.1 and -0.8 to -0.5‰. One sample from Waiotapu, the Oyster pool, has a positive delta value (0.1‰).

The hot springs from Rotorua, Waiotapu and Orakei Korako have negative δ^{37}Cl values and Cl concentrations below 1,500 ppm (Figure 3.8A). Waikite, Lake Taupo and Waimangu hot springs have Cl concentrations lower than 1,500 ppm and positive δ^{37}Cl values (Figure 3.8A). In contrast, Tokaanu has positive δ^{37}Cl values and Cl concentrations above 1,500 ppm, similar to the values from the geothermal wells. The same two groups of waters identified in Figure 3.6 can be recognized in Figure 3.8B for the set of well samples analyzed; one group represented by Cl concentrations above 1,500 ppm and positive δ^{37}Cl values and the other with concentrations below 1,500 ppm and negative δ^{37}Cl values. There is no positive correlation between δ^{37}Cl and high Cl contents in the hot spring samples (Figure 3.8A).

3.4.3.2.2 Stable Cl isotopes in geothermal wells

The δ^{37}Cl values for the samples located in the SW of the TVZ (Figure 3.5) are predominantly positive; the samples from Rotokawa have negative values, with the exception of RKA 03 (0.8‰). The δ^{37}Cl values in the Mokai samples are predominantly positive (0.0 to 0.4‰); only one sample, MK05, is negative (-0.3‰). The well samples from Wairakei, Tauhara and Ngatamariki have a positive δ^{37}Cl value of 0.5‰, 0.0‰ and 0.0‰ respectively. The samples from Kawerau located to the NE of the TVZ have negative $\delta^{37}Cl$ values from -0.1 to -0.8‰; this is the only geothermal system that is actually outside the defined central TVZ domain. In general, there is no positive correlation between $\delta^{18}O$ and $\delta^{37}Cl$ in the TVZ (Figure 3.6).

The Cl contents and the $\delta^{37}Cl$ values of geothermal fluids from deep wells are presented in Figure 3.7A. Two groups of waters can be separated in terms of Cl concentrations and isotopic compositions. The geothermal wells with Cl concentrations below 1,500 ppm appear to be related to negative $\delta^{37}Cl$ values (i.e. Kawerau, Rotokawa and Ohaaki). Wairakei, Ngatamariki, Tauhara and Mokai have Cl concentrations above 1,500 ppm and positive $\delta^{37}Cl$ values. Samples from Rotorua and Kawerau have the lowest Cl concentrations (207 to 914 ppm) although the samples come from the greatest depths (2,782 m) (Figure 3.7B). On the other side of the plot, the samples from Mokai have a narrow distribution of chloride (2,356 to 2,720 ppm) and are from depths of 1,679 to 2,593 m. In summary, Figure 3.7 suggests that the $\delta^{37}Cl$ values do not change significantly with sample depth, but a consistent spatial differentiation between waters with positive and negative chlorine isotopic values exists.

3.4.3.3 Li isotopes

3.4.3.3.1 Li isotopes in hot springs

There is no systematic relationship between the Li concentrations and $\delta^{7}Li$ values of the hot springs (Figure 3.9A) or the geothermal wells (Figure 3.9B). Figure 3.9A shows that the hot springs have a wide range in $\delta^{7}Li$ values (the Tokaanu samples were excluded from this diagram given their high Li contents in the range of 23 to 25 ppm). The lowest $\delta^{7}Li$ value was detected in one sample from the Waikite pools (-2.9‰) and the highest was found in the sample from the Oyster pool at Waiotapu (2‰). Figure 3.9A also suggests that the geothermal systems of Lake Taupo, Waikite and Waimangu have similar Li concentrations and $\delta^{7}Li$ values. Orakei Korako and Waiotapu appear close to this group but have more variability in their $\delta^{7}Li$ values. Tokaanu and Rotorua have intermediate ranges of $\delta^{7}Li$ values, from -0.8 to -0.3‰ and from -1.5 to -0.4‰ respectively.

3.4.3.3.2 Li isotopes in geothermal wells

Waters from Rotokawa have a wide distribution in $\delta^{7}Li$ values (-2.3 to 1.0‰) with only 2 positive values. In contrast, Kawerau has a smaller range of $\delta^{7}Li$ values from

0.1 to 1.4‰. The other geothermal well samples, Mokai, Ohaaki, Wairakei, Tauhara and Ngatamariki have values between these two ranges (Figure 3.9; Table 3-1).

3.5 Discussion

3.5.1 Meteoric recharge and evaporation

Previous studies have suggested that the geothermal fluids in the TVZ have been derived from meteoric waters, with additional solutes from water-rock interactions and a fluid of magmatic origin (e.g. Giggenbach, 1992). The $\delta^{18}O$ and δD values presented here confirm that the fluids are ultimately derived from meteoric waters, although some of the isotopic values have been modified by different physico-chemical processes such as mixing, boiling and evaporation. The data suggest that there are two different areas of recharge, one in the NE and one in the SW of the TVZ. However, some geothermal fields like Wairakei, Ngatamariki and Tauhara have $\delta^{18}O$ and δD values that suggest that they may have been recharged in an area located between the two main sources of meteoric water (Figure 3.4). It is noteworthy that the isotopic data suggest that the hot spring samples from Lake Taupo and Waikite, may belong to the same recharge area although they are located 60 km apart (Figure 3.6). The geographic distribution of the recharge areas in the TVZ was also confirmed by the $\delta^{18}O$ and δD values in samples from deep wells, and is consistent with values found in the literature (e.g. Hedenquist et al., 1990; Giggenbach, 1995; Giggenbach, 1996).

Evaporation has a considerable effect on the isotopic composition of some of the hot springs. Giggenbach (1996) reported higher isotopic values ($\delta^{18}O$ and δD) in the Tokaanu hot springs at the surface due to evaporation (and underground, due to phase separation of ascending geothermal fluids). The same effect is observed in this study (Figure 3.4); the three Tokaanu samples define an evaporation trend that suggests that the recharge of these hot springs comes from the SW. Other hot springs affected by evaporation are the Ruatapu cave pool at Orakei Korako, Frying Pan Lake River at Waimangu and the Oyster Pool at Waiotapu.

3.5.2 Water-rock interactions

A characteristic horizontal shift from the MWL in Figure 3.4 is the result of the isotopic exchange between the oxygen in the water and that of the rock (Craig, 1963;

Giggenbach, 1992). The highest shift in $\delta^{18}O$ values (3‰) was detected in the geothermal well samples from Kawerau, and reflect the greatest degree of water-rock interaction of the samples studied. The smallest shift in $\delta^{18}O$ values was found in the high salinity well samples from Mokai (1‰, Figure 3.4). This remarkable characteristic of the Mokai fluids was discussed by Hedenquist et al. (1990), and was interpreted as being indicative of high water-rock ratios in the geothermal system. The linear trends among Li, Cl and Br in the fluids plotted in Figure 3.2 do not support the hypothesis that these elements are derived dominantly from the host rocks. The composition of the geothermal well fluids (Figure 3.2B and C) are very similar. In Figure 3.2, some scattering in the Cl and Li data can be observed in samples from Rotokawa; however, most of the well samples fall on a trendline. The highest concentrations are found in Mokai, which has undergone the lowest amount of water-rock interaction, suggesting that the host rocks are not the main source of solutes.

In contrast, Li does appear to be affected by water-rock interactions. It has been suggested that Li is retained in minerals, such as chlorite and quartz, in the TVZ during hydrothermal alteration (Goguel, 1983). Similarly, an increase in the concentrations of Li in smectites, quartz, pumpellyite, chlorite and leucoxene relative to unaltered rhyolite, andesite and greywacke rocks, has been observed (Reyes and Trompetter, 2012). In addition, the Li isotope fractionation ($\Delta^{7}Li_{clay\text{-}solution}$) inversely correlates with temperature. In smectites, for instance, this value ranges from -1.6‰ ±1.3‰ at 250 °C to -10.0 ‰ ±1.3‰ at 90 °C (Vigier et al., 2008). This suggests that shallower hydrothermal alteration processes may result in loss of ^{7}Li in the water. This contrasts with the high Li concentrations found in geothermal well samples, representing the fluid at reservoir conditions where Li is still preserved in the fluid phase. In Figure 3.2C, there is a significant scatter of the Cl and Li concentrations with respect to the trendline defined with the geothermal well compositions (Figure 3.2D), assuming that the well samples represent fluids from the reservoir. According to this, the samples from Waimangu and two samples from Waiotapu are depleted in Li (Table 3-1). Only one sample from the Fred and Maggie's spring pool in Orakei Korako had relatively high Li values (4.7 ppm). This range in values may be explained by different degrees of Li assimilation by different minerals during hydrothermal alteration.

With the exception of Kawerau, all the other investigated reservoir fluids have low δ^7Li values. These values contrast with the Li isotopic data reported in the literature for other geothermal systems around the world (Millot et al., 2007; 2010). The Li isotopic compositions of the andesites and rhyolites in the TVZ are unknown and thus, the interaction of the reservoir fluids with these units cannot be characterized. However, reported Li isotope compositions from fresh rhyolites from Yellowstone had low δ^7Li values (-3.6 to 0.7‰), and were interpreted to be the result of crustal contamination during caldera collapse (Chan, 2003). Considering that caldera collapse is a common event in the history of the central TVZ, it is possible that the TVZ rhyolites in contact with the geothermal fluids may be ^{7}Li depleted as well. If this were the case, the low Li isotope ratios of the reservoir fluids in the TVZ may be due to water-rock interactions with a low δ^7Li host rock.

The increase in the δ^{18}O values of the fluids suggests that water-rock interaction is an important process in the TVZ; however, it cannot fully explain the source of Cl, Br and Li. A first argument supporting this statement can be presented by comparing the δ^7Li values of the waters from Rotokawa, Ohaaki and Kawerau (Figure 3.9B). These geothermal fields are located close to the east limit of the TVZ and they have basement in the Mesozoic Torlesse terrane (greywacke/argillite) (Wood, 1996). However, there are differences in the Torlesse Terrane; at Rotokawa and Ohaaki, the basement is composed of quartz-rich sandstones with a rhyolitic composition (SiO_2 70-80%), and at Kawerau, the sandstones are quartz poor of andesitic composition (SiO_2 60-64%) (Wood, 1996). At Rotokawa and Ohaaki, δ^7Li values and Li are decoupled; also all the samples from Kawerau have positive δ^7Li values. This contrasts not only with Rotokawa and Ohaaki but also with the rest of the geothermal sites in the TVZ, which have predominantly negative δ^7Li values. This observation agrees with the data presented by Millot et al. (2012). However, an interpretation explaining this difference was not provided in that work.

Lynton et al. (2005) performed experimental studies on the system quartz-muscovite-fluid at 400 and 500 °C and at 50 to 100 MPa. The experimental results as well as natural observations by Teng et al. (2006) suggested that ^{7}Li preferentially fractionates into both minerals by diffusion through interaction with a fluid of magmatic composition. The fluid in these experiments had low δ^7Li values as the heavy isotope was preferentially fractionated into quartz and muscovite. This suggests if a fluid of magmatic composition interacted with basement rocks that are relatively low in quartz (40-60%), it could generate the higher δ^7Li values of the Kawerau fluids compared to those of the reservoir fluids at Rotokawa and Ohaaki where quartz in the reservoir rocks is more abundant (70-80%).

3.5.3 The origin of chlorinity in geothermal fluids from the TVZ

There is no correlation observed between Li and Cl in terms of concentration or isotopic composition (Table 3-1). Chlorine and Br are considered to be conservative elements in magmatic systems as they are concentrated in the fluid phase during magmatic segregation (Jambon et al., 1995; Schilling et al., 1978). Several studies have demonstrated that Cl in geothermal systems associated with hydrothermal volcanism has a magmatic origin (Giggenbach, 1977; Henley and Ellis, 1983; Scott, 1989; Hurwitz et al., 2005) and that the Cl uptake by hydrothermal minerals is minimal and uncommon (Reyes and Trompetter, 2012). Our data indicate that Cl and Br concentrations in geothermal waters associated with arc-type magmatism are relatively low, when compared to rift-type waters (Figure 3.2). This is in agreement with recent data reported for geothermal waters in the TVZ (Reyes and Trompetter, 2012, and Millot et al., 2012).

Giggenbach (1977) suggested that Cl is transported as HCl during magma degassing at depth; then ascends to the reservoir rocks in the gas phase, where it is dissolved in water of meteoric origin and interacts with the feldspar in the reservoir rocks. This interaction produces NaCl which is eventually dissolved by deep reaching recharge water. The data presented thus far, suggest that water-rock interaction is unlikely to be a major source of Cl, Br and Li in these systems and so, the possibility of a magmatic source must be addressed.

3.5.4 The relationship between Cl and Br in geothermal fluids and their origin

The halogen compositions of the hot springs were found to define a trendline of slope 0.0021 (R^2=0.99), with a constant Cl/Br molar ratio of 1,072 (Figure 3.2B). A significant number of the well samples do not fall on this line but plot on a line parallel to the hot springs trendline (Figure 3.2B). In fact, some samples of the deep fluids that are associated with andesitic heat sources plot above the trendline, a possible indication of Br enrichment in a magmatic fluid, while the fluids associated with rhyolites are located below this line suggesting they are relatively depleted in Br. These variations may reflect changes in the magmatic component of the geothermal fluid. Balcone-Boissard et al. (2010) outline two possibilities to generate differences in the relative concentrations of Cl and Br in magmas. Firstly, in basaltic magmas, small amounts of Cl-bearing minerals may fractionate the halogens and modify the Cl/Br ratio. Secondly, in calc-alkaline magmas, measured Cl/Br ratios in pyroclastic rocks from several volcanos have shown considerable variations; these have been attributed to crustal contamination in subduction zones or partial melting in the upper mantle.

Figure 3.10 shows the Cl and Br concentrations, analysed using radiochemical neutron activation (RNAA) and isotope dilution mass spectrometry (IDMS), in a range of igneous standard rocks from Shinonaga et al. (1994). There is a correlation between Cl and Br in Japanese igneous rocks with compositions that range from basalts, which have low to intermediate halogen concentrations to rhyolites, which have high halogen concentrations. This trend is confirmed by using data published in Jambon et al. (1995) on MORB glasses from the Mid-Atlantic Ridge (MAR) and the East Pacific Rise (EPR). This trendline with a slope of 0.0023 (R^2= 0.95) is defined by the MAR, EPR basalts and the Japanese standard rocks (basalts and rhyolites). The distribution of these samples along the trendline suggests that the amounts of Cl and Br fractionated from a basaltic magma are proportional (molar ratio 1,072) and are transferred to glasses and hydrothermal fluids.

Giggenbach (1995) suggested that the interaction of the subducting slab and the mantle wedge, under North Island, generated a high-alumina basalt that evolved to a volatile-rich andesitic melt in the crust to form the andesitic volcanic activity and geothermal systems found at the east side of the TVZ. The high-alumina basalt in the upper mantle continues extending to the west and sits under the TVZ rift; the magmatic fractionation of this basalt evolves to form rhyolitic magmatism. As shown in Figure 3.10, the Cl and Br could be derived from a basaltic magma. There is a considerable variation in Cl and Br contents of basalts and rhyolites, but there appears to be a linear correlation in the entire data set. However, it is difficult to determine whether these variations are due to the use of different analytical methods in the determination of Cl and Br concentrations or they really represent small changes due to the history of the rocks and consequently the fluids. The distribution of Cl and Br is very similar in basalt, andesite and rhyolitic glasses to the distribution found in the TVZ (slope 0.0021). However, in a recent study located at Macquarie Island, some 1,200 km SW from New Zealand, Kendrick et al. (2012) measured Cl and Br in MORB glasses: these data are also positively correlated with a slope of 0.0033 (R^2=0.99). Samples from Kawerau, Ohaaki, Rotokawa and some hot springs sit on or very close to this trendline (Figure 3.10). The well samples related to rhyolitic magmatism, Mokai, Tokaanu, Wairakei, Tauhara and Ngatamariki plot off the Macquarie Island trendline, and appear to be more related to the acidic volcanic rocks (trachyte, pantellerite and rhyolite) analyzed by Bureau and Metrich (2003).

3.5.5 Fractionation of the chlorine isotopes in the crust

The δ^{37}Cl values measured in this study fall into two main populations: the rift-type systems (Tauhara, Wairakei, Mokai, Waikite and Waimangu) have higher Cl, Br and Li contents and positive δ^{37}Cl values compared to the arc-type geothermal systems (Rotokawa, Ohaaki, Waiotapu, Orakei Korako, Kawerau and Rotorua) which have lower Cl, Br and Li contents and predominantly negative δ^{37}Cl values (Figure 3.5). However, the Tokaanu geothermal system is characterized by high Cl, Br, and Li contents and consistently positive δ^{37}Cl values, similar to the rift-type systems. This contrasts with the andesitic origin proposed by Giggenbach (1996) on the basis of N_2, He and CO_2 contents in these waters. Taking into account the conservative character of Cl, Br and the stable Cl isotopes, as observed in the geothermal systems of the TVZ, we propose this system is predominantly influenced by rhyolitic magmatism. The chemistry and isotopic composition of the Tokaanu geothermal systems may be the result of the mixing of fluids from both rhyolitic and andesitic magmatic sources; yet the origin of salinity in the system is clearly rhyolitic.

Variations in the δ^{37}Cl values in some of the hot springs samples correlate with low pH and high δ^{18}O values (Table 3-1). Low pH and high δ^{18}O values are attributed to mixing with distilled fluids such as steam-heated waters, and evaporation (Giggenbach, 1996). The former processes is supported by the higher δ^{18}O values measured in some of the hot springs from Waiotapu (Frying pan flat spring and Oyster pool) and Orakei Korako (Devil's throat spring and Ruatapu cave pool) (Table 3-1).

Sharp et al. (2009) suggested that distillation can affect the Cl isotopic compositions of fumarole samples from Central American volcanos. A positive correlation between δ^{37}Cl and δ^{18}O has been reported in geothermal systems from Indonesia (Eggenkamp and Kreulen, 1995) and Yellowstone USA, (Zhang and Nordstrom, 2004). However, in our study, the positive or negative δ^{37}Cl values in deep geothermal wells have no correlation with δ^{18}O values (Figure 3.6). As discussed above, in the geothermal fluids studied it was observed that boiling, evaporation and mixing are capable of modifying the δ^{37}Cl values of these waters only at the surface. In addition, the current data do not support the isotopic fractionation of Cl during the transit of the geothermal fluid from the reservoir to the surface.

If a high-alumina basalt is the common source of Cl for the geothermal systems in the TVZ, then there must be another process(es) that can fractionate the Cl isotopes and result in fluids with positive and negative δ^{37}Cl values. Experiments on the behaviour of stable chlorine isotopes during fluid-vapour separation at 400 °C and 23 MPa to 450 °C and 42 MPa (Liebscher et al. 2006), suggested there was no significant isotopic fractionation and concluded that the Cl isotopes either in the fluid or the vapour will preserve the signature of the fluid responsible for magma production at depth. This implies that a deep magmatic process may be responsible for the difference in isotopic values found in the TVZ.

The Cl isotopic signature of the upper mantle under the TVZ is unknown, but data from other areas may be informative. Currently, most of the literature on the δ^{37}Cl values of the mantle is focussed on the studies of MORB. Sharp et al. (2007), analysed crust, mantle and carbonaceous chondrites and found that the δ^{37}Cl values ranged from -2.09 to 0.37‰. They also suggested there was no significant fractionation between these reservoirs and that the mantle has a homogenous composition. Bonifacie et al., (2008a) measured the isotopic value of HP metaperidotites, representing subducted material, and found these rocks to have δ^{37}Cl values $\geq$ -1.4‰. A more recent study of 22 MORB samples concluded δ^{37}Cl values for the mantle are $\leq$ -1.6‰ (Bonifacie et al., 2008b). Layne et al., (2009) analyzed glasses and melt inclusions from back-arc basin basalts, and confirmed the δ^{37}Cl values found by Bonifacie et al., (2008b). Sharp et al., (2013) based on previous data and a set of mantle-derived samples, propose a δ^{37}Cl value for the upper mantle of -0.2 ± 0.3‰, arguing that more negative values, such as the -1.6‰ δ^{37}Cl value measured by Bonifacie et al., (2008a), are due to analytical errors related to the small size of the samples investigated. However, in the present study a direct correlation between low Cl concentrations and negative δ^{37}Cl values was not identified (Table 3-1).

The δ^{37}Cl values of the geothermal fluids analyzed range from -1.0 to 0.7‰, the low end of this range is comparable with the values for MORB basalts discussed above. This suggests that the parental basaltic magma in the system is likely to have had a negative isotopic value. If we assume an end-member δ^{37}Cl value of -1.0‰, according to our lowest value measured in the Rotokawa reservoir (well NAP01), for the parental basalt, then we have to account for a 1.7‰ variation in the δ^{37}Cl values. Positive δ^{37}Cl values associated with a rhyolitic heat source have been previously documented from hot springs in Yellowstone National Park by Zhang and Nordstrom (2004), who proposed that water-rock interaction and a magmatic source gave rise to the positive δ^{37}Cl values. There are not many δ^{37}Cl data from acidic igneous rocks but a positive delta value (0.29 ‰) was detected in a rhyolite glass (Rabbit Mountain Rhyolite), and a slightly negative value (-0.06‰) in an andesite from the Pacific-Antarctic Ridge (Godon et al., 2004).

Despite the good correlation between the positive δ^{37}Cl values found in some geothermal fluids and a rhyolitic heat source, the negative values found in samples from Orakei Korako, Rotorua, and Waiotapu (geologically related to rhyolitic activity), may appear contradictory. Nevertheless, high contents of arc-type fluids related to andesitic magmas were detected by Giggenbach (1995) in the same geothermal systems. This suggests that stable Cl isotopes have the potential to identify sources of andesite and rhyolite derived hydrothermal fluids.

The model proposed by Giggenbach (1995) explained many of the geochemical differences in the chemistry of the geothermal systems in the TVZ. This study concluded that the geothermal fields located to the E in the TVZ are characterized by high CO_2 contents and 14% arc-type magmatic water, while the geothermal systems to the W were associated with rhyolitic magmas with 6% arc-type magmatic water. But a mechanism to explain the migration of the depleted high-alumina basalt in the upper mantle from E to

W was not provided. More recently, Reyners et al. (2007) recognized a zone of partial melting, attributed to the interaction between fluids from the dehydrated subducted slab and the mantle in the mantle wedge at a depth of 65 km under the W margin of the Taupo caldera. This indicates that the mantle flows from W to E under the TVZ rift, and consequently magma derived from the E cannot intrude the crust as suggested by Giggenbach (1995). However, high-alumina basalt has been reported in the central TVZ (Graham et al., 1995), which suggests there are two different kinds of this basalt, one with an arc-type volatile component and the other with a composition more homogenized by interaction with the mantle wedge under the TVZ rift (Figure 3.11).

3.5.6 The H_2O content of rhyolitic and andesitic magmas and its effect in the Cl isotopic composition of magmatic fluids

Assuming that the high-alumina basalt in the upper mantle fractionates to form andesite and rhyolite, it is conceivable that the δ^{37}Cl values of the fluid phase is modified in this process. This conclusion is supported by recent findings on magmatic differentiation controlled by crystal fractionation of mantle derived magmas in the central TVZ (Deering et al., 2011). According to that work, basalt in the lower crust with 1wt % water generates andesitic melts. A dacitic melt with higher water content (2 wt %) is trapped in the upper crust as a silicic mush, which after crystallization and loss of interstitial liquid evolves towards a rhyolitic magma (Figure 3.11). Johnson et al. (2009) proposed that H_2O and Cl are incompatible elements during the fractionation of the rhyolitic magma in the TVZ, suggesting that the rhyolites experienced vapour-saturated crystallization (this was also noted by Wallace (2005) in a suite of rhyolites from Taupo). This implies an increase in water availability by the time of crystallization; and would have to be accompanied by the fractionation of the ^{37}Cl isotope into the fluid phase.

Can the water content of a magma modify the Cl isotopic values of the magmatic-hydrothermal components of the system? As noted by Eggenkamp and Kreulen (1995) regarding the work by Howald (1960) on the isotopic fractionation of Cl in HCl gas and solutions of inorganic chlorides in glacial acetic acid, some experiments suggested that Cl fractionation occurred as a consequence of variations in the water content of the solution. For experiments with water concentration above 1.5 M, the HCl gas was enriched in ^{37}Cl, for experiments with water concentrations below 1.5 M, ^{37}Cl was depleted. With the data currently available, it is difficult to establish the extent of the Cl isotopic fractionation due to magmatic processes in the TVZ, but it is possible that the water content in the magma, along with the concentration of HCl influences, the Cl isotopic fractionation of the gas phase which is assumed here to be the main source of Cl for the geothermal systems in the TVZ.

3.6 Conclusions

The $\delta^{18}O$, δD and $\delta^{7}Li$ values of geothermal fluids of the TVZ suggest that they are meteoric waters which have interacted with their host rocks. The Li isotopes in the deep geothermal fluids suggest the fluids have interacted with unknown units that have low $\delta^{7}Li$ values, possibly rhyolites. Positive $\delta^{7}Li$ values in reservoir fluids were found at Kawerau where the low quartz content of the greywacke apparently enrich the fluid in ^{7}Li, in contrast to the rest of the geothermal systems investigated.

This study suggests there are two distinguishable sources of Cl in the geothermal waters of the TVZ, one related to andesitic magmas in the east and the other associated with predominantly rhyolitic magmatism in the west, albeit both with a common magmatic origin, a high-alumina basalt. There is no evidence of stable Cl isotope fractionation during the transit of the geothermal fluids from the reservoir to the surface, suggesting that the isotopic values are acquired at the source of the chlorinity. Our data suggest that chlorine stable isotopes are fractionated exclusively during magmatic segregation in the crust and to some extent by surface processes like evaporation and distillation in the hot spring systems. It is concluded here that Cl/Br molar ratios and stable Cl isotopes have the potential to identify andesitic and rhyolitic magmatic sources of halogens in geothermal systems.

3.7 References

Arnórsson S. and Andrésdóttir A., 1995. Processes controlling the distribution of boron and chlorine in natural waters in Iceland. Geochim. Cosmochim. Acta 20, 4125-4146.

Balcone-Boissard H., Villeman B., Boudon G., 2010. Behaviour of halogens during degassing of felsic magmas. Geochim. Geophys. Geosyst. Q09005, doi: 10.1029/2010GC003028.

Bernard R., Taran Y., Pennisi M., Tello E., Ramirez A., 2011. Chloride and Boron behaviour in fluids of Los Humeros geothermal field (Mexico): A model based on existence of deep acid brine. Appl. Geochem. 12, 2064-2073.

Bibby H. M., Caldwell T. G., Davey F. J., Webb T. H., 1995. Geophysical evidence on the structure of the Taupo Volcanic Zone and its hydrothermal circulation. J. Volcanol. Geoth. Res. 68, 29-58.

Bonifacie M., Jendrzejewski N., Agrinier P., Coleman M., Pineau F. and Javoy M., 2007. Pyrohydrolysis-IRMS determination of silicate chlorine stable isotope compositions. Application to oceanic crust and meteorite samples. Chem. Geol. 242, 187-201.

Bonifacie M., Busigny V., Mével C., Philippot P., Agrinier P., Jendrzejewski N., Scambelluri M and Javoy M., 2008a. Chlorine isotopic composition in seafloor serpentinites and high-pressure metaperidotites. Insights into oceanic serpentinization and subduction processes. Geochim. Cosmochim. Acta 72, 126-139.

Bonifacie, M., Jendrzejewski, N., Agrinier, P., Humler, E., Coleman, M., and Javoy, M., 2008b. The chlorine isotope composition of Earth's mantle: Science 359, 1518–1520.

Böhlke J. and Irwin J., 1992. Laser microprobe analyses of Cl, Br, I, and K in fluid inclusions: implications of sources in some ancient hydrothermal fluids. Geochim. Cosmochim. Acta 56, 203-225.

Browne P. R. L., Graham I. J., Parker R. J. and Wood C. P., 1992. Subsurface andesite lavas and plutonic rocks in the Rotokawa and Ngatamariki geothermal systems, Taupo Volcanic Zone, New Zealand. J. Volcanol. Geoth. Res. 51, 199-215.

Bureau H. and Métrich N., 2003. An experimental study of bromine behaviour in water-saturated silicic melts. Geochim. Cosmochim. Acta 67, 1689-1697.

Carpenter A.B., 1978. Origin and chemical evolution of brines in sedimentary basins. Oklahoma Geological Survey Circular 79, 60–77.

Chan, L. H. and Edmond, J.M., 1988. Variations in lithium isotope composition in the marine environment: A preliminary report. Geochim. Cosmochim. Acta, 52, 1711-1717.

Chan L. H., Edmond J. M. and Thompson G., 1993. A lithium isotope study of hot springs and metabasalts from Mid-Ocean Ridge hydrothermal systems. J. Geophys. Res. 98, 9653-9659.

Chan L. H., Jeffrey C. and Teagle D. H. A., 2002. Lithium and lithium isotope profiles through the upper oceanic crust: a study of seawater-basalt exchange at ODP sites 504B and 896A. EPSL. 201, 187-201.

Chan L. H., 2003. Variation of lithium isotopic composition in terrestrial systems. Goldschmidt conference abstract 2003.

Clark J. P. and Browne P.R.L., 2000. Past and present-day thermal activity between the Orakei Korako and Te Kopia geothermal areas, New Zealand. Proceedings 25th workshop Reservoir Engineering, Stanford University, Stanford, California.

Craig H., 1963. The isotopic geochemistry of water and carbon in geothermal areas. Nuclear Geology on Geothermal Areas, Spoleto, 1963. Consiglio Nazionale delle Ricerche, Laboratorio di Geologia Nucleare, Piza. 17-53.

Dean A., 2011. Lithium geochemistry of geothermal water, Taupo Volcanic Zone, New Zealand. Thesis dissertation, The University of Auckland.

Deering C. D., Bachmann O., Dufek J., Gravley D. M., 2011. Rift related transition from Andesitic to Rhyolite volcanism in the Taupo Volcanic Zone (New Zealand) controlled by crystal-melt dynamics in mush zones with variable assemblages. J. Petrol. 52, 2243-2263.

Eggenkamp H. and Kreulen R., 1995. Chlorine stable isotope variations in volcanic gasses, volcanic springs and crater lakes from Indonesia. The geochemistry of chlorine isotopes. Doctoral, Universiteit Utrecht.

Ellis A. J. and Mahon W.A.J., 1964. Natural hydrothermal systems and experimental hot-water/rock interactions, Geochim. Cosmochim. Acta 8, 1323-1357.

Flesch G., Anderson A. and Svec H., 1973. A secondary isotopic standard for ^{6}Li/^{7}Li determinations. Inter. Jour. Mass Spect. Ion Physc. 12, 265-272.

Fontes J.C. and Matray J.M. 1993. Geochemistry and origin of formation brines from the Paris basin, France: 1. Brines associated with Triassic salts. Chem. Geol. 109, 149–75.

Giggenbach W. F., 1977. The isotopic composition of sulphur in sedimentary rocks bordering the Taupo Volcanic Zone. Geochemistry 1977. N.Z. Dep. Sci. Ind. Res. Bull. 218, 57-64.

Giggenbach W. F., 1992. Isotopic shifts in waters from geothermal and volcanic systems along convergent plate boundaries and their origin. Earth Planet. Sci. Lett. 113, 495-510.

Giggenbach W. F., 1995. Variations in the chemical and isotopic composition of fluids discharged from the Taupo Volcanic Zone, New Zealand. J. Volcanol. Geoth. Res. 68, 89-116.

Giggenbach W. F., 1996. Are Tokaanu chloride waters the outflow from Hetetahi of Hipaua?. Proceeding 18th NZ Geothermal Workshop 1996. 175-182.

Giggenbach W. F., Sheppard D. S., Robinson B. W., Stewart M. K. and Lyon G. L., 1994. Geochemical structure and position of the Waiotapu geothermal field, New Zealand. Geothermics 23, 599-644.

Gleeson S.A., Turner W.A., 2007. Fluid inclusion constraints on the origin of the brines responsible for Pb-Zn mineralization at Pine Point and coarse non-saddle and saddle dolomite formation in southern Northwest Territories. Geofluids 7, 51–68.

Godon A., Webster J. D., Layne G. D. and Pineau F., 2004. Secondary ion mass spectrometry for the determination of δ^{37}Cl part II. Intercalibration of SIMS and IRMS for aluminosilicate glasses. Chem. Geol. 207, 291-303.

Goguel R., 1983. The rare alkalines in hydrothermal alteration at Wairakei and Broadlands, geotermal fields, N. Z. Geochim. Comochim. Acta 47, 429-437.

Graham, I.J., Cole, J.W., Briggs, R.M., Gamble, J.A. and Smith, I.E.M., 1995. Petrology of volcanic rocks from Taupo Volcanic Zone: A general overview. J. Volcanol. Geoth. Res. 68, 59-87.

Gravley, D.M., Wilson, C.J.N., Leonard, G.S. and Cole, J.W., 2007. Double trouble; paired ignimbrite eruptions and collateral subsidence in the Taupo volcanic zone, New Zealand. Geological Society of America Bulletin 119, 18–30.

Hedenquist J. W., Goff F., Phillips F. M. Elmore D. and Stewart M. K., 1990. Groundwater dilution and residence times, and constraints on chloride source, in Mokai geothermal system, New Zealand, from chemical, stable isotope, tritium, and 36 Cl data. J. Geophys. Res. 95, 365-375.

Henley R. W. and Ellis A. J., 1983. Geothermal systems ancient and modern: a geochemical view. Earth-Sci. Rev. 19, 1-50.

Henley R. W., Trusdell A. H. and Barton P.B., 1984. Fluid-mineral equilibria in hydrothermal systems. SEG. Reviews in Economic Geology. Vol. 1.

Hochstein M. P., 1995. Crustal heat transfer in the Taupo Volcanic Zone (New Zealand): comparison with other volcanic arcs and explanatory heat source models. J. Volcanol. Geoth. Res. 68, 117-151.

Howald R.A., 1960. Ion pairs. 1. Isotope effects shown by chloride solutions in glacial acetic acid. J. Amer. Chem. 82, 20-24.

Hurwitz S., Mariner R. H., Fehn U. and Snyder G. T., 2005. Systematics of halogen elements and their radioisotopes in thermal springs of the Cascade Range, Central Oregon, Western USA. Earth Planet. Sci. Lett. 235, 700-714.

Jambon A., Deruelle B., Dreibus G. and Pineau F., 1995. Chlorine and bromine abundance in MORB: the contrasting behavior of the Middle-Atlantic ridge and East Pacific Rise and implications for chlorine geodynamic cycle. Chem. Geol. 126, 101 – 117.

Johnson E. R., Kamenetsky V., McPhie J., Wallace P. J., 2009. Evolution of rhyolitic magmas in the crustal magmatic system beneath the Taupo Volcanic Zone, New Zealand. AGU, Fall meet., abstract #V51A-1643.

Kendrick M. A., Kamenetsky V. S., Phillips D. and Honda M., 2012. Halogen systematics (Cl, Br, I) in Mid-Ocena Ridge Basalt: a Macquarie Island case study. Geochim. Cosmochim. Acta 81, 82-93.

Kesler S.E., Appold M.S., Martini A.M., Walter L.M., Huston T.J. and Kyle J.R., 1995. Na–Cl–Br systematics of mineralizing brines in Mississippi Valley-type deposits. Geology 23, 641–4.

Kissling W. M. and Weir G. J., 2005. The spatial distribution of the geothermal fields in the Taupo Volcanic Zone, New Zealand. J. Volcanol. Geoth. Res. 145, 136-150.

Krupp R. E. and Seward T. M., 1987. The Rotokawa geothermal system, New Zealand: an active epithermal gold-depositing environment. Econ. Geol. 82:1109-1128.

Kaufmann, R.S., Frape, S., Fritz, P., and Bentley, H., 1987. Chlorine stable isotope composition of Canadian Shield brines: Geol. Assoc. of Can. Special Paper. 33: 87-93.

Kaufman R. S. 1986. $^{37}Cl/^{35}Cl$ ratios in Icelandic geothermal waters. Fifth intern. Symp. on water-rock interact. Reykjavik, Iceland. Ext. Abst. 325-328.

Kaufmann, R.S., Long, A., Campbell, D.J., 1988. Chlorine isotope distribution in formation waters, Texas and Louisiana. AAPG Bull. 72: 839–844.

Layne G. D., Kent A. J. R. and Bach W., 2009. $\delta^{37}Cl$ systematic of back-arc spreading: the Lau Basin. Geology 37, 427–430.

Liebscher A, Barnes J., Sharp Z., 2006. Chlorine isotopes vapour-liquid fractionation during experimental fluid-phase separation at 400 0C/23 MPa to 450 0C/42 MPa. Chem. Geol. 234, 340-345.

Liu, X.-M., R. L. Rudnick, S. Hier-Majumder, and M.-L. C. Sirbescu, 2010. Processes controlling lithium isotopic distribution in contact aureoles: A case study of the Florence County pegmatites, Wisconsin, Geochem. Geophys. Geosyst., 11, Q08014, doi:10.1029/2010GC003063.

Liu X.-M., Rudnick R.L., McDonough W.F. and Cummings M.L., 2012. Tracing chemical weathering of basalts using lithium isotopes: A case study from the Columbia River Basalts. Geochim. et Cosmochim. Acta in review.

Liu, X.-M., Rudnick, R.L., McDonough, W.F., Cumming, M.L., 2013. Influence of chemical weathering on the composition of the continental crust: Insights from Li and Nd isotopes in bauxite profiles developed on Columbia River Basalts. Geochim. et Cosmochim. Acta. 115: 73-91.

Lynton S. J., Walker R. J., Candela P. A., 2005. Lithium isotopes in the system Qz-Ms-fluid: an experimental study. Geochim. Cosmochim. Acta 69, 337-3347.

Magenheim A. J., Spivack A. J., Michael P. J. and Gieskes J. M., 1995, Chlorine stable isotope composition of the oceanic crust: Implications for earth’s distribution of chlorine. EPSL. 131. 427-432.

Magna T., Wiechert U.H. and Halliday A.N., 2004. Low-blank isotope ratio measurement of small samples of lithium using multiple-collector ICPMS. Inter. Jour. Mass Spect. 239, 67-76.

McCaffrey M.A., Lazar B. and Holland H.D., 1987. The evaporation path of seawater and the coprecipitation of Br and K with halite. J. Sediment. Res. 57, 928– 37.

Michel A. and Villemant B., 2003. Determintion of halogens (F, Cl, Br, I), sulfur and water in seventeen geological reference materials. Geostandards Newsletter 27, 163-171.

Millot R., Negrel P. and Petelet-Giraud E., 2007. Multi-isotopic (Li, B, Sr, Nd) approach for geothermal reservoir characterization in the Limagne Basin (Massif Central, France). Appl. Geochem. 22, 2307-2325.

Millot R., Scaillet B. and Sanjuan B., 2010. Lithium isotopes in island arc geothermal systems: Guadalupe, Martinique (French West Indies) and experimental approach. Geochim. Cosmochim. Acta 74, 1852-1871.

Millot R., Hegan A. and Negrel P., 2012. Geothermal waters from the Taupo Volcanic Zone, New Zealand: Li, B and Sr isotopes characterization. Appl. Geochem. 27, 677-688.

Moriguti T. and Nakamura E., 1998. High-yield lithium separation and the precise isotopic analysis for natural rock and aqueous samples. Chem. Geol. 145, 91-104.

Mortimer N., 1994. Origin of the Torlesse terrane and coeval rocks, North Island, New Zealand. International Geology Review 36, 891-910.

Nahnybida T., Gleeson S.A, Rusk B. and Wassenaar L., 2009. Cl/Br ratios and stable chlorine isotope analysis of magmatic-hydrothermal fluid inclusions from Butte, Montana and Bingham Canyon, Utah. Miner Deposita 44, 837-848.

Nair I. A., Hedenquist J. W., Villamor P., Berryman K. R. and Shane P. A., 2005. The A.D. 1315 Tarawera and Waiotapu eruptions, New Zealand: contemporaneous rhyolite and hydrothermal eruptions driven by an arrested basalt dike system?. Bull. Volcanol. 67, 186-193.

Qi H.P., Taylor P.D.P., Berglund M. and De Bievre P., 1997. Calibrated measurements of the isotopic composition and atomic weight of the natural Li isotopic reference material IRMM-016. Intern. Jour. Mass Spect. 171, 263-268.

Reyes, A.G., Trompetter, W.J., 2012. Hydrothermal water-rock interaction and the redistribution of Li, B and Cl in the Taupo Volcanic Zone, New Zealand. Chem. Geol. doi: 10.1016/j.chemgeo.2012.05.002.

Reyners M., Eberhart-Phillips D. and Stuart G., 2007. The role of fluids in the lower-crustal earthquakes near continental rifts. Nature. 446: 1075-1078. Doi: 10.1038.

Rittenhouse G., 1967. Bromine in oil-field waters and its use in determining possibilities of origin of these waters. AAPG Bulletin 51, 2430–40.

Robinson B. W. and Sheppard D. S., 1986. A chemical and isotopic study of the Tokaanu-Waihi geothermal area, New Zealand. J. Volcanol. Geoth. Res. 27, 135-151.

Rosenberg M. D., Bignall G. and Rae A. J., 2009. The geological framework of the Wairakei-Tauhara geothermal system, New Zealand. Geothermics 38, 72-84.

Rowland J. V., Wilson C.J.N. and Gravley D. M., 2010. Spatial and temporal variations in magma-assisted rifting, Taupo Volcanic Zone, New Zealand. J. Volcanol. Geoth. Res. 190, 89-108.

Sanjuan B., Michard G., Michard A., 1990. Origine des substances dissoutes das les eaux des sources thermals et des forages de la région Asal Ghoubbet (République de Djibouti). J. Volcanol. Geoth. Res 43:333-352.

Scott G. L., 1989. Magmatic chloride and metals in fluids, Tongonan geothermal field, Philippines. J. Volcanol. Geoth. Res. 38, 355-360.

Schilling J. G., Unni C. K., Bender M. L., 1978. Origin of chlorine and bromine in the oceans. Nature 273, 631-636.

Sharp Z. D., Barnes J. D., Brearley A. J., Chaussidon M., Fischer T. P., Kamenetsky V. S., 2007. Chlorine isotopes homogeneity of the mantle, crust and carbonaceous chondrites. Nature 446, 1062-1065.

Sharp Z. D., Barnes J. D., Fischer T. P. and Halik M., 2009. An experimental determination of chlorine isotope fractionation in acid systems and applications to volcanic fumaroles. Geochim. Cosmochim. Acta 74, 264-273.

Sharp Z., Mercer J., Jones R., Brearley A., Selverstone J. Bekker A. and Stachel T., 2013. The chlorine isotope composition of chondrites and Earth. Geochim. Cosmochim. Acta 107, 189-204.

Shinonaga T., Ebihara M., Nakahara H., Tomura K. and Heumann K. G., 1994. Cl, Br and I in igneous standard rocks. Chem. Geol. 115, 213-225.

Supri S., 2000. Assessment of fault fractures at the Mokai geothermal field, Taupo Volcanic Zone, New Zealand. Proceedings World Geothermal Congress 2000. 1771-1776.

Taylor J. W. and Grimsrud E. P., 1969. Chlorine isotopic ratios by negative ion mass spectrometry. Anal. Chem. 41, 805-810.

Teng F.Z., McDonough W.F., Rudnick R.L., Walker R.J. and Sirbescu M.L.C., 2006. Lithium isotopic systematics of granites and pegmatites from the Black Hills, South Dakota. Amer. Miner. 91, 1488-1498.

Tomascak P. B., 2004. Developments in the understanding and application of Lithium isotopes in earth and planetary sciences. Rev. Mineral. Geochem. 55, 153-195.

Vigier, N., Decarreau, A., Millot, R., Carignan, J., Petit, S., France-Lanord, C., 2008. Quantifying Li isotope fractionation during smectite formation and implications for the Li cycle. Geochim. Cosmochim. Acta. Et Cosmochim. Acta. 72: 780-792.

Walter L.M., Stueber A.M., Huston T.J., 1990. Br–Cl–Na systematics in Illinois basin fluids - constraints on fluid origin and evolution. Geology 18, 315–8.

Wallace, L.M., Beavan, J., McCaffrey, R. and Darby, D.J., 2004. Subduction zone coupling and tectonic block rotations in the North Island, New Zealand. J. Geophys. Res. 109, B12406. doi:10.1029/2004JB003241.

Wallace P. J., 2005. Volatiles in subduction zone magmas: concentration and fluxes based on melt inclusion and volcanic gas data. J. Volcanol. Res. 140, 217-240.

Wassenaar L. I. and Koehler G., 2004. On-Line technique for the determination of the δ^{37}Cl of inorganic and total organic in environmental samples. Anal. Chem. 76, 6384 – 6388.

Webster J. Tappen C. and Mandeville C., 2009. Partitioning behavior of chlorine and fluorine in the system apatite-melt-fluid. II: Felsic silicate system at 200 MPa. Geochim. Cosmochim. Acta 73, 559-581.

Wilson C. J. N. and Rowland J. V., 2011. Volcanological and tectonic insights into geothermal systema in the central Taupo Volcanic Zone, New Zealand. New Zealand Geothermal Workshop 2011.

Wilson C. J. N., Houghton B. F., McWilliams M. O., Lanphere M.A., Weaver S. D. and Briggs R. M., 1995. Volcanic and structural evolution of Taupo Volcanic Zone, New Zealand: a review. J. Volcanol. Geotherm. Res. 68, 1-28.

Wood C. P., 1992. Geology of the Rotorua geothermal system. Geothermics, N0. 1/221:25-41.

Wood P. C., 1994. Aspects of the geology of Waimangu, Waiotapu, Waikite and Reporoa geothermal systems, Taupo Volcanic Zone, New Zealand. Geothermics 23. N0 5/6: 401-421.

Wood C. P., 1996. Basement geology and structure of TVZ geothermal field, New Zealand. Proceedings 18th NZ Geothermal Workshop 1996. 157-162.

Wood C. P. and Brathwaite R. L., 1999. The basement at Kawerau geothermal field. 21st New Zealand Geothermal Workshop 1999. 101-106.

Zhang M. and Nordstrom D., 2004. Stable chlorine composition of geothermal waters from Yellowstone National Park. Proceedings of the Eleventh International Symposium on Water-Rock Interaction, 27 June-2 July 2004, Saratoga Springs.

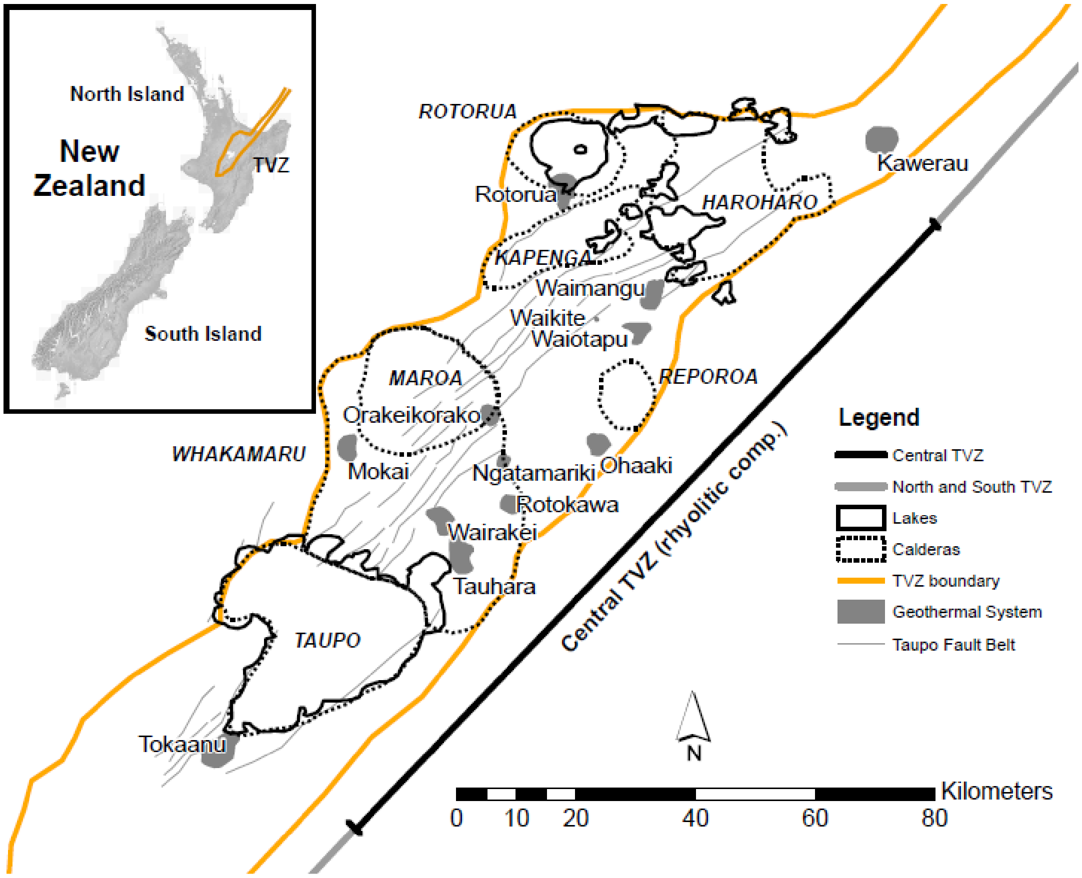

Figure 3-1 Locations of the geothermal sites.
Taupo Volcanic Zone (TVZ). Modified from Kissling and Weir (2005).

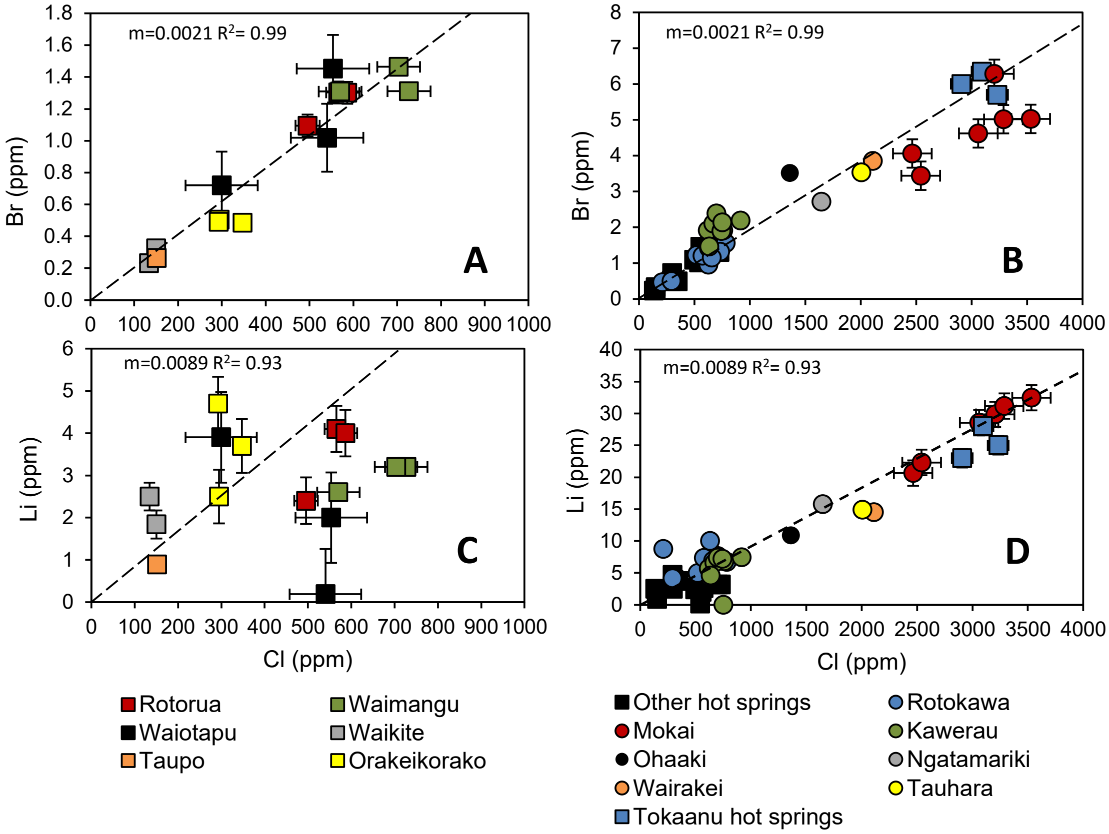

Figure 3-2 Distribution of Cl, Br and Li in hot springs (A and C) and well samples (B and D).

The Tokaanu hot springs are plotted with the well data in order to allow a better spatial definition for the rest of the hot spring samples. Trendlines are represented by dashed lines, the slope (m) and R^2 values are included. The trendline, m and R^2 values defined for the well samples (3.2D) are shown in C to highlight the differences in Li assimilation between low and high temperature hydrothermal alteration associated with hot springs and deep geothermal fluids.

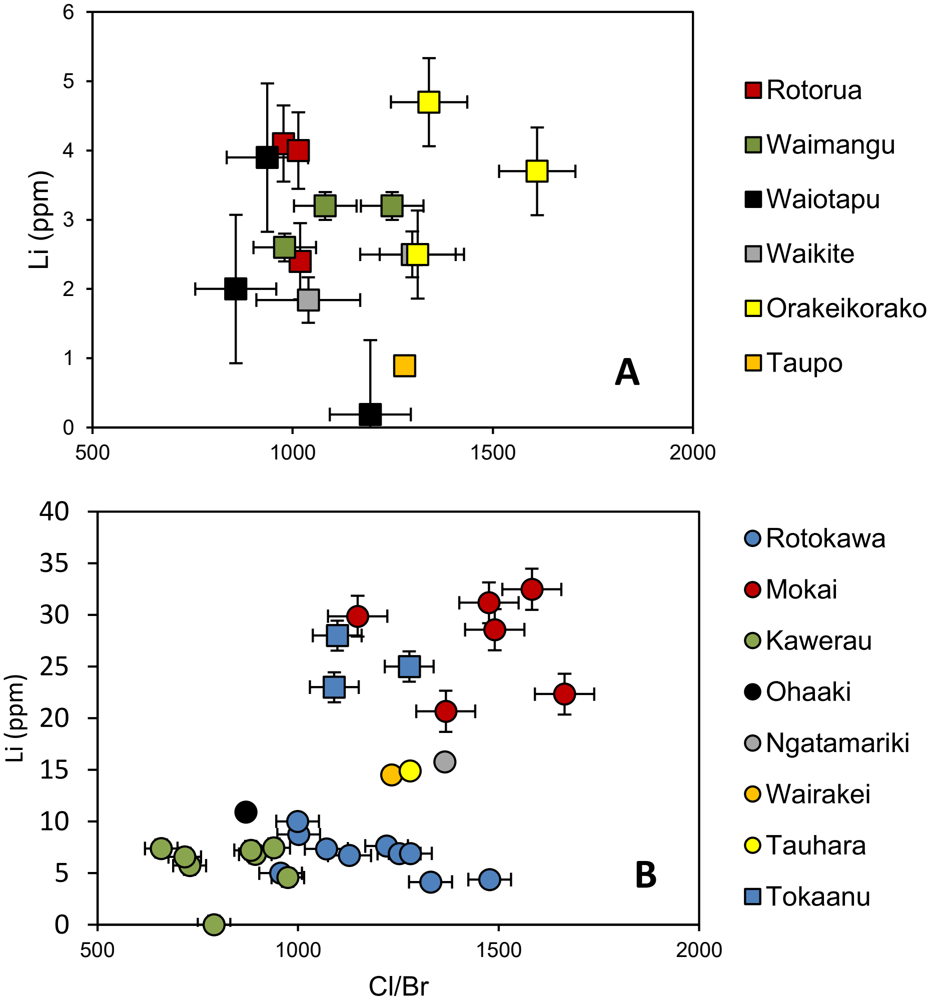

Figure 3-3 Cl/Br molar ratios vs. Li concentrations.
Hot springs (A) and geothermal wells (B). The Tokaanu hot springs are plotted along with the geothermal wells.

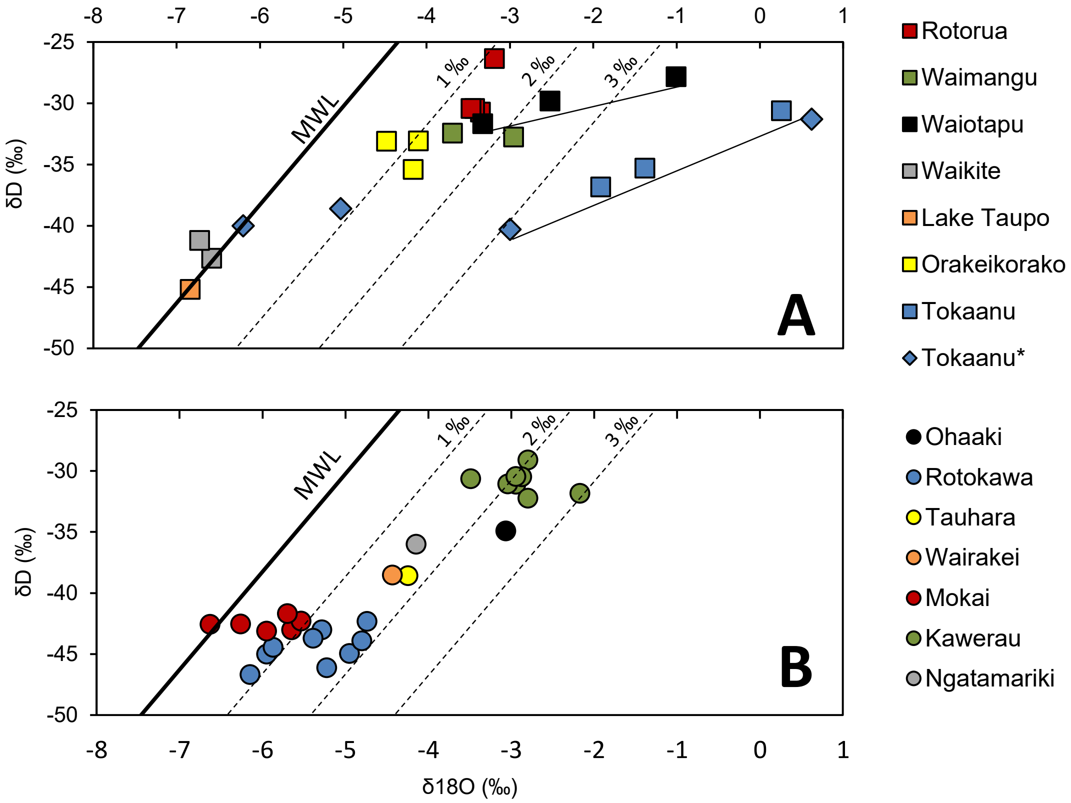

Figure 3-4 $\delta^{18}O$ vs δD values of the hot springs (A) and geothermal well samples (B). Solid lines represent evaporation trends and dashed lines depict the $\delta^{18}O$ shift representing water-rock interaction. *Data from Giggenbach (1996).

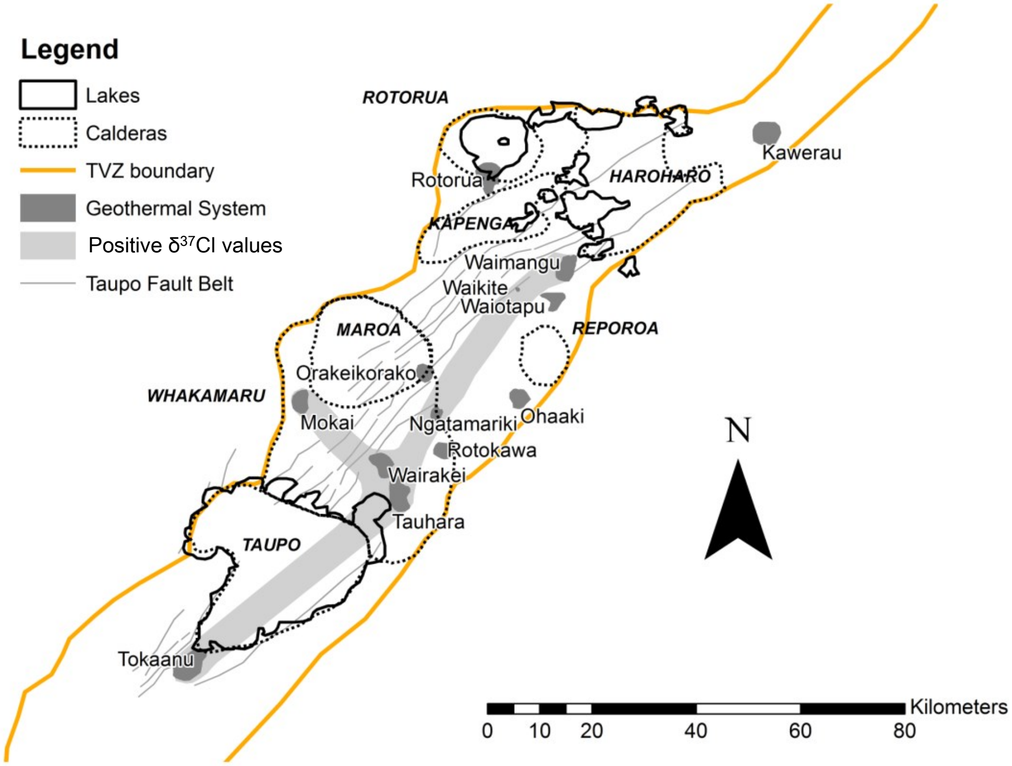

Figure 3-5 Map of the central TVZ.
Distribution of positive δ^{37}Cl values detected in the geothermal systems: Tauhara, Wairakei, Mokai, Ngatamariki, Waikite, Waimangu and Tokaanu, related to rhyolitic magmatism. The other geothermal systems: Rotokawa, Ohaaki, Kawerau, Rotorua and Orakei Korako are characterized by negative δ^{37}Cl values, related to andesitic magmatism. After Kissling and Weir (2005).

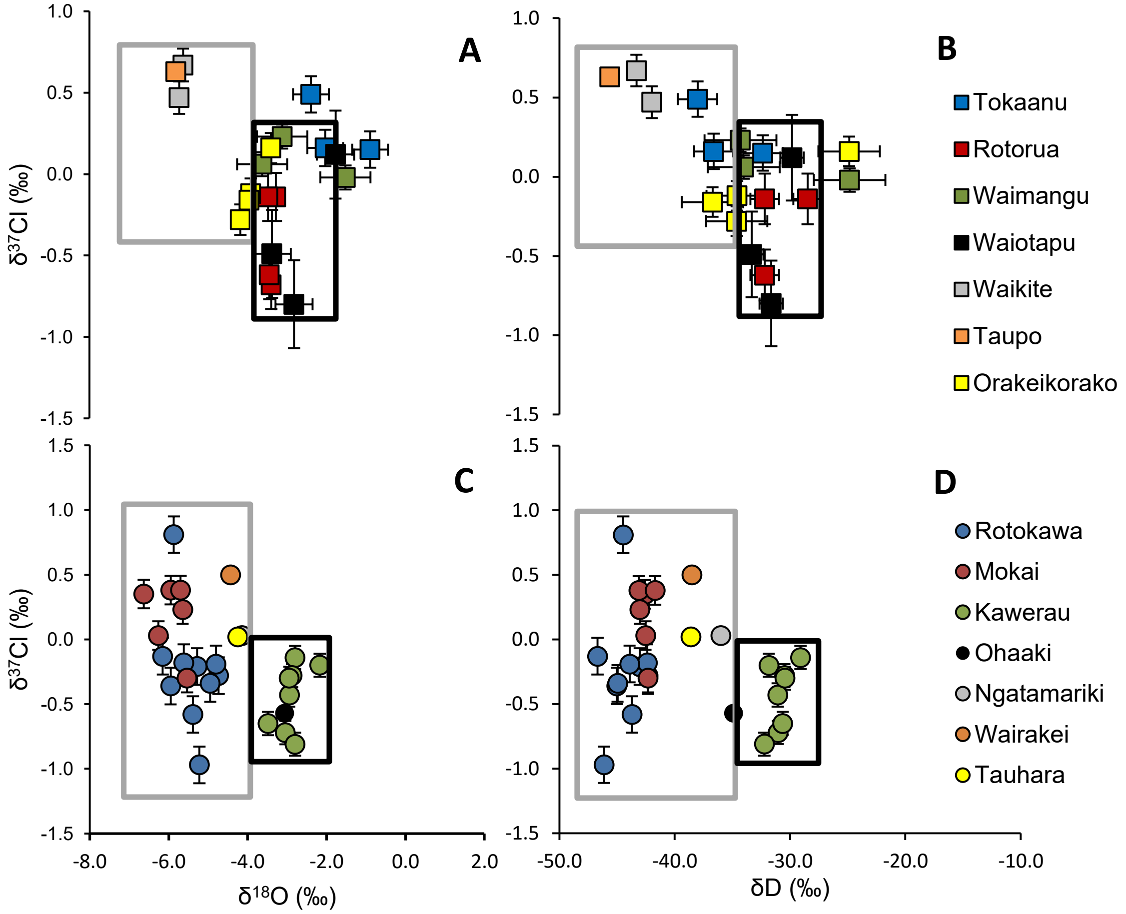

Figure 3-6 $\delta^{18}O$ and δD values vs. $\delta^{37}Cl$ values in per mil units (‰).
Diagrams A and B represent the isotopic values for hot springs and diagrams C and D are for well samples. The grey box encloses the samples associated with the recharge area to the SW and the black box includes the samples related to the recharge area to the NE in the TVZ.

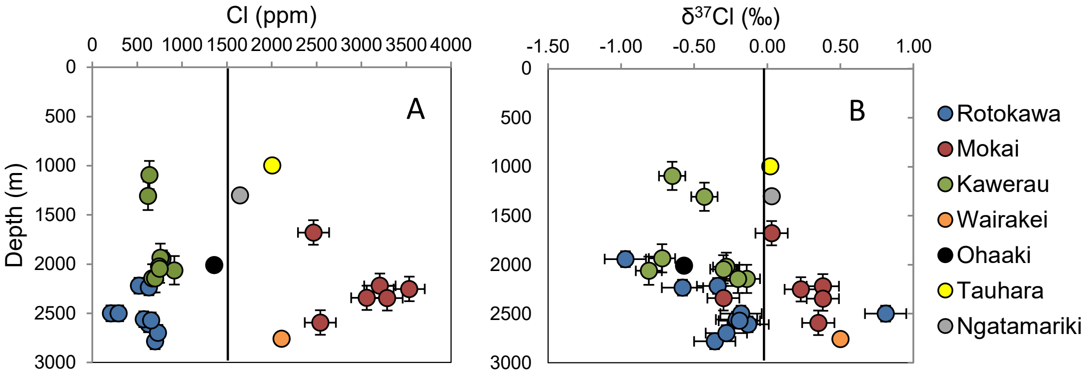

Figure 3-7 Distribution of Cl and δ^{37}Cl with depth

A) Distribution of chloride (ppm) vs depth and B) δ^{37}Cl vs depth in geothermal wells.

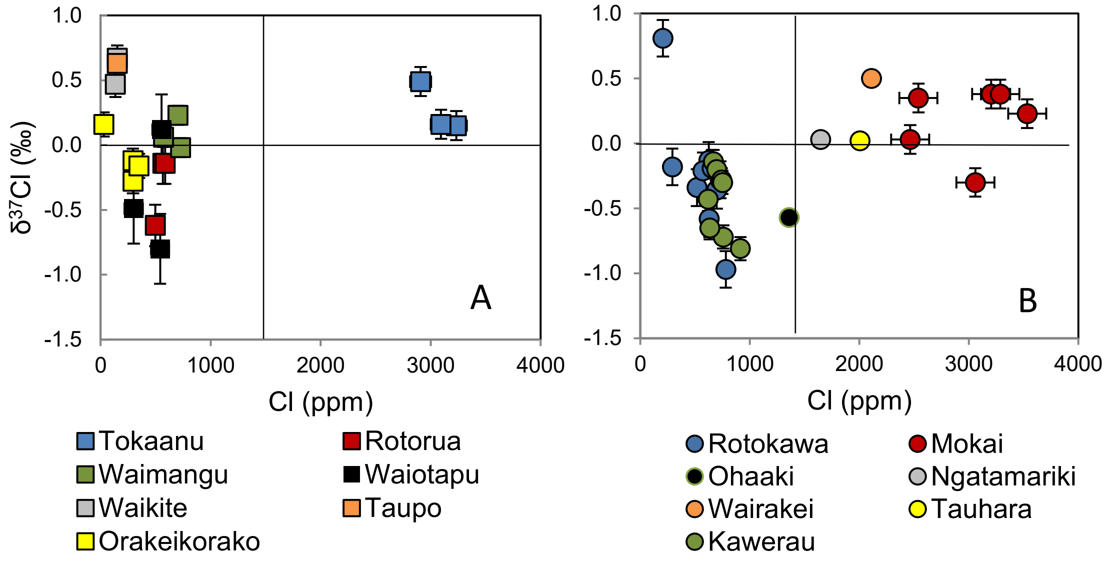

Figure 3-8 Cl concentration vs. δ^{37}Cl in hot springs (A) and geothermal wells (B).

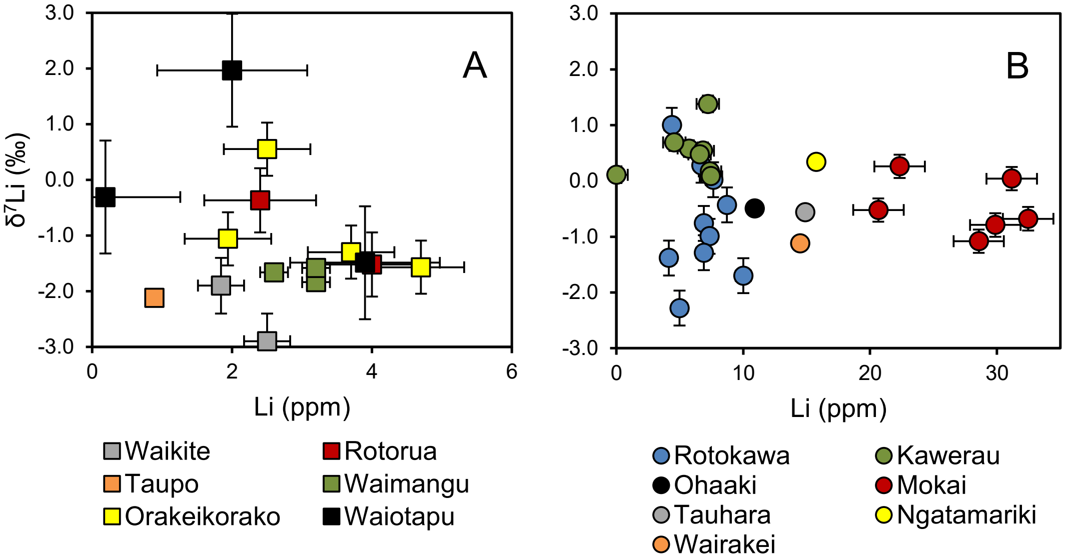

Figure 3-9 Lithium concentrations plotted against δ^7Li values.
Hot springs (A) and geothermal well samples (B). The Tokaanu samples were excluded from this diagram due to their high Li contents (23 to 25 ppm).

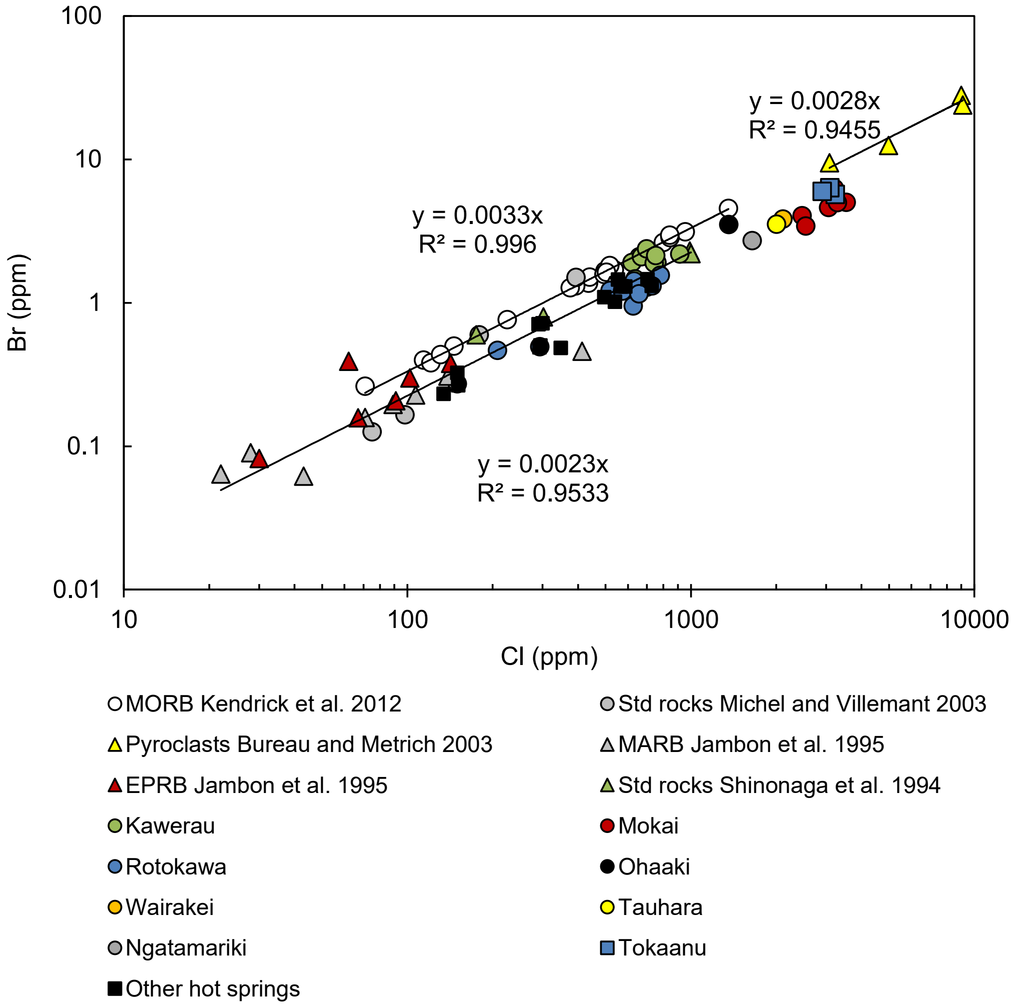

Figure 3-10 Compilation of Cl and Br data in basalts and rhyolites.
Igneous standard rocks from Shinonaga et al. (1994). MARB and EPRB glasses from Jambon et al. (1995) and references therein. Rock standards from Michel and Villemant (2003). Volcanic rocks from Bureau and Metrich (2003). Macquarie Island MORB glasses from Kendrick et al. (2012). TVZ geothermal wells and hot spring data from this study.

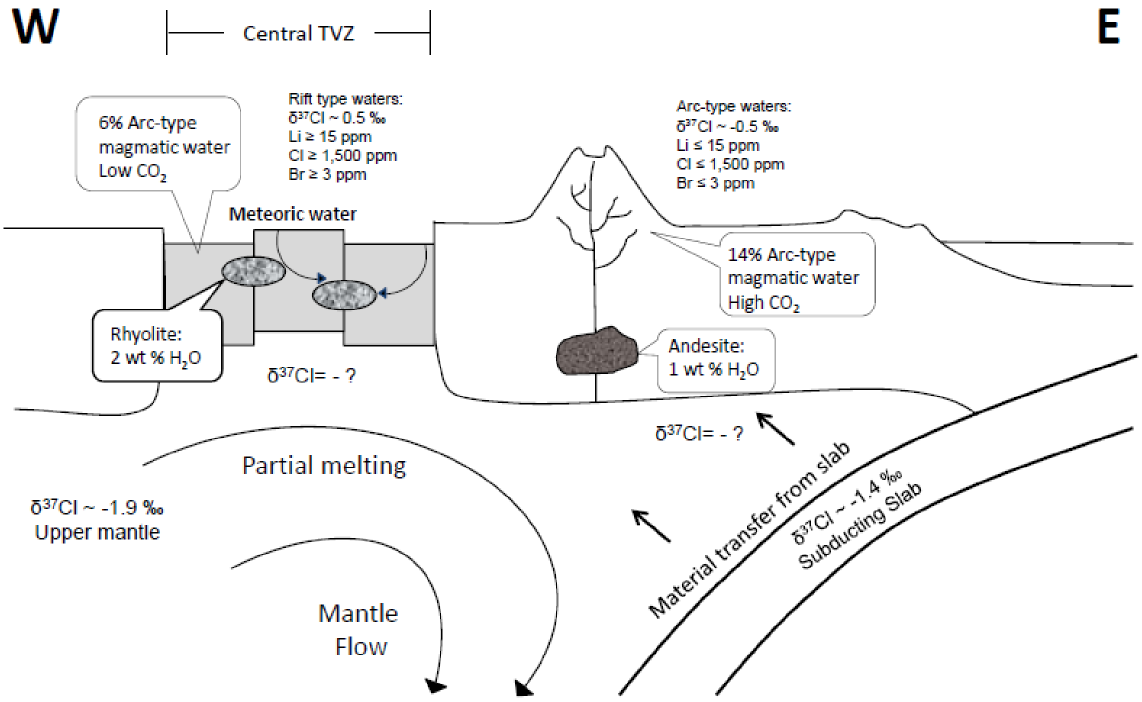

Figure 3-11 Schematic cross section W-E of the TVZ.
Front-arc, back-arc and subducting slab under North Island, New Zealand. Modified from Giggenbach (1995). δ^{37}Cl values for the subducting slab and the upper mantle after Bonifacie et al., (2008a) and Bonifacie et al., (2008b), respectively.

Table 3-1 Chemistry and stable isotope composition of geothermal waters.
Location, name, associated magmatism, sampling temperature, pH, TDS, Cl, Br, Li, Cl/Br molar, δD, δ^{18}O, δ^{37}Cl and δ^{7}Li values of the hot springs (Table 3-1a) and geothermal well samples (Table 3-1b) analyzed.

(a) Geothermal Site	Hot Spring Name	Associated Magmatism	Sampling T (°C)	pH	TDS (ppm)	Cl (ppm)	Br (ppm)	Li (ppm)	Cl/Br molar	δD (‰)	δ^{18}O (‰)	δ^{37}Cl (‰)	δ^{7}Li (‰)
Rotorua	Te Puia - cooking pool spring	Arc	95.2	7.6	1122	496	1.10	2.4	1019	-30	-3.4	-0.6	-0.4
	Te Puia - The blueys	Arc	17.3	9.8	1362	566	1.30	4.1	977	-26	-3.2	-0.1	n.a.
	Te Puia - Pohutu geyser pool	Arc	55.0	6.0	1362	586	1.30	4.0	1014	-30	-3.5	-0.1	-1.5
Waimangu	Frying pan lake river	Arc	49.5	5.7	1350	727	1.31	3.2	1249	-22	-0.6	0.0	-1.8
	Super-heated spring	Arc	94.0	8.4	1302	570	1.31	2.6	980	-32	-3.7	0.1	-1.7
	Geyser	Arc	93.4	7.6	1416	703	1.46	3.2	1081	-33	-3.0	0.2	-1.6
Waiotapu	Champagne pool	Arc	75.4	5.1	954	300	0.72	3.9	937	-32	-3.3	-0.5	-1.5
	Frying pan flat spring	Arc	93.8	2.1	2892	540	1.02	0.2	1194	-30	-2.5	-0.8	-0.3
	Oyster pool	Arc	64.9	4.8	1380	554	1.45	2.0	858	-28	-1.0	0.1	2.0
Tokaanu	Takarea no.5 spring pool	Arc	56.2	5.7	5418	3233	5.70	25.0	1277	-31	0.3	0.2	-0.8
	Hoani B spring pool	Arc	80.5	6.6	5328	3094	6.34	28.0	1098	-35	-1.4	0.2	-0.3
	Taumatapuhipuhi geyser pool	Arc	88.5	7.4	5094	2908	6.00	23.0	1090	-37	-1.9	0.5	-0.3
Waikite	Te Manaroa spring	Rift	86.6	7.5	666	150	0.33	1.8	1039	-43	-6.6	0.7	-1.9
	Waikite pools inlet spring	Rift	97.6	7.7	558	134	0.23	2.5	1299	-41	-6.7	0.5	-2.9
Tauhara/Wairakei	Lake Taupo rocky point spring	Rift	66.0	6.3	606	151	0.27	0.9	1280	-45	-6.8	0.6	-2.1
Orakei Korako	Devil's throat spring	Rift	96.8	2.4	240	295	0.51	2.5	1312	-33	-4.5	-0.3	0.6
	Fred & Maggie's spring pool	Rift	96.8	6.7	906	292	0.49	4.7	1341	-33	-4.1	-0.1	-1.6
	Ruatapu cave pool	Rift	36.4	2.4	630	27	n.a.	1.9	n.a.	-22	-3.4	0.2	-1.1
	Diamond geyser pool	Rift	87.0	7.0	888	347	0.49	3.7	1611	-35	-4.2	-0.2	-1.3

(b) Geothermal Site	Well ID	Associated Magmatism	Sampling T (°C)	pH	TDS (ppm)	Cl (ppm)	Br (ppm)	Li (ppm)	Cl/Br molar	δD (‰)	δ^{18}O (‰)	δ^{37}Cl (‰)	δ^{7}Li (‰)
Ohaaki	BR61	Arc	n/a	8.6	3108	1650	4.27	13.0	870	-35	-3.1	-0.6	-0.5
Rotokawa	RK 01	Arc	234.4	6.5	1266	700	1.29	7.6	1220	-45	-6.0	-0.4	0.0
	RK 02	Arc	233.6	6.4	702	625	0.95	4.4	1478	-47	-6.2	-0.1	1.0
	RK 03	Arc	226.6	6.4	1374	208	0.47	8.7	1002	-44	-5.9	0.7	-0.4
	NAP 01	Arc	229.4	6.4	3852	781	1.56	6.7	1128	-46	-5.2	-1.0	0.3
	NAP 02	Arc	231.3	6.2	1272	730	1.31	6.9	1252	-42	-4.7	-0.3	-0.8
	NAP 03	Arc	224.3	6.6	1182	518	1.22	5.0	956	-45	-5.0	-0.3	-2.3
	NAP 04	Arc	226.4	6.7	1392	574	1.21	7.3	1071	-43	-5.3	-0.2	-1.0
	NAP 05	Arc	182.0	7.5	1128	293	0.50	4.1	1330	-42	-5.6	-0.2	-1.4
	NAP 06	Arc	227.3	6.1	1284	630	1.42	10.0	999	-44	-5.4	-0.6	-1.7
	NAP 07	Arc	230.4	6.1	1284	657	1.16	6.9	1280	-44	-4.8	-0.2	-1.3
Kawerau	KA 01	Arc	191.1	8.2	1482	620	1.91	5.7	730	-31	-2.9	-0.4	0.6
	KA 02	Arc	204.5	7.6	1554	758	1.91	6.8	893	-31	-3.0	-0.7	0.5
	KA 03	Arc	205.5	7.6	1530	669	2.10	6.6	718	-29	-2.8	-0.1	0.5
	KA 04	Arc	184.2	7.7	1224	635	1.47	4.6	974	-31	-3.5	-0.7	0.7
	KA 05	Arc	196.0	6.8	1716	699	2.39	7.4	659	-32	-2.2	-0.2	0.2
	KA 06	Arc	210.8	6.1	1584	915	2.19	7.5	940	-32	-2.8	-0.8	0.1
	KA 07	Arc	213.6	6.5	1422	742	1.89	7.2	882	-30	-2.9	-0.3	1.4
	KA 08	Arc	247.0	5.5	1374	751	2.14	0.0	790	-30	-2.9	-0.3	0.1
Tauhara	TH14	Rift	n/a	8.7	3936	2366	4.16	18.0	1279	-39	-4.2	0.0	-0.6
Wairakei	WK247	Rift	n/a	8.5	4398	2514	4.59	17.0	1233	-39	-4.4	0.5	-1.1
Mokai	MK 01	Rift	217.0	3.6	3072	2465	4.06	20.7	1368	-43	-6.3	0.0	-0.5
	MK 02	Rift	211.1	6.3	3564	2541	3.44	22.3	1664	-43	-6.6	0.4	0.3
	MK 03	Rift	213.2	4.7	4296	3206	6.28	29.9	1149	-43	-6.0	0.4	-0.8
	MK 04	Rift	214.9	5.4	4218	3508	5.02	32.5	1583	-43	-5.6	0.2	-0.7
	MK 05	Rift	212.8	4.5	4146	3014	4.62	28.6	1490	-42	-5.5	-0.3	-1.1
	MK 06	Rift	212.6	4.5	4596	3254	5.01	31.2	1476	-42	-5.7	0.4	0.0
Ngatamariki	NG 01	Rift	n/a	8.3	2208	1647	2.71	15.8	1366	-36	-4.1	0.0	0.3

4 The origin and the effects of phase separation on the halogen compositions of magmatic-hydrothermal fluids from the Butte Porphyry-Copper Deposit: constraints from Cl/Br molar ratios and the δ^{37}Cl values of fluid inclusion leachates.

4.1 Introduction

The range of isotopic fractionation of the stable Cl isotopes in the crust, from -8‰ to +12‰ (Gleeson and Smith, 2009; Barnes et al. 2009), is relatively narrow compared to other stable isotope systems. Due to improved analytical techniques, there is a growing literature on the behaviour of the stable Cl isotopes in the upper mantle and the oceanic crust (Magenheim et al. 1995, Barnes and Sharp 2004, Barnes et al. 2008, Bonifacie et al. 2007, Bonifacie et al. 2008a, Bonifacie et al. 2008b, Layne et al. 2009). Although these studies have contributed to the understanding of the distribution of the stable chlorine isotopes in the crust and the upper mantle, there is little known about the behaviour of these isotopes in hydrothermal systems. Hydrothermal activity is important as it is involved in heat and mass transfer between the upper mantle, lower and upper crust (Hedenquist and Lowenstern, 1994; Williams-Jones and Heinrich, 2005).

Chloride is a dominant anion in magmatic hydrothermal systems. It is a conservative element in many high temperature geological environments and has the capacity to complex ore metals (Helgeson, 1964; Seward and Barnes, 1997). As documented in the literature, the Cl and Br concentrations in fluid inclusions, have the potential to help in the identification of volatile sources in the crust (e.g. Bölke and Irwin 1992, Irwin and Roedder 1995, Kendrick et al. 2001, Yardley et al. 2000; Nahnybida et al. 2009).

In the case of Porphyry Copper Deposits (PCDs), the characterization of parental magmatic hydrothermal fluids is essential to model the physical and chemical processes that form the deposits (Rusk et al. 2008a). However, currently, in magmatic hydrothermal systems such as Porphyry Copper Deposits (PCDs), the processes that may fractionate the Cl isotopes (e.g. phase separation and mixing) during the ascent of the fluid from the porphyry to higher levels in the system are still to be defined. In theory, Cl/Br molar ratios and stable Cl isotopes can be used to track the evolution of magmatic hydrothermal fluids, from magmatic segregation through phase separation and into the low temperature and distal expressions of the hydrothermal system, but such studies have not been carried out until now.

In the earliest study of its kind, Böhlke and Irwin (1992) investigated the Cl, Br, I and K composition of fluid inclusions from some PCDs by laser microprobe noble gas mass spectrometry. This study identified clear differences in Cl/Br/I ratios, which were interpreted by the authors to be characteristic of individual PCDs. The reasons for these differences in Br/Cl and I/Cl molar ratios were not explained by Böhlke and Irwin (1992), but the data demonstrated that the halogen molar ratios had potential for characterizing magmatic-hydrothermal fluids. Kendrick et al. (2001), used noble gas mass spectrometry to obtain the halogen composition of vein samples from Bingham Canyon, Silver Bell, Ray, Mission, Pinto Valley, and Globe-Miami (Arizona) PCDs. This study identified a high salinity fluid composed of a mixture of crustal and mantle fluids in samples from the potassic and propylitic alteration zones in all the PCDs analyzed.

Few studies have applied stable Cl isotopes to PCDs. An early study by Eastoe et al. (1989) analysed δ^{37}Cl values in four deposits: Bingham (Utah), Silver Bell (Arizona), El Salvador (Chile), and Panguna (Papua New Guinea). Chlorine was extracted from 250 to 500 g of early and late quartz veins using a crush and leach technique (resulting in mixed Cl from several fluid inclusion generations). This work concluded that positive δ^{37}Cl values (0.8 ‰ and 0.3 ‰) and negative δ^{37}Cl values (-1.1‰ and -0.7 ‰) were found in high and low salinity brines, respectively. The origin of the salinity in these deposits was attributed to magmatic sources, but the other processes that may fractionate the Cl isotopes were not addressed in this study. Nevertheless, this was an important contribution in the sense that it demonstrated that δ^{37}Cl values could be determined in fluid inclusion leachates. Eastoe and Guilbert (1992), using an improved precision of ± 0.2 ‰ for the δ^{37}Cl analysis, investigated the isotopic composition of fluid inclusions and biotites from Bingham Canyon, Silver Bell and Panguna. In this study, the range of δ^{37}Cl values measured in hydrothermal fluids was -1.0 to 0.5 ‰ and 0.3 to 1.7 ‰ in biotite. A negative δ^{37}Cl value measured in a vein from Bingham Canyon was interpreted as condensation of a ^{35}Cl enriched aqueous vapor. Despite the narrow variation in Cl isotopes, the higher precision obtained for the δ^{37}Cl analyses, allowed for the first discussion of possible fractionation mechanisms in high temperature geological processes. Nahnybida et al. (2009), analyzed a set of fluid inclusion samples from the Butte deposit and found that the Br/Cl elemental ratios were similar, but that the stable Cl isotopes measured in these samples had delta values from -0.8 to -2.3 ‰, which were interpreted to indicate the presence of a magmatic source with a negative δ^{37}Cl signature. Fluid inclusion leachate samples from Bingham Canyon, were also analyzed in order to determine Br/Cl molar ratios and stable Cl isotopic compositions. Negative δ^{37}Cl values (-0.9 to -4.1 ‰) and halogen molar ratios overlapping mantle values were identified in Bingham Canyon.

In this study, we analyse the halogen (Cl and Br) composition and stable Cl isotope ratios of fluid inclusions trapped at different structural levels in the Butte PCD, Montana. This allowed us to characterize the halogen compositions in most of the vein types in the deposit and to determine if the isotopic signature of the magmatic-hydrothermal fluids was modified after temperature, pressure and fluid composition variations. The Butte deposit was selected for this work for several reasons. Firstly, it is one of the deepest PCDs in the worldand formed from 5 to 9 km depth (Roberts 1975; Rusk et al. 2008a) and its geology is well constrained. Secondly, the most comprehensive fluid inclusion microthermometric study published has been carried out on the veins (over 5,000 inclusions were analysed; Rusk et al. 2008a); therefore, the samples are unusually well characterised. Thirdly, previous work has suggest that all the vein generations and alteration assemblages at Butte can be explained by the evolution of a single parental magmatic-hydrothermal fluid (Rusk et al. 2008a) and therefore, the system is ideal for assessing the effect of physical processes such as phase separation on the halogen compositions.

It has been established that Cl fractionates into the H_2O-bearing vapor phase during basaltic magma decompression as magma moves to shallower depths in the crust (Alletti et al. 2009), but the source and evolution of Cl-rich fluids in high temperature mineralizing systems is not well understood. Experiments on processes that may affect halogen distributions in hydrothermal fluids, such as phase separation, have been controversial. Published results at comparable conditions of pressure and temperature are in disagreement, probably due to different experimental conditions and the composition of the working solutions (e.g. Berndt and Seyfried, 1990; Liebscher et al. 2006). Therefore, the distribution of halogens in the vapor and liquid phases during phase separation of a supercritical fluid is still unknown. On the other hand, the effects of phase separation can also influence the stable Cl isotopes. Volcanic fumaroles in the Central American Arc System are characterized by high δ^{37}Cl values (4 to 12‰) due to a distillation process which removes $H^{35}Cl$ from the steam, indicating the presence of a boiling aqueous system (Sharp et al. 2009). However, it is unknown if similar processes operate at higher conditions of pressure and temperature and/or if such changes can be used as markers or indicators of favorable conditions for mineral precipitation in magmatic-hydrothermal systems. Our work explores different scenarios to explain the observed variations in Cl/Br molar ratios and δ^{37}Cl values at Butte. We compare the results from the Butte PCD to some new data on steam condensates from three active geothermal systems (Rotokawa, Mokai and Kawerau), located in the North Island of New Zealand, in order to facilitate a discussion on the potential effects of phase separation on the isotopic data. Based on these data, we elaborate on the mechanisms that may have been responsible for the mineralization of the Butte PCD.

4.2 Regional and property Geology

4.2.1 Butte, Montana

The Butte deposit is located in southwest Montana, some 100 km west of the Belt Mountains (Figure 4.1). Regionally, the geology in the area is characterized by the occurrence of the Boulder batholith of western Montana, which is hosted by sedimentary rocks of Middle Proterozoic to Mesozoic age (Lund et al. 2002). The Butte Granite (Lund et al. 2002; Dilles et al. 2003) is one of 15 plutons of the Boulder Batholith (Figure 4.1) that were emplaced during the Laramide orogeny (Lund et al. 2002). The Butte Granite is composed of medium to coarse grained plagioclase (40%), quartz (20%), orthoclase (20%) and hornblende and biotite (20%). The emplacement of the batholith has been dated to have occurred at 76.5 Ma (Czehura, 2006). There is evidence of volcanism in the Elkhorn Mountains, which is contemporaneous (74 to 81 Ma) with the intrusion of the Boulder Batholith and the formation of the Butte deposit (Smedes, 1966). However, owing to intense erosion and rapid uplift, volcanic units are not found at Butte (Smedes, 1966); it is thought that more than 7 km of rock has been eroded from above the Butte deposit (Houston and Dilles, 2013). The emplacement of the Boulder Batholith under the Elkhorn Mountains Volcanics has been recently proposed as a consequence of compressional tectonic conditions prevailing at the time of the intrusion (Houston and Dilles, 2013 and references therein).

The Butte Granite has been intruded by sills and dikes of aplitic, granoaplite and pegmatitic composition. These dikes were cut by the intrusion of a group of 66 Ma quartz porphyry dikes (Martin et al. 1999). The intrusion of these porphyry dikes occurred around 10 m.y. after the plutonic intrusion (Rusk et al. 2008a) and is associated with the generation of chalcopyrite-and pyrite biotitic breccias and mineralizing fluids.

The mineralization at Butte has been divided into two groups, pre-Main Stage and Main Stage (MS) (Figure 4.2A). The term pre-Main Stage refers to a dome-shaped zone of quartz-molybdenum veinlets and associated alteration assemblages (Figure 4.2B). The MS mineralization refers to large copper-rich veins that form the most economic part of the deposit (Meyer, 1968; Brimhall, 1977).

The MS mineralization, characterized by veins containing Cu, Zn, Pb, Ag, As and Mn, has been dated at 62 Ma (Snee et al. 1999). A breccia deposit named the Mountain View Breccia and a rhyolite dike dated at 58.8 Ma (Martin et al. 1999) cut the MS veins. A classification of the most commonly occurring veins at Butte has been documented in the past (Sales and Meyer, 1948; Meyer and Hemley, 1967; Meyer et al. 1968, Meyer, 1965; Roberts, 1975; Brimhall, 1977; Reed et al. 2001). In general, these studies identified five main vein types in the deposit: barren-quartz/quartz-molybdenite (BQ/QMB), Early Dark Micaceous (EDM), pale-green sericitic (PGS), gray sericitic (GS) and MS veins (Figure 4.2). These main vein types are assumed to originate as a consequence of the mobilization of Cu and Mo from a magma located deep in the crust, which is associated with low salinity hydrothermal fluids, as determined by fluid inclusion studies (Rusk et al. 2008a).

The Butte porphyry-copper mineralization is characterized by the occurrence of a potassic alteration zone composed of EDM and BQ/QMB veins, observed in the deepest drill holes intersecting the western side of the deposit, known as the Pittsmont Dome (Figure 4.2B). This alteration zone is also present to the east, where a deep normal fault, the Continental fault, uplifted the eastern portion of the Pittsmont dome some 1,250 m (Ratcliff, 1973, Rusk et al. 2008a). The mineralization in this part of the deposit is characterized by quartz, K-feldspar and chalcopyrite, and quartz veins with the highest grade molybdenite in the deposit.

Located at the top of the deposit, two alteration domes contain veins of quartz, chalcopyrite, magnetite and pyrite with K-feldspar, chlorite, quartz and PGS alteration envelopes, these veins extend to the east and west (Reed et al. 2013). BQ/QMB veins cut the EDM and the PGS veins. The MS mineralization is located above the zone known as the Anaconda dome, a dense group of veins in the N70ºE direction on the west bend located to the SE (Figure 4.2A). This group of veins vanishes in proximity to the pervasive quartz-sericite-pyrite alteration (Czehura, 2006).

According to Rusk et al. (2008a), several lines of evidence indicate that the parental mineralizing fluids at Butte had low salinities and were derived from a magmatic source with a relatively uniform chemical composition. The low salinity is recorded in fluid inclusions analyzed in early- and late-stage veins. In addition, pressure and temperature modelling of fluid inclusion data suggests that the Butte deposit was formed at depths between 5 and 9 km in the crust. This estimate was based on pressures of vein formation (200 to 250 MPa) inferred from trapping temperatures of B35 inclusions (Rusk et al. 2008a). This makes Butte the deepest formed PCD known.

4.2.2 Geothermal systems, Taupo Volcanic Zone

Fluids from the active geothermal systems: Rotokawa, Kawerau and Mokai, located in the Taupo Volcanic Zone (TVZ), North Island, New Zealand were also analyzed in this study. Andesitic and rhyolitic volcanism in the TVZ is a consequence of the subduction of the Pacific plate under the Australian plate, generating the TVZ and its intense volcanic activity (Wilson et al. 1995). According to Wilson and Rowland (2011), the Rotokawa and Kawerau geothermal systems are associated with an andesitic magmatic source located in the west margin of the TVZ, whilst the heat source of the

Mokai geothermal system, is thought to be related to the intense rhyolitic volcanism of the central TVZ. A more detail geological description can be found in Chapter 3 and references therein.

4.3 Sampled veins, fluid inclusions and geothermal fluids

Samples were obtained from barren quartz/quartz molybdenite veins from deep and moderate depth (BQ/QMB), pale green sericitic veins (PGS), gray sericitic veins (GS) and MS veins (MS) (Table 4.1).

4.3.1 Barren quartz and quartz-molybdenite veins (BQ/QMB)

Five quartz samples from depths of 1458 to 2588 m below surface (Figure 4.2A) were analyzed from deep barren quartz (BQ) and quartz molybdenite (QMB) veins. The BQ and QMB veins are differentiated by the amount of molybdenite they contain. Barren quartz veins can grade to QMB veins in just a few centimeters along the same structure, therefore, they are referred to as a single vein type (BQ/QMB). Purple anhydrite, K-feldspar, needles of rutile, and calcite are found in BQ/QMB veins. The molybdenite in QMB veins is banded and occurs parallel to quartz bands close to the margins of the veins. These veins cut the PGS and EDM veins at moderate depths. BQ/QMB veins are dominant in the deepest and hottest parts of the deposit, the potassic zone, are less common at intermediate depths and are rare at shallow depths (Rusk et al. 2008a).

4.3.2 Early dark micaceous veins (EDM)

The EDM veins comprise pyrite, chalcopyrite and magnetite and have alteration selvedges of K-feldspar, quartz, biotite, and sericite. The deep EDM veins crosscut deep BQ/QMB veins. At moderate and shallow depths in the deposit, wide alteration envelopes and the occurrence of chalcopyrite in the veins differentiate the EDM veins from other vein types. In the quartz rich core of the deposit, the EDM veins are quartz dominated, with rare chalcopyrite. Quartz dominated EDM veins contain some anhydrite, K-feldspar and molybdenite in the quartz-rich core of the deposit, the alteration envelopes are just a few mm width and include anhydrite, corundum, andalusite and plagioclase. The quartz in the veins has largely been attributed to overprinting events (Rusk and Reed, 2002) and is not a representative mineral in this vein generation.

No samples were analysed from this vein set in this study since most EDM veins are very thin and are not suitable for fluid inclusion studies.

4.3.3 Pale-green sericitic (PGS) veins

Four samples were analyzed from pale green sericitic (PGS) veins, one quartz, one pyrite and two magnetite samples. The PGS veins are common at moderate to shallow depths (1200 to 600 m) and are thought to be the vertical extension of the EDM vein type (Rusk et al. 2008). These veins contain magnetite, chalcopyrite, pyrite and quartz. The host rock around these veins is altered to an assemblage containing K-feldspar, quartz, green sericite, chlorite and minor calcite. The pale-green sericitic opaque content (magnetite, chalcopyrite and pyrite) can reach above 50 volume percent, and is higher than in EDM and QMB veins.

4.3.4 Gray sericitic (GS) veins

Five samples from gray serititic (GS) veins, four of them in quartz and one in pyrite, were analyzed. These veins are composed of pyrite and quartz with gray sericitic alteration. The alteration selvedges contain muscovite, quartz, pyrite and colorless chlorite. The GS veins are the most dominant vein type above the magnetite zone (which is defined by the abundant EDM and PGS veins). Quartz, sericite and pyrite alter the Butte Quartz Monzonite in the region between the Pittsmont and Anaconda domes and GS veins are also very common in the central zone of pervasive sericitic alteration located west of the Pittsmont dome (Figure 4.2).

4.3.5 Main stage (MS) veins

The MS veins are the youngest veins at Butte, they cross the deposit from the pervasive sericitic alteration zone to the NW and then bend to the SW (Figure 4.1). These veins can extend for kilometers and be several meters wide. The mineralogy of the veins changes gradually from a Cu-rich zone in the centre, to Cu-Zn in the middle and Mn, Pb, Zn and Ag mineralization in the external zone. In the region where this vein type occurs, the Butte Monzonite is altered to advanced argillic, sericitic and intermediate argillic assemblages. The fluid inclusions in MS veins were identified in quartz, fluorite, sphalerite and rhodocrosite (Table 4.1).

4.3.6 Fluid inclusion populations and characteristics of the samples analyzed

A classification of fluid inclusion types for the Butte deposit was developed by Rusk et al. (2008a) by describing the phases and their average volume percent present in the fluid inclusions at room temperature. For instance, a fluid inclusion classified as B20 indicates that a bubble (vapor) occupies 10 to 30% volume of the inclusion and has no halite daughter minerals. Similarly, vapor in B35 inclusions occupy 30 to 50% volume, B60 inclusions between 50 and 75% and B85 inclusions have more than 75% vapor. Some other fluid inclusion types described by Rusk et al. (2008a), include B15H, (inclusions that have a halite “H” daughter minerals at room temperature and 10 to 20 volume percent vapour content). According to this study, therefore, the following fluid inclusion types are found at Butte: B35, B60, B15H, B85, and B20.

The material analyzed was obtained from veins associated with the main alteration types at different depths. The fluid inclusion leachates were obtained from mineral separates hand-picked from the veins. The main purpose was to extract a leachate fluid representative of the dominant inclusion type in the sample. The fluid inclusion populations in the veins from the Butte deposit have been characterized by Rusk et al. (2004; 2008a). However, some fluid inclusions are common to all vein types, such as B60, B85 and B15H from moderate to shallow depths.

Salinity (wt% NaCl equiv.) of the fluid inclusions identified in the deposit are provided in Table 4.2 (Nahanybida, 2006 and Rusk et al. 2008a). The following section has a short description of each fluid inclusion type previously identified by Rusk et al. (2008a) from base to top of the deposit:

4.3.6.1 Fluid inclusion characteristics of BQ/QMB veins

The deepest BQ/QMB veins are characterized by over 90% B35 inclusions, with homogenization temperatures (Th) between 300 and 400 °C, salinities from 1 to 8 wt % NaCl equiv., 3 to 8 Mol % CO_2 and a density of 0.63 to 0.72 g/cm^3. The fluid inclusion population in BQ/QMB veins from moderate depths is dominated by B60 inclusions (50 to 80%). These inclusions homogenize to liquid, vapor and critically between 356 and 452 °C, have salinities from 1 to 7 wt % NaCl equiv., and contain 3 to 9 Mol % CO_2 and a density from 0.42 to 0.55 g /cm^3. These BQ/QMB veins formed at temperatures of 575 to 650 °C and pressures between 200 and 250 MPa, corresponding to depths from 6 to 9 km. Daughter minerals like K-feldspar, anhydrite, calcite and chalcopyrite were identified in B35 type fluid inclusions which are very common in BQ/QMB alteration veins.

For this study, nine samples from BQ/QMB veins from moderate depth were analyzed, all hosted by quartz veins.

4.3.6.2 Fluid inclusion characteristics of PGS veins

In PGS veins, B85 inclusions are dominant reaching 85% abundance, followed by B60 (35%), and B15H inclusion (< 7%). B85 inclusions homogenize from 370 to 520 °C, have salinities from 0 to 3 wt % NaCl equiv., 10 to 20 Mol % CO_2 and densities from <0.1 to 0.21 g/cm^3.

In the population of B15H inclusions analyzed, 72% of them homogenized between 175 and 412 °C, with salinities ranging from 30 to 48 wt % NaCl equiv. (average 38% NaCl equiv.), densities from 1.1 to 1.2 g/cm^3. These veins were formed at temperatures of 475 to 650 ºC and pressures between 50 and 90 MPa, corresponding to depths of 7 to 8 km. CO_2 was not detected in this inclusion type.

4.3.6.3 Fluid inclusion characteristics of GS veins

In GS veins B60 inclusions are abundant, (30 to 85%), other inclusion types like B35, B85 and B20 are present but below 30% abundance, BH15 inclusions are rare (Table 4.2). B20 inclusions homogenize from 195 to 400 °C with salinities ranging from 1 to 28 wt % NaCl equiv., at temperatures of 370 to 450 °C and pressures between 40 and 70 MPa corresponding to depths between 4 to 7 km, CO_2 was not detected in this inclusion type. The density of the fluids in this inclusion type is variable.

4.3.6.4 Fluid inclusion characteristics of MS veins

MS veins contain only B20 inclusions characterized by homogenization temperatures from 140 to 340 °C, salinities from 1 to 3.5 wt % NaCl equiv., a density of 0.9 g/cm^3 and less than 2 Mol % CO_2, at temperatures of 230 to 400 °C. The calculated pressures range between 20 and 60 MPa, corresponding to depths between 2 and 6 km. Other B20 inclusions were observed in pre-Main stage veins but are thought to be related to fractures associated with the MS mineralization.

As described above, each alteration type at Butte has a characteristic fluid inclusion population, therefore the composition of the leachates extracted from these samples are considered to be representative of the bulk salinity contained by the vein.

4.3.7 Sampling of Geothermal fluids

In a geothermal well the reservoir fluid ascends quickly to the well head, with minimum heat and pressure loss. Once at the surface, the depressurization generates a vapor fraction which fluctuates with the pressure used at the surface to separate water from vapor. In our case, we were interested in determining the concentrations of Cl in the vapour and liquid phases after separation at the surface. For the purpose of a Master's degree dissertation (Dean 2010), brine and steam condensate samples from several geothermal systems in the TVZ, including Rotokawa, Mokai and Kawerau geothermal fields were collected. A mini cyclone separator attached to the two phase line of the well was used to sample vapor and brine from the geothermal wells. The separation vapour-brine was induced at a range of sampling pressures from 135 to 449 psi. The steam samples were allowed to cool down to obtain a condensate before collection in Nalgene high density polyethylene (HDPE) bottles. After sampling, the steam condensates and the brines were sent to the University of Alberta to be analysed for Cl and Br concentrations and stable Cl isotopes.

4.4 Methods

4.4.1 Chlorine and bromine extraction procedures and analysis

Samples were processed in order to obtain representative leachates from the dominant fluid inclusions in veins at Butte. In order to analyse the Cl, Br and stable Cl isotopes in the veins, quartz, fluorite, pyrite, rhodocrosite, covellite, enargite, sphalerite and magnetite were crushed to ~2 mm size grains that were then picked by hand using a binocular microscope. A description of the mineral assemblage identified in each vein sampled is provided in Table 4.1. With the exception of the sphalerite sample Al-3 (Sph), each mineral separate was cleaned by gently heating in nitric acid (Gleeson 2003). The clean and dry samples were crushed to a powder using an agate mortar and pestle (Shepherd et al. 1985; Banks and Yardley, 1992; Gleeson, 2003). Then, 5 mL of de-ionized water was added to this powder in unreactive vials, shaken for 2 minutes and left to settle overnight. The resultant leachate was filtered using 0.2μm pore size filters in order to obtain a clean fluid suitable for ion chromatography analysis.

The leachates and the geothermal fluid condensates and brines were analysed in 7mL plastic vials for Cl and Br using a Dionex DX600 ion chromatograph (IC) equipped with an AS-14A analytical column for F, Cl, Br, NO_2, NO_3, PO_2 and SO_4. The accuracy of the method was monitored by using a DIONEX seven ion standard, which was diluted to different concentrations. Blanks were run every six samples and replicate analyses were conducted to ensure the quality of the data. The detection limit was 0.003 ppm for both Cl and Br determinations. The analytical uncertainty on all analyses was below 5%.

4.4.2 δ^{37}Cl value analyses

For the isotopic analyses, Cl was extracted by precipitating silver chloride (AgCl) from the leachate and the geothermal fluid condensates (Taylor and Grimsrud, 1969; Eggenkamp et al. 1995). The precipitate was then reacted under vacuum with CH_3I in order to obtain CH_3Cl, the analytical gas for mass spectrometry. The samples were analyzed at Environment Canada, Saskatoon in a multicollector CF-IRMS in a GV Instruments Isoprime using the method described in Wassennar and Koehler (2004). The setup was optimized to measure Cl concentrations as low as 0.2 μmol, with a precision of ± 0.2‰, by modifying the head amplifiers design and achieving $1X10^9$ Ω in the mass amplifiers 50 and 52 (Wassennar and Koheler 2004). Atlantic Seawater was used as the standard with a δ^{37}Cl value of 0‰.

4.5 Results

In order to determine the halogen composition of the leachates, all the samples were analyzed by IC for major anions (F, Cl, Br, PO_2 and SO_4). In general, the leachates had very low concentrations of Cl and Br, as described below, but also some anomalously high SO_4 concentrations exceeding 150 ppm which is the maximum detection limit of the method used. Eight samples had values significantly above the detection limit for SO_4. These very high concentrations are unlikely to reflect fluid inclusion compositions; instead they may be the result of sulfide oxidation after the pyrite in the quartz separates reacted with water. Bromine was only detected in 10 of 37 samples. Phosphate was also commonly detected, but due to the high SO_4 concentrations in some of the samples during the IC analysis, the SO_4 peak overlapped the contiguous PO_3 peak so that the PO_3 signal could not be isolated and quantified. This issue did not affect the F, Cl or Br results as they are the first ions to be analyzed and are far removed from the SO_4 peak in the chromatograph.

4.5.1 Cl/Br molar ratios

4.5.1.1 Butte leachates

The group of deep BQ/QMB veins analyzed did not have detectable Br, therefore Cl/Br molar ratios were not calculated for this vein type (Table 4.1). BQ/QMB veins at moderate depths had Cl/Br molar ratios from 2196 to 3550. PGS veins had Cl/Br molar ratios detected in two samples 435 and 2768. GS veins also had two samples with detectable Br and their Cl/Br molar ratios were 379 and 625. In MS veins only sample CZ-1 had detectable Br and the calculated Cl/Br molar ratio was 743. The halogen data obtained in our study was complemented with data from Nahnybida (2006) and Nahnybida et al. (2009) and are included in Table 4.1 and Figure 4.3 and all the data are discussed below.

4.5.1.2 Taupo Volcanic Zone fluids

Geothermal waters from Rotokawa had salinities between 702 and 3852 mg/L TDS, Mokai from 3072 to 4596 mg/L TDS and Kawerau 1224 to 1716 mg/L TDS. The geothermal fluid condensates (representative of the vapor phase) had Cl/Br molar ratios of 1338 for Rotokawa, 1285 and 1350 for Mokai and was not calculated for Kawerau (as Br was not detected in this sample). For the brines Cl/Br molar ratios from 1220 to 1478 were calculated for Rotokawa, from 1149 to 1664 for Mokai and 790 for Kawerau (Table 4.3).

4.5.2 Stable Cl isotopes

4.5.2.1 Butte

The $\delta^{37}Cl$ values of the veins analyzed are shown in Table 4.1. Only one sample from deep BQ/QMB veins was analyzed and had a $\delta^{37}Cl$ value of -0.8 ‰. BQ/QMB veins from moderate depth had positive values of 0.1 ‰ and 0.5 ‰ (Table 4.1). The four samples from PGS veins had two negative values (-0.3 ‰ and -0.4) and one positive $\delta^{37}Cl$ value of 0.4 ‰. One sample had inconsistent isotope results after several runs and is therefore not reported (11166-3805-Qz). Two samples from GS veins had $\delta^{37}Cl$ values of -0.4 ‰ and 0.1 ‰. The MS vein samples had all negative δ^{37}Cl values ranging from -1.5 to -0.2 ‰ (Table 4.1).

4.5.2.2 TVZ

Isotope values measured in the geothermal vapor samples at Rotokawa had δ^{37}Cl values from 0.41 to 0.66 ‰, Mokai from -0.68 to 0.06 ‰, and Kawerau -0.17‰. The δ^{37}Cl values of the brines from Rotokawa ranged from -0.13 to -0.36 ‰, Mokai from -0.30 to 0.38 ‰, and the sample from Kawerau had a value of -0.30 ‰ (Table 4.3).

4.6 Discussion

4.6.1 Chlorine and Br compositions of hydrothermal fluids at Butte

The concentration of an analyte in the leachate is a function of the salinity of the fluid inclusions but also the number of fluid inclusions in a given sample. Therefore, an approximation of the Cl and Br concentrations in the original hydrothermal fluids can be back calculated using the salinity data (in wt% NaCl equiv.) from the fluid inclusion populations classified by Rusk et al. (2008) and normalizing the Cl and Cl/Br data to those measurements (Banks et al. 2000). The results of these calculations are given in Table 4.2, and this includes a weighting of the different inclusion types depending on their abundance. The following section discusses the results from the deepest to shallowest veins.

We did not detect Br in any of the deep BQ/QMB samples, but Nahnybida et al. (2009) published a Cl/Br molar ratio (1667) for sample 11172-3740 in the potassic zone (Table 4.2). If this value (1667) is representative of the original Cl/Br molar ratio of the hydrothermal fluid, and assuming a salinity of less than 10 wt % equiv. NaCl for deep B20 secondary fluid inclusions (Rusk et al. 2009), then B20 and B35 inclusions contributed on average 49 and 40 ppm Br respectively, to the leachate (Table 4.2).

In the case of BQ/QMB samples at moderate depths with no detectable Br (11135-4326 (Qz) and 11135-4947 (Qz)), chlorine appears to be derived from B60 inclusions, the most abundant fluid inclusion type in these veins. The variation of wt% NaCl equiv. and the abundance of secondary B20 inclusions appears to control the detection of Br in the fluid inclusion leachates. BQ/QMB veins at moderate depths also contain BH15 fluid inclusions but this type of inclusion is considered here only as potential source of Cl, as Br is excluded from the halite lattice during crystallization (Kesler, 1995).

PGS veins are dominated by vapour-rich B85 inclusions which account for most of the Cl in the leachate but there is also a contribution from BH15 fluid inclusions. Samples 10772-0 (Py) and 11166-3805 (Qz) from PGS veins had detectable Br concentrations, with Cl/Br molar ratios of 435 and 2768, respectively (Table 4.1). Fluid inclusion abundances for these samples are not available, but based on the predominance of B85 inclusions in this vein type reported by Rusk et al. (2008a), it can be concluded that Br may be contained in a less abundant inclusion type like B20 or B60.

According to data reported by Nahnybida et al. (2009) for GS veins (Table 4.2), the B60 inclusion type appears to be the main source of Cl and Br in their samples, although the calculated Br concentrations here suggest there is an important Br contribution from B20 inclusions in the leachates analyzed in this study. Two GS vein samples analyzed in our study had detectable Br (Table 4.1), allowing for the calculation of Cl/Br molar ratios (379 and 625).

MS veins are dominated by B20 inclusions (~100%) with salinities of 1 to 3.5 wt% NaCl equiv., different to the pre-Main stage B20 type which have a higher range in salinity (1 to 20 wt% NaCl equiv.) (Rusk et al. 2008a). Therefore, both Cl and Br concentrations in the fluid inclusions are expected to be low. The MS vein samples analyzed in the present study had undetectable Br with the exception of sample CZ1 with a Cl/Br ratio of 743 (Table 4.1). Two analysis of sample CZ1 were conducted by Nahnybida (2006); and they obtained Cl/Br molar ratios of 608 and 108. In the same study, two more MS samples were reported with Cl/Br molar ratios of 534 and 722 (Table 4.1). This suggests that the B20 MS fluid inclusions are relatively Br enriched.

In pre-Main stage veins B20, B35 and B60 fluid inclusions contain Br resulting in different Cl/Br molar ratios. This contrasts with the Br concentrations of MS veins, where the Br budget is dominated by B20 MS fluid inclusions, the most abundant fluid inclusion type in this vein type.

In summary, this suggests that Br concentrations in the system overall are relatively low and its distribution in fluid inclusions (and the leachates) may be controlled by processes which occurred during the evolution of the hydrothermal system. These possibilities will be discussed later in more detail.

4.6.2 The source of halogens and the isotopic composition of the parental magmatic-hydrothermal fluid at Butte

Chlorine/bromine molar ratios have been measured before in inclusions from the Butte deposit by Irwin and Roedder (1995), who reported Cl/Br molar ratios between 649 and 1818. Kendrick et al. (2001), used noble gas spectrometry to calculate Cl/Br molar ratios in quartz samples from the potassic zone from Bingham Canyon, Silverbell, Ray, Mission, Pinto Valley and Globe-Miami. Their data ranged from 535 to 1149. These values overlap Cl/Br molar ratios measured by Jambon et al. (1995) in samples from the Mid-Atlantic Ridge Basalt (MARB) (828 to 2026), the East Pacific Rise Basalt (EPRB) (826 to 848), and the Mid-Ocean Ridge Basalt (MORB) values reported in Kendrick et al. (2012a) (612 to 670). Based on these studies, approximate Cl/Br molar ratios for the upper mantle range from 612 to 2026 (Figure 4.3).

The fluids trapped in the BQ/QMB veins represent the supercritical parental magmatic-hydrothermal fluid in the Butte system. Two samples thought to be representative of the supercritical fluid in the potassic zone at Butte were measured and reported in Nahnybida (2006), and have Cl/Br molar ratios of 1175 (Br/Cl: 0.85×10^{-3}) and 1667 (Br/Cl: 0.60×10^{-3}). Based on the values mentioned above, reported in the literature, we suggest that a mantle-like signature is present in the Butte deposit.

Only one B35-dominated fluid inclusion sample in deep BQ/QMB veins, was measured for stable Cl isotopes (11172-4187-Qz) and this had a delta value of -0.8 ‰. We suggest that this value therefore, may represent the isotopic composition of the parental magmatic-hydrothermal fluid.

According to published δ^{37}Cl values, the upper mantle has a value of $\leq$-1.6‰ (Bonifacie et al. 2008b; Layne et al. 2009). Bernal et al. (2014) published δ^{37}Cl values of geothermal fluids related to andesitic and rhyolitic heat sources in the Taupo Volcanic Zone, North Island New Zealand, and argued that negative δ^{37}Cl values (average -0.4‰) are preserved in fluids from geothermal systems associated with andesitic magmas, whilst positive δ^{37}Cl values (average +0.4‰) are indicative of rhyolitic sources. In other words, the geothermal fluids preserve the chlorine isotopic signature of the parental magma at depth. Assuming that the parental hydrothermal fluid at Butte had a uniform composition which evolved to form all the alteration assemblages found in the deposit (Rusk et al. 2008a; Reed et al. 2013), then the negative δ^{37}Cl value of this fluid reflects the isotopic composition of the magmatic source. Therefore, the isotopic data support the hypothesis that the fluids deep in the Butte deposit have a mantle signature, and suggest that mafic magmatism may have an important role in forming the Butte PCD system.

Mafic magmas can exsolve SO_2 and chalcophile elements more efficiently into the aqueous phase than felsic magmas (Maughan et al. 2002; Hattori and Keith, 2001), which have low sulfur solubility as the iron content of the magma is depleted during fractionation (Hattori and Keith, 2001). Following Reed et al. (2013), the availability of SO_2 is crucial for the development of the Pre-Main stage and MS veins at Butte. The role of SO_2 is to reduce the pH of the hydrothermal fluid as temperature decreases, the interaction of this acidic fluid with the host rock produced the alteration assemblages characteristic of the Butte PCD. According to Chiaradia et al. (2012) mafic-intermediate magma reservoirs can release Cu and S-bearing fluids which recharge shallower porphyry systems to form large Cu deposits. The Butte deposit, is associated with felsic magmatism, but a pulse of mafic-intermediate magma recharging a felsic magmatic chamber at depth can provide the required Cu and SO_2 to the hydrothermal fluid in order to mineralize the host rock at shallower depths. Hattori et al. (2002) showed that mafic and felsic magma mixing processes were important at Bingham Canyon and in the volcanic system at Mount Pinatubo. Although an input from a mafic source into the Butte system was suggested by Rusk et al. (2008a), there is currently no evidence of mafic rocks in the pit. Nevertheless, Smedes (1966) described basaltic, andesitic and rhyolitic lavas in the lower unit of the Elkhorn Mountains Volcanics, indicating a full magmatic evolution of the volcanic system thought to be contemporaneous with the Boulder Batholith. The occurrence of intermediate-mafic magmatism in the area at the time of the intrusion of the Boulder Batholith (and the Butte Granite), therefore, suggests that the interaction between felsic and mafic magmas, may have played a role in the formation of the Butte system and in defining the halogen signature of the deep veins.

4.6.3 Evolution of the mineralizing fluid in BQ/QMB veins

If the original halogen composition of the magmatic fluid is contained in fluid inclusions from deep BQ/QMB veins, then it evolved chemically, since the BQ/QMB samples from moderate depth trapped fluids with Cl/Br molar ratios from 2196 to 3550. These values partially overlap previous measurements (1175 to 2410) in Nahnybida (2006). We will discuss two main processes that could lead to these diverse Cl/Br molar ratios: phase separation and/or changes in the halogen composition of the magmatic source.

Experiments to assess the effects of phase separation on the halogen composition of fluids resembling marine hydrothermal systems with a Na-K-Ca-Cl-H_2O composition were carried out by Berndt and Seyfried, (1990) at 425 to 450 °C and 33 to 38 MPa; they concluded that Br and Cl do not fractionate from each other and both are concentrated preferentially in the brine. These results were challenged by Liebscher et al. (2006), who argued that in their experiments, under similar conditions of pressure and temperature (380 to 450 °C and 22.9 to 41.7 MPa), Br is enriched in the liquid phase with respect to Cl. Both experiments were carried out with different starting solutions, the initial wt% NaCl composition of the initial fluids used in Berndt and Seyfried (1990) is unknown, but in addition to Br they added Li, Sr, Ba and B to their experimental solution, whilst Liebscher et al. (2006), used fluids with initial salinities between 0.44 and 9.05 wt% NaCl and investigated the pure H_2O-NaCl-NaBr system. This difference in salinity and additional components may have had an effect on the experimental results as discussed in Liebscher et al. (2006), making the findings uncertain and perhaps inapplicable in our case.

In an attempt to identify firsthand the effects of phase separation in hydrothermal fluids, we investigated the chemical composition of co-existing vapor and brine from geothermal fluids. The expectation was that these magma-sourced fluids may have had a comparable chemical composition to the deep Butte hydrothermal fluid, and therefore, may be more representative than the fluids used in the experimental studies with seawater (Table 4.3).

The chemistry of brine and condensate samples is shown in Table 4.3. The data in this table show that the Cl and Br concentrations in the vapor are very small with respect to the brine, but also that there is no significant alteration of the Cl/Br molar ratios in the vapor and brine after phase separation. Our empirical data, therefore, is in agreement with the study of Berndt and Seyfried, (1990). If a similar process occurred at Butte, the change in the range of Cl/Br molar ratios in the potassic zone of the Butte PCD (1175 to 3550) cannot be explained by phase separation but is solely a function of differences in the source of the halogens as the system develops. The range of Cl/Br molar ratios in deep BQ/QMB veins (1175 to 2410) (Table 4.1) fall within the published upper mantle values range of 612 to 2026 (Jambon et al. 1995; Kendrick et al. 2012) (Figure 4.3). Therefore, the Cl/Br molar ratios of the potassic zone may largely reflect the interaction between felsic and mafic magmas, generating a range of Cl/Br molar ratios of the hydrothermal fluid that depended on the predominance of one magma type over the other.

It has been recently proposed that hot magmatic fluids in the Butte PCD were able to reach more than 2 km without extensive overall cooling or thermal equilibration required for hydrothermal alteration (Mercer and Reed, 2013).This process can modify the ^{37}Cl/ ^{35}Cl ratio of the brine as a rapid ascent of the hydrothermal fluid can potentially lead to kinetic isotope fractionation. Stable Cl isotopes delta values for BQ/BMQ veins are negative in general, with the exception of two samples with slightly positive values (0.1 and 0.5‰).

Two kinetic processes are examined in order to explain the δ^{37}Cl values measured in the fluid inclusion leachates: distillation and phase separation. Distillation is a kinetic fractionation process affecting stable Cl isotopes, as proposed in Sharp et al. (2009). During experiments simulating the effect of condensation in volcanic fumaroles (restricted to small fractures and rock dissolution spaces), these workers proposed that the heavy Cl isotope is enriched in the gas phase (HCl) with respect to the aqueous fluid as a result of condensation at depth. At Butte it is possible that an isotopically enriched HCl gas was later re-incorporated by the hydrothermal fluid shifting its isotopic composition to higher values at locations in the veins where water/rock ratios were low. The occurrence of negative and positive δ^{37}Cl values in the same vein type supports local modification of the isotopic signature, possibly occurring in reduced volumes of hydrothermal fluid. We are not aware of any stable Cl isotope fractionation study at supercritical conditions to support the process described by Sharp et al. (2009), but Berndt and Seyfried (1990), based on the relative concentrations of B, Li, Cs and Rb in marine vent fluids at supercritical conditions inferred brine condensation, vapor evolution and remixing occurring in small regions of the cracking front of submarine hydrothermal systems.

The effect of phase separation on the Cl isotopic composition of geothermal fluids (Table 4.3), can help to interpret the isotope values in the fluid inclusion leachates analyzed. Our data for the Rotokawa wells indicate that after phase separation δ^{37}Cl is enriched in the vapor phase. Conversely, for the Mokai and Kawerau wells this shift is not observed, suggesting that during phase separation either ^{37}Cl or ^{35}Cl can favor the steam phase; an indication of kinetic fractionation. In the case of the geothermal brines, the highest fractionation between liquid and vapour was 1.03‰ (±0.2‰) and the lowest -0.13 ‰ (±0.2‰) (Table 4.3). It is to be expected that, at supercritical conditions such as those at Butte, the fractionation of the Cl isotopes would be smaller than that observed in the geothermal fluids; therefore, kinetic isotope effects due to phase separation may not fully explain our data and phase separation in combination with brine condensation, vapor evolution and remixing, as identified by Bernt and Seyfried (1990), cannot be discounted. Therefore, it is possible that the hydrothermal fluid at Butte experienced a shift to higher Cl isotope values as consequence of unmixing. This affected only the small concentration of Cl retained by the vapor phase, and most of the hydrothermal fluid preserved its original (negative) isotopic signature.

4.6.4 Evolution of the mineralizing fluid, PGS and GS veins

Overall, our data indicate a significant change to fluids with lower Cl/Br molar ratios in PGS and GS veins, compared with the deep and moderate depth BQ/QMB veins representative of the parental magmatic hydrothermal fluid (Table 4.1). The first occurrence of low Cl/Br molar ratios coincides with the change from transient lithostatic to hydrostatic pressure in the deposit (Rusk et al. 2008a, Reed et al. 2013 and Mercer and Reed 2013) (Figure 4.4A). Phase separation in combination with brine condensation, vapor evolution and remixing may have been increasingly important mechanisms at these depths, resulting in the fractionation of Cl from Br as the hydrothermal fluid decompressed and cooled to form PGS and GS veins. However, other processes such as the ingress of an external Br-rich fluid, water rock interaction and mineral precipitation may be important as well; these options will be discussed in turn.

Bromine can be incorporated into the magmatic hydrothermal fluid by mixing with Br-rich external fluids. One potential source of these fluids would be highly evaporated seawater brines which have Cl/Br molar ratios below the seawater value of 650 (Rittenhouse, 1967; Carpenter, 1978). Only two samples with detectable Br, 10772-0-Py and 11052-7007-Qz from PGS and GS veins, respectively have such low values (Table 4.1). Another possibility is a fluid which has acquired Br from organic sources of Br, such as hydrocarbons (Kendrick et al. 2012b). However, the host rocks are unlikely to have hydrocarbons and the input of significant organic material is not reflected in the chemistry of the inclusions. Equally, if either of these two sources were present, Br-rich fluids would be more commonly detected in the veins analyzed (Table 4.1 and 4.2).

A geochemical modeling study was conducted by Reed et al. (2013), which simulated the chemical interaction between a magmatic-hydrothermal fluid and the Butte granite. The model predicted that a magmatic fluid at 1 kbar and 600 °C, subsequently cooled to 200 °C, can reproduce all the alteration assemblages observed at Butte, including the advanced argillic and sericitic alteration characteristic of the MS mineralisation, and showed that changes in pH and chemistry due to the neutralization of the acidic fluid with the host rock is the main mechanism that generates the alteration assemblages. Therefore, it is not necessary to invoke an external source of solutes in the genesis of the Butte deposit. This conclusion is supported by the negative values of most of the stable Cl isotopes measured in fluid inclusions at Butte (Table 4.1), which indicates a magmatic source of halogens. This suggests that the variations in the Cl/Br molar ratios and δ^{37}Cl values observed in our study during the evolution of a single hydrothermal fluid have to be explained by a closed system process or processes. We consider the possibility that Cl was incorporated into a mineral phase, removing Cl more efficiently from the hydrothermal fluid than phase separation, and therefore, decreasing the Cl/Br molar ratios as a more plausible option.

In magmatic hydrothermal systems, Cl can be retained by a few minerals such as apatite, amphibole and biotite. At Butte, apatite has been reported only at EDM veins formed at around 600 °C (Reed et al. 2013), but amphibole is associated with hydrothermal alteration occurring at temperatures above 450 °C, and biotite is common in veins formed above 350 °C (Reed et al. 2013). Chlorine concentrations in the apatite and amphibole are not available to estimate how much Cl was retained by these minerals, but published electron microprobe data on shreddy biotites in EDM/PGS veins indicate that Cl is present in this mineral from 0.06 to 0.09 wt% (Mercer and Reed, 2013). In addition, there are biotite breccias and biotite crackle veins reported at the deepest parts of the deposit (Roberts, 1975, Rusk et al. 2008a, Reed et al. 2013 and Mercer and Reed, 2013). However, there are not enough data available on the Cl contents, distribution or total amount of biotite at Butte to conduct a Cl mass balance calculation. Considering the low salinity of the original hydrothermal fluid, (2 to 5 wt% NaCl equiv.: Rusk et al. 2008a) and the common occurrence of secondary biotite and perhaps amphibole in some of the deepest veins of the deposit (EDM veins), it is quite possible that the hydrothermal fluid was already depleted in Cl with respect to Br at the time PGS and GS veins were formed, producing the low Cl/Br molar ratios measured in these veins.

In terms of the stable Cl isotopes, the range in δ^{37}Cl values in PGS veins (-0.4 to 0.4‰) and GS veins (-1.6 to 0.1‰) (Figure 4.4B), may reflect a complex combination of different isotopic fractionation mechanisms. On the one hand, kinetic fractionation may have modified the isotopic signature as discussed before, but later equilibrium isotopic fractionation may have been involved during mineral precipitation. If Cl is partitioned into the biotite, the hydrothermal fluid would be depleted in ^{37}Cl, which according to Schauble et al. (2003), is concentrated in the mineral phase (as Cl is bonded to +2 cations (i.e. $FeCl_2$) in biotite). This mechanism cannot be ruled out and to better understand the extent of the isotopic fractionation in biotite, the analyses of stable Cl isotopes in this mineral are needed.

4.6.5 Evolution of the mineralizing fluid, MS veins

In our study MS vein samples had undetectable Br with the exception of sample CZ1, which had a Cl/Br molar ratio of 743. MS mineralization is thought to have been formed by decompressed magmatic hydrothermal fluids that later mixed with meteoric waters (Rusk et al. 2008b); this dilution may explain the low concentrations of Br in the inclusions in these veins. However, as discussed before, some higher δ^{37}Cl values would be expected as consequence of these physico-chemical processes. Instead, all the isotope values measured in MS fluid inclusion leachates in our study and previous studies are highly depleted (-2.0 to -0.2 ‰) overlapping the isotope values measured in the pre-Main stage potassic zone and the parental magmatic hydrothermal fluid (-2.0 to -0.8 ‰) (Table 4.1).

This commonality suggests that the pre-Main stage and MS mineralisation have a common magmatic-hydrothermal source. However, this interpretation is not supported by the Cl/Br molar ratios reported in Nahnybida et al. (2009), which ranged from 534 to 1008 in MS veins and from 1175 to 2410 measured in the potassic zone. Spatial relationships indicate that the pre-Main stage veins are cut by MS vein lodes (Rusk et al. 2008b). In a genetic model of the Butte porphyry Cu-Mo system (Mercer and Reed, 2013), two episodes of hydrofracturing were associated with fluid pulses that reached the upper parts of the deposit (> 2 km).. The first episode is related to EDM, PGS, DGS (GS veins with K-feldspar) and GS alteration. The second episode was associated with BQ/QMB veins and more recent GS veins. The rapid ascent of the hydrothermal fluid is supported by the lack of alteration envelopes in BQ/QMB veins (Rusk et al. 2008a, Reed et al. 2013 and Mercer and Reed, 2013). If a single magmatic fluid produced all the observed assemblages (Rusk et al. 2008a; Reed et al. 2013), this suggests that the hydrothermal fluid in both events had similar chemical characteristics.

We propose, based on our data, that a later injection of magma in the Butte Granite may have generated additional pulses of magmatic-hydrothermal fluid responsible for the generation of the MS mineralization. This fluid may have been able to move faster than the previous hydrothermal fluid injections due to less resistance to hydraulic fracturing by a weakened and altered host rock. The lower Cl/Br molar ratio measured in MS veins (722), compared with the value published in Nahnybida (2006) for the potassic zone in pre-Main stage veins (1175 to 2410) (Table 4.1), indicates some evolution of the magmatic source between these two mineralization events as evidenced by the δ^{37}Cl signature. Unlike the earlier, pre-Main stage hydrothermal events, the MS pulse reached shallower depths and encountered meteoric water. Assuming that the fast transit from the intrusion depths to the meteoric water contact was an adiabatic process, minimal vapor and temperature loss would be expected before contact with meteoric water. Decompression and mixing with low salinity cold waters may have quenched down the hydrothermal fluid quickly and dissolved the vapor phase as it formed. As a result, the MS fluid inclusions do not have the highδ^{37}Cl values derived from unmixing processes such as those that occurred in the pre-Main Stage hydrothermal fluids.

As this last episode unfolded, the pressure increased and hydraulic fracturing and brecciation developed. This allowed for new incursions of modified hydrothermal fluid, giving place to vein mineralization. Under these circumstances the hydrothermal fluid would have a similar Cu content to the original magmatic-hydrothermal fluid, explaining the high grades found in MS veins. However, after mixing with meteoric water this fluid would have lower salinities than the 2 to 5 wt% NaCl equiv. fluids in the pre-Main stage potassic zone (Rusk et al. 2008a).

The MS veins have negative δ^{37}Cl values, as mentioned before, only sample CZ-1 (QZ) has detectable Br and its molar ratio (743) may be an indication of an upper mantle component in the hydrothermal fluid. In addition, the δ^{37}Cl value measured in this sample was -0.7 ‰, very close to the value of the deepest sample analyzed for this study and in Nahnybida (2006) for BQ/QMB veins (-0.8 ‰) (Table 4.1). However, the wide difference in Cl/Br molar ratios in these two vein types suggests that the magmatic source, thought to be a mixture of felsic and mafic magmas, evolved with time to lower Cl/Br molar ratios. Despite these variations in the elemental halogen composition of the hydrothermal fluid, the δ^{37}Cl signature of its magmatic source persisted during the Butte mineralisation.

In summary, the evolution of the hydrothermal fluid in the Butte PCD is complex, but at different depths in the deposit the hydrothermal fluid is characterized by its halogen and stable Cl isotope compositions. The deepest veins (BQ/QMB) preserve the isotopic and halogen composition of the source magmas. As the fluid evolves and moves to shallower depths in the deposit, processes such as phase separation and water-rock interactions modify both the Cl isotopes and the Cl/Br molar ratios of the fluid inclusions (PGS and GS veins). The youngest and shallower veins (MS) trapped fluid inclusions with compositions resembling the deepest hydrothermal fluid, which have not been affected by physico-chemical processes, this supports renewed input from the magmatic source was responsible for the Cu mineralization of the MS veins at Butte.

4.7 Conclusions

In the present study we report high Cl/Br molar ratios in deep and moderate depth BQ/QMB veins, compared to low Cl/Br molar ratios from shallower PGS and GS veins. We assessed several possibilities to explain this variation: an external source of Br available to PGS and GS veins, distillation and phase separation during cooling and decompression of the hydrothermal fluid, and the retention of Cl or Br by a mineral phase. Of these options we consider that both phase separation and the retention of Cl by biotite may have affected the halogen element concentrations and the isotope values in the system.

In the potassic zone (BQ/QMB veins), where the effects of phase separation are minimal, the variations in the Cl/Br molar ratios are attributed to the interaction between felsic and mafic magmas, reflected in a range of Cl/Br molar ratios of the hydrothermal fluid. For the shallower veins (PGS and GS) we used Cl/Br molar ratios measured in vapors and brines from three different geothermal fluids as an empirical comparator of vapor-brine Cl/Br fractionation. These data show that during phase separation only small concentrations of Cl and Br were partitioned from the brine to the vapor, and after phase separation the Cl/Br molar ratios were preserved in both phases. From these observations, and the experimental data, we conclude that the large range of Cl/Br molar ratios measured in our study (379 to 3550) cannot be explained purely by unmixing of the hydrothermal fluid. In upper veins, we suggest that Cl was incorporated in biotite and that the low Cl/Br molar ratios in PGS and GS veins are the product of Cl uptake by this mineral. The higher δ^{37}Cl values measured in some moderate depth BQ/QMB, PGS and GS veins can be explained by a combination of several processes such as phase separation, brine condensation, vapor formation and remixing, occurring locally in cracks and fractures. However, this fractionation is presumed to be restricted to the small concentration of Cl transferred from the brine to the vapor phase; most of the Cl (contained by the brine) preserved its original isotopic signature.

The similarity of the low δ^{37}Cl values in fluid inclusions in veins that have trapped the parental magmatic hydrothermal fluids, the deep BQ/QMB veins and the younger, and economically important, MS veins (-0.8‰ and -0.7‰ respectively), supports the hypothesis that the hydrothermal fluid at Butte has a single source which evolved to form all the alteration assemblages found in the deposit (Rusk et al. 2008a and Reed et al. 2013). The data also confirm a common and persistent mantle-like signature during the formation of the Butte PCD. Based on the behaviour of Cl, Br and the stable Cl isotopes observed in pre-Main Stage alteration veins, we propose that MS mineralization was produced by a final pulse(s) of magmatic-hydrothermal fluid released from a deep porphyry intrusion, similar to previous intrusions modeled by Mercer and Reed (2013). This latest pulse was different in that it reached shallower depths and encountered meteoric water already in fractures and conduits connected to the surface. The vapor generated during this interaction was mostly removed or dissolved by the meteoric water, but the hydrothermal fluid preserved the metal content of its magmatic source, explaining the high grades characteristic of the MS mineralization.

4.8 References

Alletti M., Baker D. Scaillet B., Aiuppa A. Moretti R. and Ottolini L., 2009. Chlorine partitioning between a basaltic melt and H_2O-CO_2 fluids at Mount Etna. Chem. Geol. 263, 37-50.

Banks D. A. and Yardley B. W. D., 1992, Crush-leach analysis of fluid inclusions in small natural and synthetic samples. Geochim. Cosmochim. Acta. 56, 245-248.

Barnes J. D and Sharp Z. D., 2005. A chlorine isotope study of DSDP/ODP serpentinazed ultramafic rocks: Insights into serpentinization process. Chem. Geol. 1413, 1-20.

Barnes J. D., Sharp Z. D. and Fischer T. P., 2008. Chlorine Isotope variations across the Izu-bonin-Mariana arc. The Geol. Soc. Amer. 36, 883-886.

Barnes J. D., Sharp Z. D., Fischer T. P., Hilton D. R. and Carr M. J., 2009. Chlorine isotopic variations along the Central American volcanic front and back arc. Geochem. Geophysics Geosys. 10, 11- 17 p.

Bernal N. F, Gleeson S. A, Dean A., Liu X. M. and Hoskin P., 2014. The source of halogens in geothermal fluids from the Taupo Volcanic Zone, North Island, New Zealand. Geochim. Cosmochim. Acta. 126, 265-283.

Berndt M. and Seyfried W., 1990. Boron, bromine, and other trace elements as clues to the fate of chlorine in mid-ocean ridge vent fluids. Geochim. Cosmochim. Acta. 54, 2235-2245.

Bonifacie M., Monnin C., Jendrzejewski N., Agrinier P. and Javoy M., 2007. Chlorine stable isotopic composition of basement fluid of the eastern flank of the Juan de Fuca Ridge (ODP Leg 168). Earth Planet. Sci. Lett. 260, 10-22.

Bonifacie, M., Busigny, V., Mevel, C., Philippot, P., Agrinier, P., Jendrzejewski, N., Scambelluri, M., and Javoy, M., 2008a. Chlorine isotopic composition in seafloor serpentinites and high-pressure metaperidotites: Insights into oceanic serpentinization and subduction processes: Geochim. Cosmochim. Acta. 72, 126–139.

Bonifacie, M., Jendrzejewski, N., Agrinier, P., Humler, E., Coleman, M., and Javoy, M., 2008b. The chlorine isotope composition of Earth's mantle: Science, 359, 1518–1520.

Böhlke J. and Irwin J., 1992. Laser microprobe analyses of Cl, Br, I, and K in fluid inclusions: implications of sources in some ancient hydrothermal fluids. Geochim. Cosmochim. Acta. 56, 203-225.

Brimhall G.H., Jr., 1977. Early fracture-controlled disseminated mineralization at Butte, Montana: Econ. Geol. 72, 37–59.

Carpenter A. B., 1978. Origin and chemical evolution of brines in sedimentary basins. Cir-Okla. Geol. Surv. 79, 60-77.

Chiaradia M., Ulianov A., Kouzmanov K. and Beate B., 2012. Why large porphyry Cu deposits like high Sr/Y magmas?. Scient. Rep. 2:685/DOI:10.1038/srep00685.

Czehura S., 2006. Butte – A world class ore deposit. 2006 SME annual meeting and exhibit & 7th ICARD, St. Louis, Missouri.

Eastoe C., Guilbert J. and Kaufmann R., 1989. Preliminary evidence for fractionation of stable chlorine isotopes in ore-forming hydrothermal systems. Geology 17, 285-288.

Eastoe C. and Guilbert J., 1992. Stable chlorine isotopes in hydrothermal processes. Geochim. Cosmochim. Acta. 56, 4247-4255.

Eggenkamp H. and Kreulen R., 1995. Chlorine stable isotope variations in volcanic gasses, volcanic springs and crater lakes from Indonesia. The geochemistry of chlorine isotopes. Doctoral, Universiteit Utrecht.

Gleeson S. A., 2003. Bulk analysis of electrolytes in fluid inclusions. Fluid inclusions: Analysis and interpretation, Short course series 32, 233-246.

Gleeson S. A. and Smith M. P., 2009. The sources and evolution of mineralizing fluids in iron oxide-copper-gold systems, Norrbotten, Sweden: Constraints from Br/Cl ratios and stable Cl isotopes of fluid inclusion leachates. Geochim. Cosmochim. Acta. 73, 5658-5672.

Hattori K. and Keith J., 2001. Contribution of mafic melt to porphyry copper mineralization: evidence from Mount Pinatubo, Philippines, and Bingham Canyon, Utah, USA. Miner. Dep. 36:799-806.

Hattori, K. H., 2002. Role of oxidized, sulfur-rich mafic magmas for porphyry copper mineralization. Abstracts with Programs. The Geol. Soc. of Ame. October, 2002, 34, 6, 88.

Hedenquist J. and Lowenstern J., 1994. The role of magmas in the formation of hydrothermal ore deposits. Nature 370, 519-527.

Houston, R.A., 2002. Geology and structural history of the Butte district, Montana: Unpublished M.S. thesis, Corvallis, Oregon, Oregon State University, 45 p.

Houston R. and Dilles J., 2013. Structural Geologic Evolution of the Butte District, Montana. Soc. of Econ. Geol. 108, 1397-1424.

Irwin J. and Roedder E., 1995. Diverse origins of fluid in magmatic inclusions at bingham (Utha, USA), Butte (Montana, USA), St. Austell (Cornwall, UK), and Ascension Island (mid-Atlantic, UK), indicated by laser microprobe analysis of Cl, K, Br, I, Ba + Te, U, Ar, kr, and Xe. Geochim. Cosmochim. Acta. 59, 295-312.

Jambon A., Deruelle B., Dreibus G. and Pineau F., 1995. Chlorine and bromine abundance in MORB: the contrasting behavior of the Middle-Atlantic ridge and East Pacific Rise and implications for chlorine geodynamic cycle. Chem. Geol. 126, 101-117.

Kendrick M., Burgess R., Patrick R. and Turner G., 2001. Fluid inclusion noble gas and halogen evidence on the origin of Cu-Porphyry mineralizing fluids. Geochim. Cosmochim. Acta. 65, 2651-2668.

Kendrick M. A., Kamenetsky V. S., Phillips D. and Honda M., 2012a. Halogen systematics (Cl, Br, I) in Mid-Ocena Ridge Basalt: a Macquarie Island case study. Geochim. Cosmochim. Acta. 81, 82-93.

Kendrick M., Woodhead J. and Kamenetsky V., 2012b. Tracking halogens through the subduction cycle. Geology 40, 1075-1078.

Kesler S., Appold M., Marin A., Walter L., Hudson T and Kyle R., 1995. Na-Cl-Br systematics of mineralizing brines in Mississippi Valley-type deposits. Geology 23, 641-644.

Layne G. D., Kent A. J. R. and Bach W., 2009. δ^{37}Cl systematic of back-arc spreading: the Lau Basin. Geology 37, 427–430.

Lund K., Aleinkoff J., Kunk M., Unruh D., Zeihen G., Hodges W., Du Bray E., and O'Neill J., 2002. Shrimp U-Pb and 40Ar/39Ar age constraints for relating plutonism and mineralization in the Boulder batholith region, Montana. Econ. Geol. 97, 241–267.

Magenheim A. J., Spivack A. J., Michael P. J. and Gieskes J. M., 1995. Chlorine stable isotope composition of the oceanic crust: Implications for earth's distribution of chlorine. EPSL 131, 427-432.

Martin M.W., Dilles, J.H., and Proffett, J.M., 1999. U-Pb geochronologic constraints for the Butte porphyry system [abs.]: Geological Society of America Abstracts with Programs, 31, no. 7, p. A380.

Maughan D., Keith J., Christiansen E., Pulsipher T. Hattori K. and Evans N., 2002. Contributions from mafic alkaline magmas to the Bingham porphyry Cu-Au-Mo deposit, Utah, USA. Miner. Dep. 37, 14-37.

Meyer C., and Hemley, J.J., 1967. Wall rock alteration, in Barnes, H.L. ed., Geochemistry of hydrothermal ore deposits: New York, Holt, Rinehart and Winston, Inc., p. 166–232.

Meyer C., Shea, E., Goddard, C., and staff, 1968. Ore deposits at Butte, Montana, *in* Ridge, J.D. ed., Ore deposits of the United States 1933–1967 [Graton-Sales volume]: New York, American Institute of Mining, Metallurgical, and Petroleum Engineers 2, 1363–1416.

Miller R.N., ed., 1973. A field meeting held August 18–21, 1973, Butte, Montana, sponsored by the Society of Economic Geologists, U.S. Geological Survey, and Anaconda Company, Geological Department.

Nahnybida T., 2006. Halogen and stable chlorine isotope analysis of quartz hosted fluid inclusions from porphyry Cu deposits. Master of Science thesis. Department of Earth and Atmospheric Sciences, University of Alberta.

Nahnybida T., Gleeson S.A, Rusk B. and Wassennar L., 2009. Cl/Br ratios and stable chlorine isotope analysis of magmatic-hydrothermal fluid inclusions from Butte, Montana and Bingham Canyon, Utha. Doi:10.1007/s00126-009-0248-0.

Proffett, J.M., 1973. Structure of the Butte district, Montana, *in* Miller, R.N., ed., A field meeting held August 18–21, 1973, Butte, Montana: Sponsored by the Society of Economic Geologists, U.S. Geological Survey, and Anaconda Company, Geol. Dep., G1–12.

Reed M.H., 1999. Zoning of metals and early potassic and sericitic hydrothermal alteration in the Butte, Montana, porphyry Cu–Mo deposit [abs.]: Geol. Soc. Ame., Abstracts with Programs, 31, 7, A381.

Reed, M., and Rusk, B., 2001. Insights into supercritical hydrothermal processes from numerical models of potassic hydrothermal alteration, and SEM-CL imaging of vein quartz at Butte, Montana, *in* Toshiyuki, H., ed., Proceedings from the Workshop on Potential Thermal Extraction from Deep-seated Rock Masses: Sendai, Japan, Tohoku University, p. 37–53.

Reed M., Rusk B. and Palandri J., 2013. The Butte magmatic-hydrothermal system: One fluid yields all alteration and veins. Econ. Geol. 108, 1379-1396.

Roberts S. A. 1975. Early hydrothermal alteration and mineralization in the Butte district, Montana: Unpublished Ph.D. dissertation, Harvard University, 157 p.

Rusk B.G., and Reed, M.H., 2002. Scanning electron microscope-cathodoluminescence of quartz reveals complex growth histories in veins from the Butte porphyry copper deposit, Montana: Geology 30, 727–730.

Rusk B., Reed, M., Dilles, J.H., Klemm, L., and Heinrich, C.A., 2004. Compositions of magmatic hydrothermal fluids determined by LA-ICP-MS of fluid inclusions from the porphyry copper-molybdenum deposit at Butte, Montana: Chem. Geol. 210, 173–199.

Rusk B., Reed M., and Dilles J., 2008a. Fluid inclusion evidence of magmatic-hydrothermal fluid evolution in the porphyry copper-molybdenum deposite at Butte, Montana. Econo. Geol. 103, 307-334.

Rusk B.G., Miller, B.J., and Reed, M.H., 2008b. Fluid-inclusion evidence for the formation of Main stage polymetallic base-metal veins, Butte, Montana, USA, *in* Spencer, J.E., and Titley, S.R., eds., Ores and orogenesis: Circum-Pacific tectonics, geologic evolution, and ore deposits: Ariz. Geol. Soc. Dig. 22, 573-581.

Sales R., and Meyer, C., 1948. Wall rock alteration at Butte: American Institute of Mining and Metallurgical Engineers, Transactions 46, 4–106.

Sharp Z. D. and Barnes J. D., 2004. Water-soluble chlorides in massive seafloor serpentinites: a source of chloride in subduction zones. EPSL. 226, 243-254.

Sharp Z. D., Barnes J. D., Fischer T. P. and Halik M., 2009. An experimental determination of chlorine isotope fractionation in acid systems and applications to volcanic fumaroles. Geochim. Cosmochim. Acta 74, 264-273.

Seward, T.M. and Barnes, H.L., 1997. Metal transport by hydrothermal ore fluids, In: Barnes, H.L. (Ed.), Geochem. Hydroth. Ore Dep. 3rd Ed., 435–486.

Shepherd T. J., Rankin A. H. and Alderton D.H.M., 1985. A practical guide to fluid inclusion studies. Blackie, London, 239.

Smedes H., 1966. Geology and igneous petrology of the Northern Elkhorn Mountains, Jefferson and Broadwater Counties, Montana. USGS professional paper 510.

Snee, L., Miggins, D., Geissman, J., Reed, M., Dilles, J., and Zhang, L., 1999. Thermal history of the Butte porphyry system, Montana [abs.]: Geological Society of America Abstracts with Program, 31, 380.

Taylor J. W. and Grimsrud E. P., 1969. Chlorine isotopic ratios by negative ion mass spectrometry. Anal. Chem. 41, 805-810.

Wassenaar L. I. and Koehler G., 2004. On-Line technique for the determination of the δ^{37}Cl of inorganic and total organic in environmental samples. Anal. Chem. 76, 6384- 6388.

Williams-Jones, A.E., Heinrich, C.A., 2005. 100th Anniversary special paper: vapor transport of metals and the formation of magmatic-hydrothermal ore deposits. Econom. Geol. 100, 1287–1312.

Wilson C. J. N., Houghton B. F., McWilliams M. O., Lanphere M.A., Weaver S. D. and Briggs R. M., 1995. Volcanic and structural evolution of Taupo Volcanic Zone, New Zealand: a review. J. Volcanol. Geotherm. Res. 68, 1-28.

Wilson C. J. N. and Rowland J. V., 2011. Volcanological and tectonic insights into geothermal system in the central Taupo Volcanic Zone, New Zealand. New Zealand Geothermal Workshop 2011.

Yardley B. W. D., Gleeson S. A., Bruce S., Banks D. A., 2000. Origin of retrograde fluids in metamorphic rocks. Jour. Geochem. Expl. 69-70, 281-285.

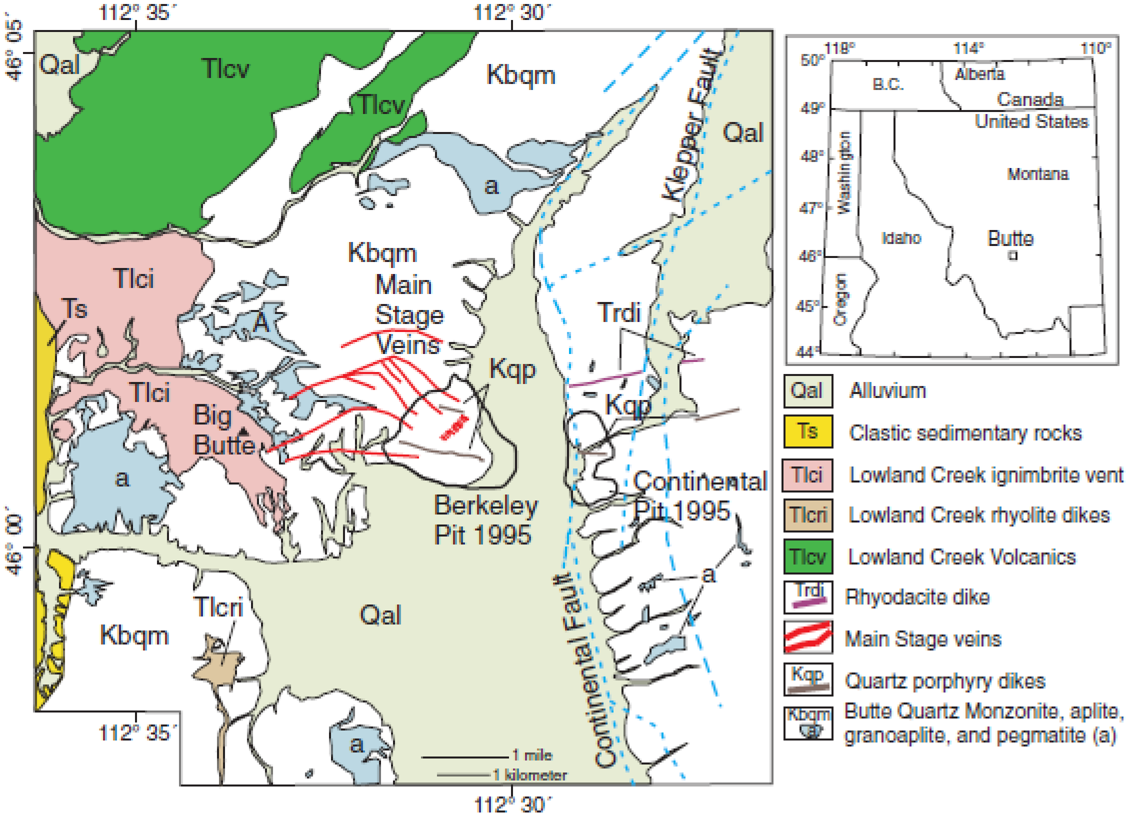

Figure 4-1 Location map of the Butte Deposit.
The Berkeley and Continental pits (modified after Hudson (2002), Proffett (1973), and unpublished reports of the Anaconda Company).

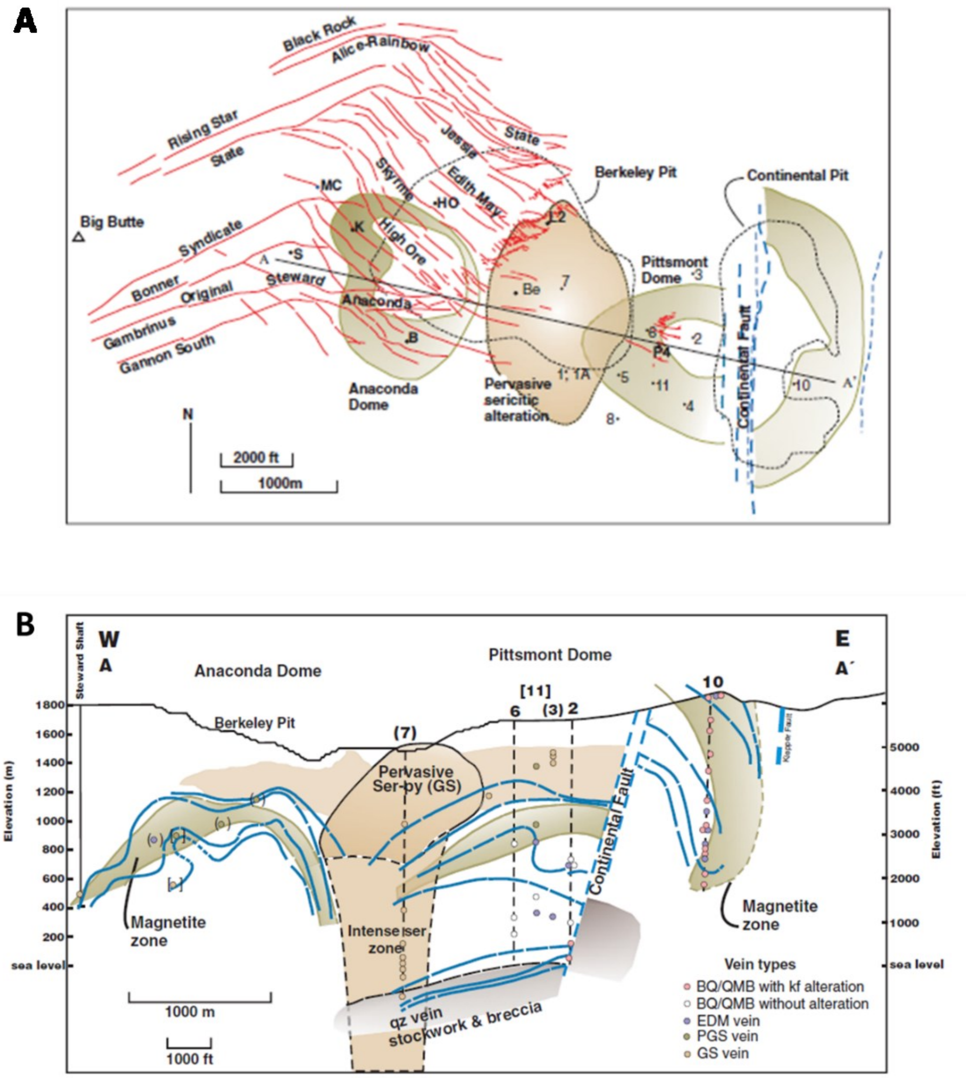

Figure 4-2 Geologic map and cross section of the Butte PCD.

Distribution of MS and pre-Main stage mineralization at the Butte PCD. A) Plan view of the MS and pre-Main stage mineralization at Butte. The subsurface position of pre-Main stage porphyry Cu centers the Pittsmont and Anaconda domes are shown in green, and MS veins are shown in red. A zone of pervasive sericitic alteration separating the two porphyry Cu mineral centers is shown in tan. The locations of several mine shafts are also indicated: S = Steward, K = Kelly, MC = Mountain Consolidated, Be = Berkley, HO = High Ore, L2 = Leonard, P4 = Pittsmont #4, and B = Belmont. B) East-west geologic cross section (A-A') of pre-Main stage porphyry Cu-Mo mineralization. The two mineral centers are the Anaconda dome in the west, and the Pittsmont dome in the east. The Continental fault displaces the eastern part of the Pittsmont dome upward by ~1,300 m.

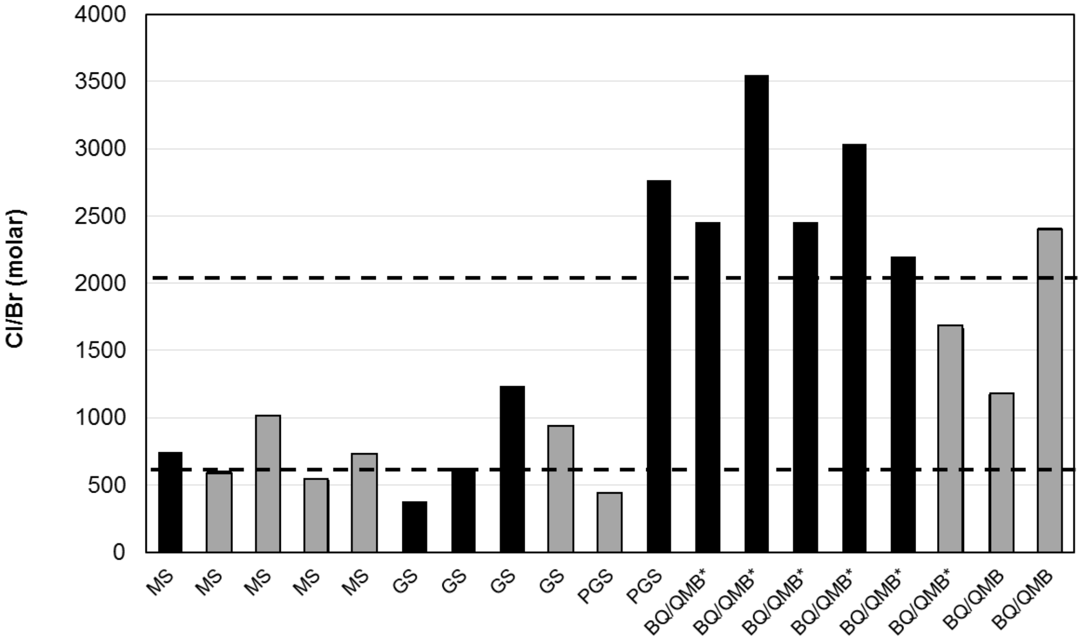

Figure 4-3 Cl/Br molar ratios from alteration veins of the Butte PCD.
The dashed lines represent the range of upper mantle values (Jambon et al. 1995; Kendrick et al. 2012). Gray histograms are data from Nahnybida (2006). Moderate depth BQ/QMB values are shown by an asterisk.

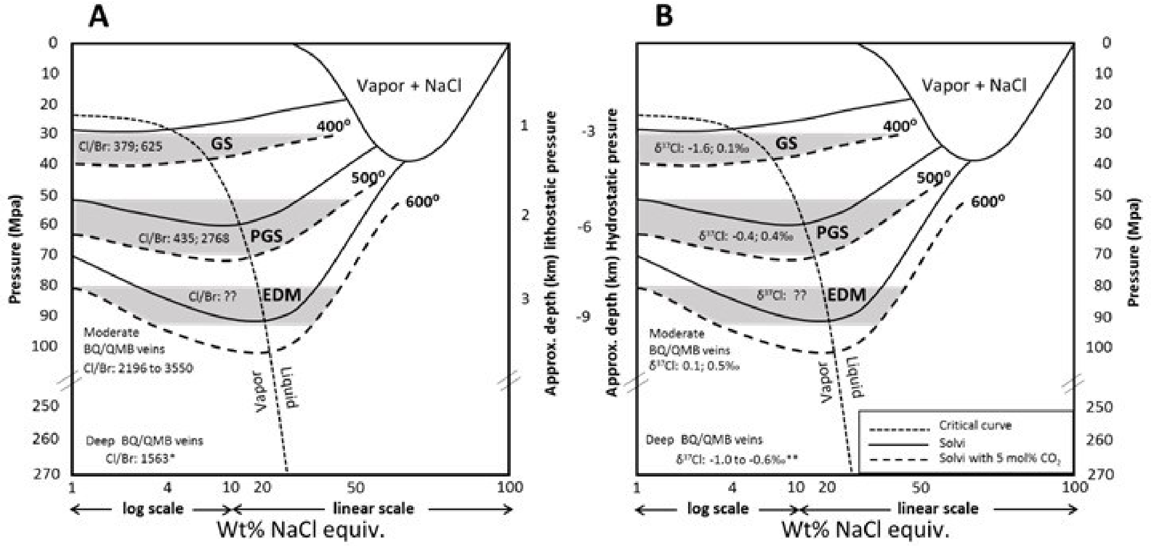

Figure 4-4 Phase diagram representing the system H_2O-NaCl.
This diagram also includes pressure and temperature conditions of brine evolution. A) Measured Cl/Br molar ratios transitioning from high values in BQ/QMB veins to low values in PGS and GS veins. B) δ^{37}Cl values for pre-Main stage veins (modified after Rusk et al. 2008a) showing higher δ^{37}Cl values than the deepest and hottest hydrothermal fluids contained by BQ/QMB inclusions. Data not available for EDM veins. *Nahnybida et al. (2009). **Nahnybida (2006).

Table 4-1 Cl and Br concentrations and δ^{37}Cl values from alteration veins at Butte.
Text in bold from Nahnybida (2006). Qz: quartz; Py: pyrite; Cov: covelite; Mt: Magnetite; Mo: Molybdenite; Rod: rhodochrosite; Sph: sphalerite, Fl: Fluorite; tr: traces; n.d.: not detected; n.c.: not calculated; n.m.: not measured.

Vein types	Sample ID	Main vein minerals	Alteration Zone	Cl (ppm)	Br (ppm)	Cl/Br molar	Br/Cl (X10^{-3}) molar	δ^{37}Cl (‰)
Main Stage (MS)	10551-1 (Qz)	Qz (90) and En (10)	Main Stage	8.07	n.d.	n.c.	n.c.	-0.9
	10551-1 (En)	Qz (25) and En (75)	Main Stage	2.63	n.d.	n.c.	n.c.	-1.5
	Lex-5 (Py)	Sp (20), Py (65), Cpy (10) and Qz (5)	Main Stage	14.88	n.d.	n.c.	n.c.	n.m.
	CZ-1 (Qz)	Py (5), En (5) and Qz (90)	Main Stage	5.38	0.016	743	1.35	-0.7
	X-2004 (Qz)	Qz (100)	Main Stage	2.54	n.d.	n.c.	n.c.	-0.2
	CZ-2 (Py)	Py (70), Cp (15) and Qz (15)	Main Stage	0.80	n.d.	n.c.	n.c.	-1.4
	CZ-2 (Cov)	Py (20), Cp (10) and Cov (70)	Main Stage	0.58	n.d.	n.c.	n.c.	-0.4
	11169-1171 (Py)	Py (90) and En (10)	Main Stage	2.94	n.d.	n.c.	n.c.	-0.2
	11169-1171 (En)	Py (5) and En (95)	Main Stage	1.57	n.d.	n.c.	n.c.	n.m.
	3440 (Fl)	Fl (100)	Main Stage	5.82	n.d.	n.c.	n.c.	-0.7
	Al-3 (Qz)	Qz (80), Rod (10) and Sph (10)	Main Stage	2.96	n.d.	n.c.	n.c.	-1.5
	Al-3 (Rod)	Qz (10), Rod (85) and Sph (5)	Main Stage	2.07	n.d.	n.c.	n.c.	-0.8
	Al-3 (Sph)	Qz (20), Rod (10) and Sph (70)	Main Stage	5.23	n.d.	n.c.	n.c.	n.m.
	Bum-03-20 (Qz)	Qz (100)	Main Stage	9.75	n.d.	n.c.	n.c.	-1.0
	CZ-1 (Qz)	**Qz (100)**	**Main Stage**	**0.81**	**0.003**	**608**	**1.65**	**-1.3**
	CZ-1 (Qz)	**Qz (100)**	**Main Stage**	**4.91**	**0.011**	**1008**	**0.99**	**n.m.**
	AL-2 (Qz)	**Qz (100)**	**Main Stage**	**1.18**	**0.005**	**534**	**1.87**	**-1.1**
	X35564 (Qz)	**Qz (100)**	**Main Stage**	**0.96**	**0.003**	**722**	**1.38**	**-2.0**
Gray Sericitic (GS)	11052-7182 (Qz)	Qz (100)	Perv. Sericitic	20.34	n.d.	n.c.	n.c.	n.m.
	11185-4790 (Py)	Py (100)	Perv. Sericitic	3.13	n.d.	n.c.	n.c.	-0.4
	11052-7007(Qz)	Py (5), En (3) and Qz (92)	Perv. Sericitic	3.35	0.020	379	2.64	0.1
	11166-2091 (Qz)	Py (5), En (1) and Qz (94)	Perv. Sericitic	20.81	n.d.	n.c.	n.c.	n.m.
	I-15-1 (Py)	Py (80) and Qz (20)	Perv. Sericitic	5.94	0.021	625	1.6	n.m.
	11052-7025 (Qz)	**Qz (100)**	**Perv. Sericitic**	**4.916**	**0.009**	**1233**	**0.81**	**-1.6**
	11052-6215 (Qz)	**Qz (100)**	**Perv. Sericitic**	**4.52**	**0.011**	**927**	**1.08**	**-1.0**
Pale-Green Sericitic (PGS)	10772-0 (Py)	Py (75), Cp (10) and Qz (15)	Sericitic	16.63	0.086	435	2.3	0.4
	11185-2091 (Mt)	Mt (85), Cp (5), Py (5) and Qz (5)	Sericitic	8.26	n.d.	n.c.	n.c.	-0.3
	11166-3805 (Mt)	Qz (5) and Mt (95)	Sericitic	7.34	n.d.	n.c.	n.c.	-0.4
	11166-3805 (Qz)	Qz (90) and Mt (10)	Sericitic	30.02	0.024	2768	0.36	n.m.
(BQ/QMB) at moderate depths.	11169-2933 (Qz)	Qz (100)	Potassic	14.58	0.013	2453	0.41	n.m.
	11155-3384 (Qz)	Qz (100)	Potassic	5.77	n.d.	n.c.	n.c.	n.m.
	80-10 (Qz)	Qz (90) and Py (10)	Potassic	37.24	0.024	3550	0.28	n.m.
	11135-3872 (Qz)	Qz (100)	Potassic	16.28	0.015	2456	0.41	n.m.
	11185-3260 (Qz)	Qz (95) and Mo (5)	Potassic	15.39	0.011	3034	0.33	n.m.
	11135-4326 (Qz)	Qz (100)	Potassic	6.44	n.d.	n.c.	n.c.	n.m.
	11169-4999 (Qz)	Qz (100)	Potassic	18.72	0.019	2196	0.46	n.m.
	11135-4947 (Qz)	Qz (100)	Potassic	3.71	n.d.	n.c.	n.c.	0.5
	Kelly 4700 (Qz)	Qz (100)	Potassic	8.38	n.d.	n.c.	n.c.	0.1
	11135-4967 (Qz)	**Qz (100)**	**Potassic**	**2.95**	**0.004**	**1667**	**0.60**	**-1.0**
	11135-4967 (Qz)	**Qz (100)**	**Potassic**	**7.36**	**n.d.**	**n.c.**	**n.c.**	**-0.8**
BQ/QMB deep veins	11172-2329 (Qz)	Qz (100)	Potassic	3.18	n.d.	n.c.	n.c.	n.m.
	11172-2946 (Qz)	Qz (100)	Potassic	13.18	n.d.	n.c.	n.c.	n.m.
	11172-1734 (Qz)	Qz (100)	Potassic	8.28	n.d.	n.c.	n.c.	n.m.
	11172-4187 (Qz)	Qz (100)	Potassic	9.27	n.d.	n.c.	n.c.	-0.8
	11172-2800 (Qz)	Qz (100)	Potassic	6.38	n.d.	n.c.	n.c.	n.m.
	11172-3740 (Qz)	**Qz (100)**	**Potassic**	**1.56**	**0.003**	**1175**	**0.85**	**-1.3**
	11172-3740 (Qz)	**Qz (100)**	**Potassic**	**9.61**	**0.009**	**2410**	**0.41**	**n.m.**

Table 4-2 Estimated Cl and Br concentrations in fluid inclusion types.
Values obtained by using the average Cl concentration for fluid inclusion type and weighted by percentage of abundance. Text in bold from Nahnybida (2006).

Vein types	Sample	Fluid Inclusion type	Abun. %	Cl/Br molar	Min. wt% NaCl equiv.	Max. wt% NaCl equiv.	Min. Cl ppm	Max. Cl ppm	Ave. Cl ppm	Calc. Cl ppm	Calc. Br ppm	δ^{37}Cl (‰)
Main Stage (MS)	**CZ1**	**B20$_{MS}$**	**100**	**1008**	**1**	**4**	**6100**	**24400**	**15250**	**15250**	**37**	**-1.3**
	AL2	**B20$_{MS}$**	**100**	**534**	**1**	**4**	**6100**	**24400**	**15250**	**15250**	**37**	**-1.1**
	X3564	**B20$_{MS}$**	**100**	**722**	**1**	**4**	**6100**	**24400**	**15250**	**15250**	**37**	**-2.0**
Gray Sericitic (GS)	**11052-6215 (Qz)**	**B20**	**5**	**926**	**1**	**20**	**6100**	**122000**	**64050**	**3202.5**	**156**	**-1.3**
		B35	**0**		**1**	**8**	**6100**	**48800**	**27450**	**0**	**0**	
		B60	**90**		**1**	**7**	**6100**	**42700**	**24400**	**21960**	**60**	
		B85	**5**		**0**	**3**	**0**	**18300**	**9150**	**457.5**	**22**	
	11052-7025 (Qz)	**B20**	**5**	**1235**	**1**	**20**	**6100**	**122000**	**64050**	**3202.5**	**117**	**-1.6**
		B35	**0**		**1**	**8**	**6100**	**48800**	**27450**	**0**	**0**	
		B60	**90**		**1**	**7**	**6100**	**42700**	**24400**	**21960**	**45**	
		B85	**5**		**0**	**3**	**0**	**18300**	**9150**	**457.5**	**17**	
Pale Gray Sericitic (PGS)	11185-2091 (Mt)	BH15	6	n.c.	30	48	183000	292800	237900	14274	n.c.	
		B20	4		1	20	6100	122000	64050	2562	n.c.	
		B35	2		1	8	6100	48800	27450	549	n.c.	
		B60	3		1	7	6100	42700	24400	732	n.c.	
		B85	85		0	3	0	18300	9150	7777.5	n.c.	
BQ/QMB veins at moderate depth	11135-3872 (Qz)	BH15	3	2456	30	48	183000	292800	237900	7137	n.c.	n.m.
		B20	20		1	20	6100	122000	64050	12810	59	
		B35	17		1	8	6100	48800	27450	4666.5	25	
		B60	50		1	7	6100	42700	24400	12200	22	
		B85	10		0	3	0	18300	9150	915	8	
	11135-4326 (Qz)	B20	4	n.c.	1	20	6100	122000	64050	2562	n.c.	n.m.
		B35	15		1	8	6100	48800	27450	4117.5	n.c.	
		B60	80		1	7	6100	42700	24400	19520	n.c.	
		B85	1		0	3	0	18300	9150	91.5	n.c.	
	11135-4947 (Qz)	B20	3	n.c.	1	20	6100	122000	64050	1921.5	n.c.	0.5
		B35	12		1	8	6100	48800	27450	3294	n.c.	
		B60	80		1	7	6100	42700	24400	19520	n.c.	
		B85	5		0	3	0	18300	9150	457.5	n.c.	
	11135-4967 (Qz)	**B20**	**2**	**1667**	**1**	**20**	**6100**	**122000**	**64050**	**1281**	**87**	**-0.8**
		B35	**40**		**1**	**8**	**6100**	**48800**	**27450**	**10980**	**37**	
		B60	**50**		**1**	**7**	**6100**	**42700**	**24400**	**12200**	**33**	
		B85	**10**		**0**	**3**	**0**	**18300**	**9150**	**915**	**12**	
BQ/QMB deep veins	**11172-4187 (Qz)**	**B20**	**3**	**n.c.**	**1**	**10**	**6100**	**61000**	**33550**	**1006.5**	**n.c.**	**-0.8**
		B35	**94**		**1**	**8**	**6100**	**48800**	**27450**	**25803**	**n.c.**	
		B60	**2**		**1**	**7**	**6100**	**42700**	**24400**	**488**	**n.c.**	
		B85	**1**		**0**	**3**	**0**	**18300**	**9150**	**91.5**	**n.c.**	
	11172-3740 (Qz)	**B20**	**<2**	**1563**	**1**	**10**	**6100**	**61000**	**33550**	**2100**	**49**	**-1.3**
		B35	**100**		**1**	**8**	**6100**	**48800**	**27450**	**27450**	**40**	
		B60	**0**		**1**	**7**	**6100**	**42700**	**24400**	**0**	**0**	
		B85	**0**		**0**	**3**	**0**	**18300**	**9150**	**0**	**0**	

Notes:
n.c.: no calculated
n.m.: no measured

Table 4-3 Halogens and stable Cl isotopes in geothermal fluids.
Cl, Br, Cl/Br molar ratios, Cl isotope ratios and fractionation factors (vapor and brine).

Location	Well	Cl ppm	Br ppm	Cl/Br molar	δ^{37}Cl ‰	$10^3 \ln \alpha$ ‰
Rotokawa	RKA 01 brine	699.701	1.290	1220	-0.36	-1.02
	RKA 01 vapor	8.355	0.014	1338	0.66	
	RKA 02 brine	625.378	0.953	1478	-0.13	-0.59
	RKA 02 vapor	0.330	n.d.	n.c.	0.46	
	NAP 02 brine	730.474	1.313	1252	-0.28	-0.84
	NAP 02 vapor	4.217	n.d.	n.c.	0.56	
	NAP 07 brine	656.753	1.155	1280	-0.19	-0.60
	NAP 07 vapor	10.733	n.d.	n.c.	0.41	
Mokai	MK 01 brine	2465.125	4.056	1368	0.03	0.30
	MK 01 vapor	0.620	n.d.	n.c.	-0.27	
	MK 02 brine	2541.068	3.437	1664	0.35	1.03
	MK 02 vapor	61.909	0.108	1285	-0.68	
	MK 03 brine	2468.431	4.837	1149	0.38	0.32
	MK 03 vapor	17.052	0.028	1350	0.06	
	MK 04 brine	2356.237	3.558	1490	-0.30	-0.13
	MK 04 vapor	2.070	n.d.	n.c.	-0.17	
Kawerau	KA 08 brine	750.724	2.138	790	-0.30	-0.13
	KA 08 vapor	4.543	n.d.	n.c.	-0.17	

Notes:
n.d.: not detected
n.c.: not calculated

5 The stable chlorine isotope composition of scapolites from iron oxide-copper-gold (IOCG) deposits and regional Na-Cl metasomatic alteration, Norrbotten County, Sweden.

5.1 Introduction

The ability of the halogen elements to be incorporated in mineral structures is determined by their ionic radii, electronegativities and electron affinities. In general, the halogens F and Cl, with smaller radii and larger electronegativites and electron affinities, are more readily incorporated in non-halide minerals than other halogens. Only a few non-halide minerals can accommodate significant amounts of Cl in their structures, despite the abundance of Cl in some geologic environments. Some of these Cl-bearing minerals, such as apatite, amphibole, biotite and scapolite, are found in alteration assemblages in ore deposits. Scapolite can also form as a result of metasomatic processes, metamorphism and as a primary phase in igneous rocks (Mora and Valley, 1989; Dong, 2005; Mi and Pan, 2015). Iron-oxide Cu-Au deposits (IOCG), are found in cratonic areas or continental margins; these deposits occur in different types of host rocks, including plutonic granitoids, (meta)-andesitic volcanic rocks, and mainly (meta)-siliclastic and/or metabasic rocks (Williams et al., 2005). Fluid inclusion studies on these deposits show that the mineralising fluid is commonly a Cl-rich brine (Williams et al., 2005; Chiaradia et al. 2006) and the alteration assemblages associated with these deposits commonly contain Cl-rich scapolite. A variety of fluid sources have been suggested for the brines that form IOCG deposits including magmatic and metamorphic fluids, formation waters and/or mixtures of these end members (e.g. Barton and Johnson, 1996, 2000, Frietsch et al., 1997, Williams et al. 2005, Chiarada et al., 2006, Pollard 2000, 2006, Oliver et al., 2004, Fisher and Kendrick, 2008; Kendrick et al., 2008a). Chiaradia et al. (2006) reported Cl and Sr isotopic data from three IOCG deposits (Candelaria, Raul-Condensable and Sossego) and suggested the mineralising fluids were the result of mixing between a magmatic fluid and a basinal brine.

A temporal and spatial association between the Kiruna type iron oxide-apatite (IOA) and IOCG deposits has been suggested in the past (Williams et al. 2005). IOCG deposits are characterized by the occurrence of Cu-sulphide ± Au hydrothermal ores with abundant (> 20%) hematite or magnetite (e.g., Corriveau, 2007; Smith et al., 2012). These deposits are associated with batholitic granitoids and pervasive alkali metasomatism (Williams et al. 2005). A- to I-type magmatism and alkaline-carbonatites stocks are also related to IOCG mineralisation (Corriveau, 2007). In the Norrbotten region, IOA deposits are restricted to the Kiruna and Galliväre areas, whereas the IOCG deposits are found in the Karelian greenstones and in volcanic rocks of Svecofennian age (Wanhainen at al., 2012).

Gleeson and Smith (2009) determined the halogen contents and Cl stable isotope compositions of fluid inclusions in quartz veins from IOA and IOCG systems in Norrbotten, Sweden. The fluid inclusion leachates from veins in the IOCG deposits had low δ^{37}Cl values (-5.6‰ to -1.3‰) and it was suggested that the Cl in these fluids had a magmatic, and ultimately a mantle, source but their isotopic composition had been modified by crystallization of scapolites (and micas), which had progressively lowered δ^{37}Cl values of the residual fluids. There are no experimental constraints on the direction or magnitude of chlorine isotope fractionation factors between brines and silicate minerals. However, theoretical calculations of equilibrium fractionation of Cl isotopes between solid monovalent chloride NaCl- and KCl-saturated brines and the divalent-metal chlorides $FeCl_2$ and $MnCl_2$, which may serve as a proxy for the fractionation behavior of structurally bound Cl^- in micas and amphiboles indicates that ^{37}Cl is partitioned into the divalent chloride (Schauble et al. 2003). The magnitude of the calculated fractionation ranges from 2 to 3‰ at 25 °C to <1‰ at hydrothermal temperatures of 300 to 350 °C. These calculations suggest that there should only be a small partitioning of the ^{37}Cl isotope into amphiboles or micas relative to monovalent chloride brines (e.g. NaCl, KCl). The Cl isotope fractionation between brines and scapolite is unknown but given that Cl in scapolite is mostly bonded to the monovalent cation Na^+, the theoretical expectation is that scapolite would have less of an affinity for ^{37}Cl than amphiboles or micas.

Kusebauch et al. (2015) reported δ^{37}Cl values of -0.7 to 0.0‰ and Br/Cl molar ratios of 0.004 to 0.007 for scapolites from the Bamble sector, SE Norway. This study discounted the presence of meta-evaporites or mantle sources in the halogen compositions of the fluids in the Bamble sector based on halogen ratios.

In this study, we have analysed the halogen concentration and the Cl isotope composition of scapolites from the Nunasvaara and the Greenstone and porphyry-hosted Cu deposits at Pahtohavare, Kallosalmi, Sarkivaara and Gruvberget (Figure 5.1). This work tests the hypothesis of Gleeson and Smith (2009) and also provides an empirical estimate of the direction and magnitude of the Cl isotope fractionation factor between scapolite and hydrothermal fluids at temperatures between 300-500°C. On the basis of the halogen content and Cl isotope data, the sources of chlorine in scapolite associated with regional metasomatism and ore-forming processes are discussed.

5.2 Geology background and previous studies

The IOCG-type deposits of Norrbotten County, Sweden (Figure 5.1) are hosted by a Paleoproterozoic sequence (~1.9 Ga) of Svecokarelian metavolcanic and metasedimentary rocks known as the Greenstone and Porphyry Groups (Carlon 2000; Bergman et al., 2001). The Karelian Greenstone group is composed of volcanic rocks of tholeiitic to komatiitic composition overlying the Archaean basement (Ekdahl, 1993). The Porphyry Group consists of basalt, trachyandesite and rhyodacite-rhyolite units that are intruded by the syenitic- to quartz syenitic-composition Kiruna porphyries. The Porphyry Group may have acquired their current character as a result of metasomatic overprinting of an older calc-alkaline association (Martinsson, 1997). These units were originally assigned an age of ~1880 Ma (Romer et al., 1994), but U-Pb analyses of cores of titanite grains from the hanging wall to the Luossavaara ore body suggest a minimum age of 2050 Ma (Storey et al., 2007). Albitisation and scapolitisation occurred at a regional scale, but the timing of regional Na alteration is relatively poorly constrained. Smith et al. (2009) presented a single LA-ICPMS U-Pb age of titanite from Na-altered diorite at Nunasvaara of 1903±8 Ma – an age which is pre- to syn- the main iron-oxide apatite (IOA) mineralisation at Kirunavaara and potentially elsewhere.

IOCG deposits are associated with high salinity brines, which are responsible for the presence of Na-rich alteration, albite and scapolite (Williams et al., 2001, Kendrick et al., 2007, 2008a,b, Gleeson and Smith 2009). In the Norrbotten district, some mineralising fluids are Ca-rich, probably due to the dissolution of limestone during interaction of these fluids with calc-silicate skarns in the area (Wanhainen et al. 2003, Smith et al., 2012). Chlorine stable isotopes have previously been analysed from fluid inclusion leachates extracted from quartz veins in the region (Gleeson and Smith, 2009). Scapolite and quartz rarely occur directly together, as scapolite occurs as an alteration phase in the wall rock, and quartz in veins. However, the scapolite alteration in the vicinity of ore deposits is directly associated with chalcopyrite mineralisation, as is quartz at Pahtohavare, Kallosalmi and Gruvberget. Some quartz veins appear cutting scapolite alteration. Also, scapolite, actinolite and quartz have been observed co-existing in the same assemblage. The precipitation of scapolite is therefore, interpreted to be related to the same fluids responsible for mineralization in these deposits.

5.2.1 Origin of the Samples

Scapolite is directly associated with IOCG mineralisation and also with barren regional units. Scapolite-bearing samples for this study were taken from regional Na-Cl metasomatic assemblages (RM), from scapolite altered metabasic rocks in the vicinity of iron oxide-apatite or iron oxide-copper-gold deposits (IOCG-M), and from intense Na-alteration zones in which the original character of the rock has been obscured by alteration (Na-metasomatites or ‘Na-Skarns’; IOCG-PS) (Figure 5.2).

5.2.1.1 Regional Na-Cl metasomatism (RM)

Regional Na-Cl metasomatism is developed throughout the Norrbotten area, southern Norway and Fennoscandinavia. In stratigraphic settings, RM occurs as massive layers and structurally controlled disseminations, stringers and veinlets (Freitsch et al., 1997). Sodium metasomatism in the region has previously been interpreted to be a result of the metamorphism of evaporites in the volcano-sedimentary sequence (Frietsch et al., 1997), and in other IOA-IOCG districts a strong case has been made for the direct association of regional Na-alteration with the mobilisation of metals that are subsequently concentrated in mineral deposits (Barton and Johnson, 1996, 2000; Oliver et al., 2004). The regional metasomatic samples in this study are not associated with ore. Samples were taken from regional alteration assemblages at Nunasvaara, where the contact of a diorite intrusion with brecciated metasediments is exposed. Both the diorite and the host sediments are altered and contain scapolite and albite, with igneous and breccia matrices now dominated by actinolite and abundant accessory titanite (Figure 5.2). A second group of samples were taken from well preserved pillow basalts on the banks of the Torneälven River. Here basalts are altered to scapolite-albite-actinolite-bearing assemblages, cut by veins containing scapolite, actinolite, chlorite and magnetite (Figure 5.2).

5.2.1.2 IOCG-Scapolite altered Metabasic Rocks (IOCG-M)

More intense scapolite alteration is developed around many of the ore deposits in the region, typically, but not exclusively, in metabasic protoliths (e.g. Frietsch et al., 1997; Martinsson, 2004; Edfelt et al., 2005; Smith et al., 2007). Samples of scapolite from metabasic hosts in the immediate vicinity of ore deposits were taken from Pahtohavare (Martinsson, 1997; Lindblom et al., 1996) and Kallosalmi (Wägman and Ohlsson, 2000). Pahtohavare is a previously mined Cu-(Au) deposit hosted in folded, greenschist-facies slates and metabasic rocks (Figure 5.2). Ore is associated with albitisation and scapolitisation in both lithologies, commonly with overprinting potassic alteration. Samples were taken from altered metabasic rocks in core, and from a metadolerite dyke exposed in the open pit. Kallosalmi is an unmined prospect in which strongly Na-altered metabasic rocks host carbonate-associated Cu mineralisation. Samples were taken from altered metabasic rocks in drill core.

5.2.1.3 IOCG scapolite rich alteration/Na skarn (IOCG-PS)

Samples were taken from Pahtohavare and Kallosalmi (described above) where intensely scapolitised and albitised rocks with little relict texture directly host chalcopyrite mineralisation (Figure 5.3). Similar mineralisation was sampled at Sarkivaara (Wägman and Ohlsson, 2000) where intense scapolite-albite alteration hosts chalcopyrite-molybdenite mineralisation. Samples from Gruvberget (Martinsson and Virkkunen, 2004) were taken from altered metavolcanic rock within 2 m of the contact with a magnetite-hematite-apatite body, with overprinting Cu mineralisation. The alteration consists of the development of albite and scapolite with actinolite, overprinted by K-feldspar alteration (Figure 5.2). The rock is also associated with abundant, large (>1cm) titanite crystals.

5.3 Methods and analytical techniques

5.3.1 Electron microprobe analysis (EMPA)

Electron microprobe analyses of scapolite in thin sections were carried out using a Cameca SX50 electron microprobe at the Natural History Museum, London. Beam conditions were set at 20Kv and 20nA with a spot size of 1mm. The instrument was calibrated using well characterised silicate, sulphide, halide and oxide mineral standards for Na, Mg, Si, S, Cl, Ca, Ti, Fe, and Sr, and synthetic KBr for K. The data were empirically corrected for peak overlaps using analyses of standards following the techniques outlined in Williams (1996).

5.3.2 X-ray Fluorescence Microprobe

Bromine analyses were carried out on an XRF Microprobe (XRFM) at the University of Saskatchewan, using the same instrument and analytical protocols described in Pan and Dong (2003). Briefly, the XRF microprobe consists of a 2.0 kW X-ray generator, a concave (Johansson) LiF (220) (R=250 mm) monochromator, a sampler holder attached to a petrographic microscope, and an energy-dispersion X-ray spectrometer. The X-ray generator is operated at a voltage of 45 kV and a current of 20 mA. The X-ray beam (0.1 to 2.5 mm) is focused from the LiF monochromator, and is collimated by a conical collimator of 0.2 to 2.5 mm in dimension. A calibration curve for Br was first established from four international reference materials and was further evaluated by using the Br contents in a suite of Cl-rich minerals (i.e., chlorapatite, scapolite and sodalite) determined by instrumental neutron activation analysis (INAA; Pan and Dong, 2003). Scapolite grains of ~100 μm in diameter for X-ray microprobe analyses were carefully selected under a petrographic microscope to minimize mineral and fluid inclusions. The counting times for samples with less than 10 ppm Br, was increased from 10 to 45 minutes. The precision of the method is reflected in the relative standard deviation, which was less than 5% for Br concentrations over 10 ppm, and 10% for concentrations below 10 ppm. The calculated detection limit in the analysis of single mineral grains is ~1 ppm Br (Pan and Dong, 2003).

5.3.3 Cl extraction by Pyrohydrolysis

Rock samples containing scapolite were crushed and sieved to sizes from 100 to 250 µm. Then singular scapolite grains were carefully separated by hand and weighed. Before pyrohydrolysis each sample was cleaned by immersing the scapolite grains in a HNO_3 solution and gently heating (Gleeson 2003). After that, the samples were rinsed with deionized water and dried in the oven overnight.

A pyrohydrolysis apparatus was built at the University of Alberta in order to extract the Cl contained in scapolite separates (Figure 5.4). The purpose of this technique is to remove the Cl present in the structure of a mineral by melting a small sample mass (~100 to 150 mg). The volatiles released during the reaction are carried by a steam flow to a distillation tube obtaining an aqueous solution. The pyrohydrolysis set up used was modified from the one described by Bonifacie et al. (2007) in order to allow for the direct analysis of the Cl concentration in the recovered solution by ion chromatography (IC). The objective was to avoid the use of a NaOH collecting solution, as further chemical treatment is required to neutralize the high pH of the Cl-bearing solution, potentially leading to contamination. The use of a boiling reservoir and a condensation tube in the present set-up, was modified from the pyrohydrolysis apparatus described in Barnes and Sharp (2006). A nebulizer is usually used to control the flow of water vapor (i.e. Whitehead and Thomas, 1985; Magenheim et al. 1994; Bonifacie et al. 2007).

The sample was mixed with five parts V_2O_5 (Whitehead and Tomas, 1985), then the mixture was transferred to the reaction tube, which was placed in a position coincident with the central area of the heating element inside the furnace to ensure the homogeneous heating and melting of the sample. A stream of water steam carried the volatiles from the furnace to the condensation tube where the solution containing Cl^- from the mineral sample is recovered.

Deionized water was heated in the boiling water reservoir and analyzed by IC to assess if any Cl flowed back from the reaction tube, however Cl was not detected in any of the analyses. The total duration of each extraction was 1 hour, including a pre-heating stage from 400 ºC to 1,200 °C of 15 minutes and a melting stage of 45 minutes at 1,200 °C.

Chlorine in scapolites was measured by EPMA in mineral grains and by IC in pyrohydrolysis solutions. Based on the Cl wt % obtained by microprobe analysis, the Cl yield after pyrohydrolysis was calculated (Table 5.1). Most of the pyrohydrolyzed samples were scapolite separates with the exception of sample RM01 (73% scapolite) and three Gruvberget samples (PN14, PN15 and PN16) (34% scapolite) with different grain sizes. The other minerals in these samples are included in Table 5.1. With the exception of the PN16 sample, the other three samples have a Cl yield of over 100%. Errors induced during counting of the scapolite separates could have affected the final yield. Two PN21 samples, had very low yields (24 and 38 %) that were reproduced in several pyrohydrolysis runs. In this case, the source of error is perhaps due to a lower percentage of the actual scapolite grains identified in the sample rather than the efficiency of the Cl extraction method. The efficiency of the pyrohydrolysis extraction was established by using a well characterized biotite sample. This biotite was used as internal standard and was run three times for comparison. The recovered solution was then analysed by IC obtaining Cl yields between 89 and 95% (Table 5.2).

5.3.4 Ion chromatography

Chloride and bromide concentrations in the pyrohydrolysis solutions were analysed at the University of Alberta in the Department of Earth and Atmospheric Sciences using a Dionex DX600 ion chromatograph with an AS-14A analytical column. A seven ion standard, blanks and an internal quality control standard were run along with the samples. Replicate analyses of standards and unknown were also carried out. The reported data have a calculated uncertainty of 5%. The detection limits for Br and Cl were 0.005 ppm.

5.3.5 Stable Cl isotopes

The Cl extracted from scapolite samples by pyrohydrolysis was contained in an aqueous solution after distillation. The Cl^- in this solution was precipitated as AgCl following the procedures described by Wassenaar and Koehler (2004), based on the early work by Eggenkamp (1994) and Magenheim et al. (1994). The solution was reacted with $AgNO_3$ to produce AgCl. The AgCl precipitates were retained on 0.45 μm glass filters and dried overnight. The AgCl samples were then reacted under vacuum with CH_3I at 80 °C for 48 hours to produce CH_3Cl, the analytical gas. The isotopic compositions were measured on a ThermoElectron MAT 253 mass spectrometer at the University of Texas-Austin under continuous flow. Delta values are reported in per mil notation relative to SMOC (standard mean ocean chloride). The precision of the method is ±0.2 ‰ based on the reproducibility of three seawater standards and one internal serpentinite standard.

5.4 Results

5.4.1 Major- and trace-element geochemistry of scapolites

5.4.1.1 Regional Na-Cl Metasomatism (RM)

This alteration type is represented by two samples from Nunasvaara and three samples from the Torneälven River outcrops. Sodium concentrations are high in sample RM01 (119920 ppm) and the lowest in sample RM12 (9635 ppm). Scapolites in samples RM07 and RM05 have Na concentrations of 92710 and 89660 ppm, respectively (Table 5.3 and Figure 5.5A). Overall, the Nunasvaara RM scapolites are characterized by relatively low Ca, intermediate K (Figure 5.5A and B) and low to intermediate SO_4 and Cl contents, (Figure 5.6). Sample RM07 has the highest Fe concentrations of all the samples analysed (Figure 5.5B) but its SO_4-CO_3-Cl composition is comparable with all the other Torneälven samples (Figure 5.6). Scapolites related to regional alteration have similar Cl and CO_3 compositions to the proximal metabasites (IOCG-M), but have higher SO_4 contents (Figure 5.6). Scapolites from Nunasvaara have the highest Cl contents in the samples analyzed, ~35000 ppm by both XRF microprobe and electron microprobe (Table 5.3). In the samples from Nunasvaara, Br was not analyzed.

The scapolites from Torneälven River have similar Cl concentrations (between 27070 and 27360 ppm by EPMA). In the Torneälven River samples, Br concentrations vary from 76 to 88 ppm. The Cl/Br molar ratios and the Br concentrations of the Torneälven River samples occur close together when Cl/Br molar ratios are plotted against Br concentrations (Figure 5.7A). RM scapolites have Cl/Br molar ratios that range from 639 to 770 (Figure 5.7A and B).

5.4.1.2 IOCG-Scapolite altered Metabasic Rocks (IOCG-M)

This alteration type is represented by three samples from Pahtohavare. Sodium concentrations in MB02 and MB10 are similar, 94660 and 94190 ppm, respectively. IOCG-M scapolites have intermediate Ca, Na and K compositions (Figure 5.5A). The

IOCG-M scapolites also have high K compositions, but data were only collected on two samples (Figure 5.5B). The IOCG Metabasic scapolites (IOCG-M) also have intermediate concentrations of Na, Cl and CO_3 concentrations are relatively high, but SO_4 contents are low and characteristic of the Pahtohavare scapolites (Figure 5.6). Scapolites associated with proximal metabasites (IOCG-M) have high Cl contents, whereas their low CO_3 contents appear to be characteristic of this alteration type (Figure 5.6). Chlorine concentrations are between 25000 and 28000 ppm in samples MB03 and MB10, respectively (Table 5.3). Sample MB02 contains some of the lowest Br concentrations measured in this set of samples; 36 ppm. The IOCG-M samples have a wide range in Cl/Br molar ratios (Figure 5.7A). Although only two samples were analysed for Na/Br molar ratios they fit well on the trend line depicted in Figure 5.7B.

5.4.1.3 IOCG-Proximal Scapolite-rich alteration/Na-Skarn (IOCG-PS)

The samples of this alteration type come from four deposits; three from Kallosalmi, two from Pahtohavare, four from Gruvberget and one from Sarkivaara. Sodium was only measured in six out of the ten samples from IOCG-PS alteration and ranges from 62330 ppm (PN19) to 104490 ppm (PN17) (Table 5.3). The sample with the highest Ca relative to Cl and Na is PN19 (Fig 5.5A), which belongs to the Sarkivaara deposit. IOCG-PS scapolites vary substantially in Cl and Ca contents. The IOCG-PS scapolites have the highest and lowest K and S contents of the three groups (Figure 5.5B). Scapolites from Sarkivaara are characterized by the highest SO_4 and CO_3 and intermediate Cl concentrations. The Gruvberget scapolites have intermediate to high SO_4 concentrations with low CO_3. Pahtohavare and Kallosalmi scapolites are characterized by low SO_4. Within the IOCG-PS scapolites, the Kallosalmi and the Pahtohavare samples have the highest Cl and CO_3 concentrations, respectively (Figure 5.6). Scapolites associated with proximal ore are divided in two compositional groups, one characterized by high Cl contents and the other with higher SO_4 compositions (Figure 5.6).

All samples have a range of Cl compositions from 10000 to 33000 ppm (Table 5.3). Chlorine concentrations in Kallosalmi (PN09, PN20 and PN21) and Pahtohavare (PN17 and PN18) samples are the same (33000 ppm via XRF microprobe). Electron microprobe analysis yielded a higher value for sample PN09 (36080 ppm) but lower for sample PN21 (30000 ppm). Gruvberget and Sarkivaara samples have the lowest Cl concentrations by both XRF microprobe and electron microprobe analyses. Chlorine in sample PN19 is particularly low, at 10000 ppm by XRF microprobe and 13170 ppm by EPMA.

The most remarkable characteristic of the of IOCG-PS scapolites is the high halogen contents detected in two samples. Sample PN19 has the lowest Cl/Br molar ratios of the samples analyzed (271), contrasting with sample PN14 that has the highest (2363), which is the highest amongst all scapolites analyzed in this study and published elsewhere (Pan and Dong, 2003; Hammerli et al. 2013, 2014) (Table 5.3).

5.4.2 Stable Cl isotopes

A scapolite from Nunasvaara belonging to the RM alteration group (RM01) yielded a δ^{37}Cl value of -0.1‰ (Table 5.3). Torneälven River samples have δ^{37}Cl values ranging from 0.0 to +0.3‰. Two scapolite samples from IOCG-M alteration at Pahtohavare yielded values of +0.2‰. Ten scapolite samples from IOCG-PS alteration had δ^{37}Cl values ranging from -0.1‰ to +1.0‰; the lowest values are from PN15 and PN18, and the highest from PN17. Scapolite samples from Kallosalmi tend to be slightly enriched in ^{37}Cl (+0.4‰ to +0.6‰) compared to Gruvberget scapolites (-0.1‰ to +0.3‰). The Sarkivaara sample has the second highest δ^{37}Cl value of the IOCG-PS alteration scapolites (+0.9‰).

5.5 Discussion

5.5.1 Chemical characteristics of scapolites

The chemical composition of the scapolites analysed indicate that they are all variations of marialitic scapolite with 1.0 to 3.6 wt % Cl, and 4.6 to 13.6 wt % CaO (Table 5.4). These ranges are comparable with the compositions of marialites from the Tienshan Fe Skarn deposit, China (Pan and Dong, 2003), the Marcona Magnetite deposit, Peru (Chen et al., 2010), and the Manto Verde IOCG, Chile (Benavides et al., 2007).

The differences in major-element chemistry in combination with the halogen contents of these marialites can provide some constraints on their origin. In Figure 5.7A, the three groups of scapolites overlap in the middle of the general trend, where four RM samples are located. The IOCG PS scapolites encompass almost the entire range of chemical compositions found in the other two mineralisation types; however, these samples are characterized by higher mass percentages of Ca and K. Although the IOCG PS scapolites do have higher Ca contents, Cl and Na still are the dominant anion and cation (Figure 5.7A).

The anion contents of the group of samples investigated (Figure 5.6), represent two compositional trends departing from high Cl concentrations. The first trend defined by IOCG-PS scapolites increases towards high SO_4 concentrations from Pahtohavare to Sarkivaara; the Cl-SO_4 trend. The second trend goes from high Cl to some of the highest CO_3 concentrations; the Cl-CO_3 trend, represented by samples from Kallosalmi and Pahtohavare. The RM scapolites appear associated with both IOCG compositional trends; scapolites from Nunasvaara follow the Cl-SO_4 trend, whilst scapolites from Torneälven are more related to the Cl-CO_3 trend. In any case, the range of compositions of the IOCG related alteration encompasses that of the regional metasomatic scapolites. Based on the age of the regional alteration at Nunasvaara 1903±8 Ma (Smith et al., 2009), it is possible that the RM scapolites may have been assimilated or recycled during the intrusion of the magmatic systems that are contemporaneous with IOCG mineralisation, dated at 1.88 to 1.85 Ga (Billström and Martinsson, 2000). This possibility will be explored in the next section in light of the halogen contents of these scapolites.

5.5.2 Origin of halogens in the Norrbotten Scapolites

It has been suggested that the regional metasomatic scapolites of Norrbotten were generated by the low- to medium-grade regional metamorphism of evaporite-bearing assemblages (Frietsch et al., 1997). Experiments with scapolite solid solutions at 750ºC and 4 kbar (Orville, 1975) found that the composition albite + halite favors the formation of marialite ($Na_4Al_3Si_9O_{24}Cl$), which suggests that the occurrence of marialite-rich scapolite is correlated with high NaCl activities. As a result, at these pressure and temperature conditions, Ellis (1978) suggested that regional Cl-rich scapolite is formed from the metamorphism of evaporite beds. In addition, this has been confirmed by more recent studies that have also suggested that the reaction of plagioclase with halite and calcite during regional metamorphism can also generate scapolite (Mora and Valley, 1989; Frietsch et al; 1997). However, the redistribution of Na, Cl and other components during regional metamorphism and circulation of hydrothermal fluids associated with magmatic intrusions have also been recognized as important processes in the Norrbotten region (Frietsch et al., 1997 and references therein).

Based on the halogen contents of IOCG-PS scapolites (Figure 7A), two end members are observed, one identified in the Sarkivaara scapolite with the lowest Cl/Br molar ratio (271), and the other represented by the Gruvberget scapolites with the highest Cl/Br molar ratios (942 to 2,363). The scapolites from these two deposits are also characterized by relatively high to intermediate SO_4 and high to intermediate CO_3 contents (Figure 5.6). The halogen compositions of IOCG-M scapolites fall between these two end members, but the samples with low Cl/Br molar ratios have the highest Br contents detected (Table 5.3). IOCG-M scapolites at Pahtohavare are characterized by low SO_4 and high Cl contents, with a range of low to intermediate CO_3 relative concentrations (Figure 5.6). RM scapolites from the Torneälven River have low Cl/Br molar ratios (639 to 770) bracketing seawater (650). Although Br was not analysed in samples from Nunasvaara their SO_4-Cl-CO_3 compositions are comparable with the Kallosami, Gruvberget and Pahtohavare scapolites.

Pan and Dong (2003), using XRF microprobe analysis of single grain scapolite samples, identified a marialite-fluid halogen distribution coefficient (K_D) of 0.97±0.08. K_D is defined as the concentration of the element in the mineral divided by the concentration of the element in the fluid or melt: $(Cl/Br)_{scapolite}/(Cl/Br)_{fluid}$. This small K_D value indicates that the Cl/Br molar ratio of the marialite resembles the Cl/Br molar ratio of the hydrothermal fluid, as observed in the Norrbotten scapolites (Figure 5.7B).

In Figure 5.7B, increasing halite dissolution results in fluids with high Na and Cl concentrations (e.g., Kesler et al. 1995). Formation waters with high Cl/Br and Na/Br ratios (greater than seawater) therefore, have been interpreted to contain additional Cl derived from halite dissolution in upper crustal environments. However, high Cl/Br molar ratios are also typical of magmatic fluids (e.g. Sanjuan et al., 1990, Böhlke and Irwin, 1992; Gleeson and Turner, 2007; Kendrick et al., 2012). A compilation of Cl/Br molar ratios of geothermal fluids associated with magmatic sources suggested that values between 600 and 2000 are indicative of magmatic origin (Böhlke and Irwin, 1992). However, lower Cl/Br molar ratios were measured in fluid inclusion leachates from the Bingham Canyon and the Butte porphyry copper deposits (Nahnybida et al., 2009) extending the range down to 271. Formation waters with high Br contents, and low Cl/Br ratios (less than seawater) are considered to have attained their salinity from a seawater source, where evaporation has resulted in the precipitation of halite, leaving the residual brine enriched in Br (Walter et al., 1990; Kesler et al., 1995). According to Figure 5.7B, and the Cl/Br molar ratios represented in Figure 5.7A, both evaporated seawater and halite dissolution and/or magmatic sources of salinity can be found in scapolites from the three types of alteration (RM, IOCG-M and IOCG-PS). However, evaporative residual brines are dominant at Sarkivaara and are also present in some Pahtohavare scapolites. This contrasts with the halogen sources of the regional-scale alteration scapolites from the Bamble Sector, SE Norway, where both magmatic sources and remobilization of meta-evaporites were ruled out (Kusebauch et al. 2015).

As mentioned before, the regional Na-alteration dated at 1903 ± 8 Ma (Smith et al., 2009), predates early Cu-mineralisation, dated from 1.88 to 1.85 Ga (Billström and Martinsson, 2000). The RM scapolites, although from one locality, have a restricted range in compositions unlike the IOCG-related scapolites, which have a wide range of chemical compositions. The early and late Cu-mineralisation in Norrbotten is associated with magmatic intrusions and magmatic-hydrothermal events (Gleeson and Smith 2009). The possible interaction with magmatic-hydrothermal fluids derived from mafic to felsic magmas (Bergman et al. 2001; Kathol and Martinsson, 1999; Romer et al., 1992) in combination with water-rock interaction with a high diversity of protoliths may explain the wide range of chemical compositions found in IOCG scapolites (Figs. 5.5A and 5.5B).

5.5.3 Isotopic fractionation between mineralising fluids and scapolites

The distribution of δ^{37}Cl values vs Cl/Br molar ratios (Figure 5.8) shows that some scapolites from all three alteration types plot within the evaporative brine field. However, the data from most of the scapolite samples analysed in the present study plot outside both the magmatic and evaporative brine fields. Ten of these scapolites have high Cl/Br molar ratios derived from halite dissolution or magmatic hydrothermal systems and do not support a pristine magmatic origin for the scapolite-forming fluid (Figure 5.8). However, to assess the original δ^{37}Cl values in the hydrothermal fluid, it is important to have an understanding of the chlorine isotope fractionation between the fluid and the scapolite.

A previous study on fluid inclusion leachates obtained a range of predominantly negative δ^{37}Cl values for fluid inclusions in the Norrbotten area (Gleeson and Smith, 2009). These values range from -5.6 to -1.3‰ in Greenstone- and Porphyry-hosted Cu-Au deposits and between -2.4 to +0.5‰ for Cu-Au deposits in the Nautanen Deformation Zone (NDZ); however overall, the majority of the samples had δ^{37}Cl values ranging from -3.5 to 0‰. These authors suggested that the lowest values were produced by fractionation processes between the hydrothermal fluids and minerals, like scapolite, in the alteration assemblages. The analysed quartz is found in veins that are spatially related to scapolite-bearing alteration (Gleeson & Smith) but it is unknown if isotopic equilibrium was attained between the two phases. This study offers a test to this hypothesis as we have analysed scapolite from the alteration selvage of a vein sample with a known fluid inclusion composition (MB02).

If equilibrium was attained in the formation of the hydrothermal scapolite, Rayleigh fractionation calculations can model the evolution of fluid δ^{37}Cl values measured in fluid inclusions from IOCG deposits at Norrbotten (Gleeson and Smith, 2009). More recently, fractionation calculations have been used to model δ^{37}Cl values measured in scapolite and amphibole alteration minerals associated with a shear zone in the Bamble sector, SE Norway (Kusebauch et al. 2015). In Kusebauch et al. (2015), the initial and remaining δ^{37}Cl values of the hydrothermal fluid are calculated assuming theoretical fractionation factors and measured δ^{37}Cl values in bulk-rock, amphibole and scapolite. This work concludes that the observed decrease in δ^{37}Cl values in the bulk-rock with increasing distance to a shear zone can be explained by a Rayleigh fractionation or a combination of Rayleigh and kinetic fractionation. Unlike this study, in the present work, the δ^{37}Cl composition of both fluid and scapolite are available for one sample (PAH88217). In that sample, the fluid inclusions yielded a δ^{37}Cl value of -1.7‰ (Gleeson and Smith, 2009) whereas the scapolite (this study) yielded a value of +0.2‰. From these two values it is possible to calculate a fluid-scapolite Cl-isotope fractionation factor ($\Delta^{37}\mathrm{Cl}_{\mathrm{scp-fluid}}$) of +1.9‰. This assumes that the analyzed fluid in the fluid inclusion was in isotopic equilibrium with the scapolite.

The main purpose of the Rayleigh fractionation model was to determine if this inferred fractionation factor was able to reproduce the low δ^{37}Cl values measured by Gleeson and Smith (2009).

The Cl isotope co-evolution of fluid and scapolite can be described by a Rayleigh fractionation model (Figure 5.9) using an equation adapted from Faure (1986):

$\delta^{37}Cl_{fluid} = (1000+ \delta^{37}Cl_{o\text{-}fluid})*F^{(\alpha-1)} -1000$ (1)

where $\delta^{37}Cl_{o\text{-}fluid}$ and $\delta^{37}Cl_{fluid}$ are the initial and final isotopic compositions of the hydrothermal fluid, respectively; F is the fraction of Cl left in the hydrothermal fluid after isotope fractionation between the scapolite and the hydrothermal fluid, and α is the observed isotope fractionation factor at a given temperature. Measurement of the Cl isotope composition of MORB samples suggests that the upper mantle has a δ^{37}Cl value ≤ -1.6‰ (Bonifacie et al. 2008 and Layne et al. 2009). Although this negative value for the upper mantle has been debated (Bonifacie et al. 2008), it is used here as the initial composition of the fluid ($\delta^{37}Cl_{o\text{-}fluid}$). As depicted in Figure 5.9, using this value we obtained several curves representing the isotope fractionation and the progressive decrease of Cl in the hydrothermal fluid as consequence of Cl uptake by the mineral phase. For comparison, the isotope fractionation coefficients used in our study and those reported in Kusebauch et al. (2015) for the Bamble scapolites are modeled. Although the isotope fractionation coefficients considered by Kusebauch et al. (2015) reproduced upper mantle values, the Rayleigh fractionation model applying the empirical +1.9‰ isotope fractionation value, is the only one that reproduces the lowest fluid inclusion δ^{37}Cl values measured in the set of samples reported in Gleeson and Smith (2009).

This large empirical fractionation factor between scapolite and fluid is not supported by the predictions for monovalent chlorides proposed by Schauble et al. (2003). According to their study small isotope fractionations should be expected between a brine with high NaCl activity and scapolite at equilibrium, between 0.37 and 0.68‰ at temperatures from 300 to 600 °C. Theoretical predictions by Schauble et al. (2003) were confirmed by Kusebauch et al. (2015) in scapolites from the Bamble Sector, SE Norway. However, the fractionation coefficients used by Kusebauch et al. (2015) (1.0005, 1.0007 and 1.0010) to model the Rayleigh fractionation of the hydrothermal fluid at Bamble, cannot produce the low δ^{37}Cl values measured in the fluid inclusions (Figure 5.9). This suggests either that isotopic equilibrium was not attained in our system or that such low fractionation factors may not be applicable to the Norrbotten scapolites.

There are some differences between the scapolites from Norrbotten and the Bamble Sector. For instance, the Norrbotten scapolites are classified as marialites whilst the Bamble scapolites vary from meionite to marialite perhaps reflecting different sources of salinity and water-rock interaction histories. According to Kusebauch et al. (2015) the Cl identified in the Bamble scapolites has a marine pore fluid origin. This contrasts with the Norrbotten scapolites, which contain Cl from diverse sources (Gleeson and Smith, 2009; this study). Also, at the Pahtohavare deposit, other Cl minerals such as amphibole and biotite have low Cl contents, well below 1 wt% (Alain, 2014), which contrasts with higher Cl contents reported in these minerals by Kusebauch et al. (2015) for the Bamble Sector. Furthermore, in our study the scapolite formation is associated with $CaCl_2$-rich and CO_2-bearing fluids (Gleeson and Smith, 2009), versus the high Na^+, Cl^- and CO_2 fluids identified in the Bamble scapolites (Kusebauch et al. 2015).

Unfortunatelly, the theroretical isotope fractionation estimates by Schauble et al. (2003) do not include $CaCl_2$-rich brines. None the less, assuming equilibrium, the observed isotope fractionation (+1.9‰) indicates that ^{37}Cl was preferentially accomodated in the A site of the scapolite structure. This suggests that the stable Cl isotope partition between the $CaCl_2$-rich brine and the scapolite may be different to the estimates for NaCl brines in equilibrium with silicate minerals considered by Schauble et al. (2003).

It is possible however, that the relatively high empirical fractionation factor obtained here indicates that fluid and mineral were not in isotopic equilibrium and therefore the values from the Norrbotten scapolites may reflect a kinetic isotope fractionation process. This interpretation is supported by data from other samples in this study. For example, there were high $\delta^{37}Cl$ values found in scapolites from two locations, Pahtohavare (+1.0‰) and Sarkivaara (+0.9‰) (Table 5.3). The Pahtohavare and Sarkivaara samples have Cl/Br molar ratios of 554 and 271, respectively, which are consistent with typical Cl/Br molar ratios for evaporitic brines. If we use the inferred fractionation factor (+1.9‰) the calculated $\delta^{37}Cl$ value for the hydrothermal fluid is around -1.0‰, which is too low for an evaporitic brine. This assumes that the variations in δ^{37}Cl values for marine Phanerozoic evaporites (0.0 and 0.9‰) (Eastoe et al. 1999; Eastoe et al. 2007) also apply to Paleoproterozoic evaporites.

If the scapolite investigated in the present study and the hydrothermal fluid did not reach isotopic equilibrium, the low δ^{37}Cl values identified in fluid inclusions by Gleeson and Smith (2009) must be explained by some other process. These may include water-rock interaction, kinetic isotope fractionation or an unknown source of Cl. None of these options can be assessed in light of the lack of experimental data that quantify the behavior of the stable Cl isotopes water rock interaction. Future work should focus on fractionation experiments.

5.6 Conclusions

The scapolites investigated from the Norrbotten County have a predominantly marialitic composition. Some chemical variations are present particularly in samples from IOCG-PS alteration, which are more Ca and S enriched and Na and Cl depleted. In contrast, IOCG-M scapolites are more Cl and Fe rich, but depleted in Ca. The RM scapolites have intermediate compositions. In addition, relative SO_4-Cl-CO_3 compositions and temporal correlations suggest that RM scapolites may have been incorporated or recycled into the later IOCG alteration. This is also confirmed by the halogen compositions of Kallosalmi, Gruvberget, Pahtohavare, Nunasvaara and Torneälven scapolites. Some scapolite samples from Pahtohavare and the sample from the Sarkivaara deposit contain lower than seawater Cl/Br molar ratios (554 and 271), indicating the presence of evaporative residual brines. All the other scapolites had Cl/Br molar ratios related to seawater, magmatic or evaporitic sources.

Based on the chemistry of these scapolites, it is concluded here that the RM alteration resulted from a hydrothermal fluid of homogeneous composition, owing to a more restricted availability of protoliths and fluids. Whilst, IOCG-M and IOCG-PS alterations had several sources including: magmatic, metamorphic and evaporitic (halite and residual brine) sources.

Measured δ^{37}Cl values in fluid inclusions (Gleeson and Smith, 2009) and spatially related scapolite in one of the samples allowed the calculation of an empirical isotope fractionation of +1.9‰ between the mineral and the fluid. This value contradicts predictions for isotope fractionation between a silicate mineral such as scapolite and a monovalent hydrothermal fluid with high NaCl activities. However, using a Rayleigh fractionation model starting with an inferred upper mantle value of -1.6‰, we reproduced the lowest δ^{37}Cl values reported by Gleeson and Smith (2009) in fluid inclusions from deposits of the Norrbotten County. Conversely, if the scapolite investigated in the present study and the hydrothermal fluid did not reach isotopic equilibrium, the low δ^{37}Cl values identified in fluid inclusions by Gleeson and Smith (2009) must be explained by some other unknown process. These may include water-rock interaction, kinetic isotope fractionation or an unknown source depleted in δ^{37}Cl. Our results suggest that more that experiemental data on fractionation factors for the scapolite-hydrothermal fluid system are needed to test the theoretical predictions proposed by Schauble et al. (2003).

The complex geologic history of the Norrbotten district is reflected in the chemical and isotopic composition of its mineral alteration. Owing to the persistence of regional metamorphism and the recurrence of magmatic episodes, the hydrothermal fluids contain both recycled and new components that formed the proximal scapolites. Whilst halogen and Cl isotope compositions of IOCG alteration appear more representative of the original hydrothermal fluids, more research has to be done to better understand the evolution of the Cl isotopes in RM scapolites, and the extent of the Cl isotopic fractionation at high temperatures between hydrothermal fluids and Cl-bearing minerals.

5.7 References

Alain V. 2014. Mineral chemistry and texture paragenesis of alteration minerals in the Patohavare Cu-Au deposit, Sweden. Master’s Thesis. Luleå university of Technology.

Barnes J. D. and Cisneros M., 2012. Mineralogical controls on the chlorine isotopic composition of altered oceanic crust. Chem. Geol. 326-327: 51-60.

Barnes, J.D., and Sharp, Z.D., 2006. A chlorine isotope study of DSDP/ODP serpentinized ultramafic rocks: insights into the serpentinization process. Chem. Geol. 228, 246- 265.

Barton M. D. and Johnson D. A., 1996. Evaporitic-source model for igneous-related Fe oxide-(REE–Cu–Au–U) mineralisation. Geology 24, 259–262.

Barton, M. D. & Johnson, D. A., 2000. Alternative brine sources for Fe-oxide Cu-Au systems: Implications for hydrothermal alteration and metals. In: Porter, T. M. (ed.) Hydrothermal Iron Oxide Copper-Gold and Related Deposits: A Global Perspective. Adelaide: Austra. Min. Foun., 43-60.

Benavides J., Kyser T., Clark A., Oates C., Zamora, R. Tarnovschi R., Castillo B., 2007. The Mantoverde iron oxide-copper-gold district, III region, Chile; the role of regionally derived, nonmagmatic fluids in chalcopyrite mineralisation. Econ. Geol. 102, 415-440.

Bergman S., Ku¨ bler L. and Martinsson O., 2001. Description of the Regional Geological and Geophysical Maps of Northern Norrbotten County (East of the Caledonian Orogen). Geological Survey of Sweden (Sveriges Geologiska Underso¨kning). Ba56, 110.

Billström K. and Martinsson O., 2000. Links between epigenetic Cu–Au mineralisations and magmatism/deformation in the Norrbotten County, Sweden. In: 2nd GEODE Fennoscandian Shield Field Workshop on Palaeoproterozoic and Archaean Greenstone Belts and VMS Districts in the Fennoscandian Shield, Lulea University of Technology, Research Report 06, p. 6.

Bonifacie M., Jendrzejewski N., Agrinier P., Coleman M., Pineau F. and Javoy M., 2007. Pyrohydrolysis-IRMS determination of silicate chlorine stable isotope compositions. Application to oceanic crust and meteorite samples. Chem. Geol. 242, 187-201.

Bonifacie, M., Jendrzejewski, N., Agrinier, P., Humler, E., Coleman, M., and Javoy, M., 2008. The chlorine isotope composition of Earth's mantle: Science 359, 1518–1520.

Böhlke J. and Irwin J., 1992. Laser microprobe analyses of Cl, Br, I, and K in fluid inclusions: implications of sources in some ancient hydrothermal fluids. Geochim. Cosmochim. Acta 56, 203-225.

Chen H., Clark A. and Kyser K., 2010. The Marcona magnetite deposit, Ica, south-central Peru: A product of hydrous, iron-oxide-rich melts?. Soc. Econ. Geol. 105, 1441-1456.

Chiaradia M., Banks D. A., Cliff R., Marschik R. and de Haller A., 2006. Origin of fluids in iron oxide–copper–gold deposits: constraints from δ^{37}Cl, Sr^{87}/Sr^{86} and Cl/Br. Mineral Deposits. 41, 565–573.

Corriveau L., 2007. Iron oxide copper-gold deposits: a Canadian perspective. Mineral Deposits of Canada: a Synthesis of Major Deposit-Types, District Metallogeny, the Evolution of Geological Provinces and Exploration Methods. Geol. Asso. Can. Min. Dep. Div., Spe. Vol. 5, 307-328.

Dong P., 2005. Halogen-element (F, Cl and Br) behaviour in apatites, scapolite, and sodalite: an experimental investigation with field applications. Thesis. Department of Geological Sciences. University of Saskatchewan. 234p.

Edfelt, Å. Armstrong, R. N., Smith, M. P. & Martinsson, O., 2005. Alteration aragenesis and mineral chemistry of the Tjärrojäkka apatite-iron and Cu (-Au) occurrences, Kiruna area, northern Sweden. Mineral. Dep. 40, 409-434.

Ellis D., 1978. Stability and phase equilibria of chloride and carbonate bearing scapolite at 750 and 400 bar. Geochim. et Cosmochim. Acta. 42, 1271-1281.

Faure G., 1986. Principles of Isotope Geology. second ed. J.Wiley and Sons, p. 589.

Fisher L. A. and Kendrick M. A., 2008. Metamorphic fluid origins in the Osborne Fe oxide–Cu–Au deposit, Australia: evidence from noble gases and halogens. Min. Dep. 43, 483–497.

Frietsch, R., Tuisku, P., Martinsson, O. & Perdahl, J. A. 1997. Early Proterozoic Cu-(Au) and Fe ore deposits associated with regional Na-Cl metasomatism in northern Fennoscandia. Ore Geol. Rev. 12, 1-34.

Gleeson S. A. 2003. Bulk analysis of electrolytes in fluid inclusions. Fluid inclusions: Analysis and interpretation, Short course series 32, 233-246.

Gleeson, S.A., and Smith, M.P., 2009. The sources and evolution of mineralising fluids in Fe oxide-apatite and iron oxide-copper-gold systems, Norrbotten, Sweden: Constraints from stable Cl isotopes of fluid inclusion leachates. Geochim. Cosmochim. Acta 73, 5658-5672.

Gleeson S.A., Turner W.A., 2007. Fluid inclusion constraints on the origin of the brines responsible for Pb-Zn mineralisation at Pine Point and coarse non-saddle and saddle dolomite formation in southern Northwest Territories. Geofluids 7, 51–68.

Hammerli J, Rusk B, Spandler C, Emsbo P, Oliver N.H.S., 2013. In situ quantification of Br and Cl in minerals and fluid inclusions by LA-ICP-MS: A powerful tool to identify fluid sources. Chem. Geol. 337-338, 75-87.

Hammerli J., Spandler C., Oliver N.H.S., Rusk B., 2014, Cl/Br of scapolite as a fluid tracer in the earth's crust: insights into fluid sources in the Mary Kathleen Fold Belt, Mt. Isa Inlier, Austra. Jour. Met. Geol. 32, 93-112.

Jambon A., De´ruelle B., Dreibus G. and Pineau F., 1995. Chlorine and bromine abundance in MORB: the constrasting behaviour of the Mid-Atlantic Ridge and East Pacific Rise and implications for chlorine geodynamic cycle. Chem. Geol. 126, 101–117.

Johnson L. H., Burgess R., Turner G., Milledge J. H. and Harris J. W., 2000. Noble gas and halogen geochemistry of mantle fluids: comparison of African and Canadian diamonds. Geochim Cosmochim. Acta 64, 717–732.

Kendrick M. A., Mark G. and Phillips D., 2007. Mid-crustal fluid mixing in a Proterozoic Fe oxide–Cu–Au deposit, Ernest Henry, Australia: evidence from Ar, Kr, Xe, Cl, Br, and I. Earth Planet. Sci. Lett. 256, 328–343.

Kendrick M. A., Honda M., Gillen D., Baker T. and Phillips D., 2008a. New constraints on regional brecciation in the Wernecke Mountains, Canada from He, Ne, Ar, Kr, Xe, Cl, Br and I in fluid inclusions. Chem. Geol. 255, 33–36.

Kendrick M. A., Baker T., Fu B., Phillips D. and Williams P. J., 2008b. Noble gas and halogen constraints on regionally extensive mid-crustal Na–Ca metasomatism, the Proterozoic Eastern Mount Isa Block, Australia. Precambrian Res. 163, 131–150.

Kendrick M. A., Kamenetsky V. S., Phillips D. and Honda M., 2012, Halogen systematics (Cl, Br, I) in Mid-Ocena Ridge Basalt: a Macquarie Island case study. Geochim. Cosmochim. Acta 81, 82-93.

Kesler S. E., Appold M. S., Martini A. M., Walter L. M., Huston T. J. and Kyle J. R., 1995. Na–Cl–Br systematics of mineralising brines in Mississippi Valley-type deposits. Geology 23, 641–644.

Kusebauch C., John T., Barnes J. and Klügel A and Austrheim H., 2015. Halogen element and stable chlorine isotope fractionation caused by fluid–rock interaction (Bamble Sector, SE Norway). Jour. Petrol. doi:10.1093/petrology/egv001.

Layne G. D., Kent A. J. R. and Bach W., 2009. δ^{37}Cl systematic of back-arc spreading: the Lau Basin. Geology 37, 427–430.

Lindblom, S., Broman, C. & Martinsson, O., 1996. Magmatic-hydrothermal fluids in the Pahtohavare Cu-Au deposit in greenstone at Kiruna, Sweden. Mineral. Dep. 31, 307-318.

Martinsson, O., 1997.Tectonic setting and Metallogeny of the Kiruna Greenstones. Doctoral thesis, Lule University of Technology.

Martinsson, O., 2004. Geology and Metallogeny of the Northern Norrbotten Fe^Cu^Au Province. In: Allen, R. L., Martinsson, O. & Weihed, P. (eds) Svecofennian Ore-Forming Environments: Volcanic-Associated Zn-Cu-Au-Ag, Intrusion-Associated Cu-Au, Sediment- Hosted Pb-Zn, and Magnetite-Apatite Deposits of Northern Sweden, Soc. Econ. Geol. Guidebook Series 33, 131-148.

Martinsson, O. and Virkkunen, R., 2004. Apatite Iron Ores in the Gällivare, Svappavaara, and Jukkasjä rvi Areas. In: Allen, R. L., Martinsson, O. & Weihed, P. (eds) Svecofennian Ore-Forming Environments: Volcanic-Associated Zn-Cu-Au-Ag, Intrusion-Associated Cu-Au, Sediment-Hosted Pb-Zn, and Magnetite-Apatite Deposits of Northern Sweden, Soc. Econ. Geol. Guidebook Series 33,167-172.

Mora, C.I. and Valley, J.W., 1989. Halogen-rich scapolite and biotite: Implications for metamorphic fluid-rock interaction. The Amer. Mineral. 74, 721-737.

Nahnybida T., Gleeson S.A, Rusk B. and Wassenaar L., 2009. Cl/Br ratios and stable chlorine isotope analysis of magmatic-hydrothermal fluid inclusions from Butte, Montana and Bingham Canyon, Utah. Miner. Deposita 44, 837-848.

Oliver, N. H. S., Cleverley, J. S., Mark, G., Pollard, P. J., Bin Fu, , Marshall, L. J., Rubenach, M. J., Williams, P. J. & Baker, T., 2004. Modeling the role of sodic alteration in the genesis of iron oxide-copper-gold deposits, eastern Mount Isa block, Australia. Econ. Geol. 99, 1145-1176.

Orville M. P., 1975. Stability of scapolite in the system Ab-An-NaCl-$CaCO_3$ at 4kb and 750ºC. Geochim. Cosmochim. Acta. 39, 1091-1105.

Pan Y. and Dong P., 2003. Bromide in scapolite-group minerals and sodalite: XRF microprobe analysis, exchange experiments, and application to skarn deposits. The Can. Mineral. 41, 559-540.

Pollard P. J., 2000. Evidence of a magmatic fluid and metal source for Fe-oxide Cu–Au mineralisation. In Hydrothermal Iron Oxide Copper–Gold and Related Deposits: A Global Perspective (ed. T. M. Porter). Austral. Mineral Found. 27–41.

Pollard P. J., 2006. An intrusion-related origin for Cu–Au mineralisation in iron oxide–copper–gold (IOGC) provinces. Min. Dep. 41, 179–197.

Romer R.L., Kjösnes B., Korneliussen A., Lindah, I., Skysseth T., Stendal, H. & Sundvoll B, 1992. The Archaean-Proterozoic boundary beneath the Caledonides of northern Norway and Sweden: U-Pb, Rb-Sr and Nd isotopic data from the Rombak-Tysfjord area: Norges Geologiske Undersøkelse, Rapport 91, 225, 67 p.

Romer, R.L., Martinsson, O., and Perdahl, J.-A., 1994. Geochronology of the Kiruna iron ores and hydrothermal alterations: Econ. Geol. 89, 1249–1261.

Sanjuan B., Michard G., Michard A., 1990. Origine des substances dissoutes das les eaux des sources thermals et des forages de la région Asal Ghoubbet (République de Djibouti). J. Volcanol. Geoth. Res 43,333-352.

Sharp Z., Barnes J., Brearley A., Chaussidon M., Fischer T. and Kamenetsky V., 2007. Chlorine isotope homogeneity of the mantle, crust and carbonaceous chondrites. Nature, Lett. 446, nature05748.

Schauble E., Rossman G. and Taylor H., 2003. Theoretical estimates of equilibrium chlorine-isotope fractionations. Geochimica and Cosmochimica Acta. 67. 17: 3267-3281.

Smith, M. P., Coppard, J., Herrington, R. & Stein, H., 2007. The geology of the Rakkurijärvi Cu-(Au) prospect, Norrbotten: A new IOCG deposit in Northern Sweden. Econ. Geol. 102, 393-414.

Smith, M.P., Storey, C.D., Jeffries, T.E., and Ryan, C., 2009. In Situ U-Pb andTrace Element Analysis of Accessory Minerals in the Kiruna District, Norrbotten, Sweden: New Constraints on the Timing and Origin of Mineralisation. J. Petrol. 50, 2063-2094.

Smith M.P., Gleeson S.A., and Yardley B.W.D., 2012, Hydrothermal fluid evolution and metal transport in the \Kiruna District, Sweden: Constraining metal behaviour in aqueous and aqueous-carbonic brines. Geochim et Cosmochim, Acta. 102: 89-112.

Walter, L. M., Stueber, A. M., and Huston, T. J., 1990. Br-Cl-Na systematics in Illinois Basin fluids: Constraints on fluid origin and evolution: Geology 18, 315–318.

Wanhainen C., Broman C., and Marinsson O., 2003. The Aitik Cu-Au-Ag deposit in northern Sweden: a product of high salinity fluids. Mineral. Dep. 38, 715-726.

Wanhainen C., Broman C., Martinsson O., and Magnor B., 2012. Modification of a paloeproterozoic porphyry-like system: Integration of structural geochemical, petrographic, and fluid inclusion data from the Aitik Cu-Au-Ag deposit, northern Sweden. Ore Geol. Rev. 48, 306-331.

Wägman, K. & Ohlsson, L. G., 2000. Exploration opportunities in Norrbotten: Municipality of Kiruna. Stockholm: Mineral Resources Information Office, Sveriges Geologiska Undersökning, 278 p.

Whitehead D. and Tomas J. E., 1985. Use of a Nebulizer in pyrohydrolytic Decomposition of silicate materials for determination of fluorine and chlorine. Anal. Chem. 57, 2421-2423.

Williams P.J., Barton M.D., Johnson D.A., Fontboté L., de Haller A., Mark G., Oliver N.H.S., Marschik R., 2005. Iron oxide–copper–gold deposits: geology, space–time distribution, and possible modes of origin. In: Hedenquist JW, Thompson JFH, Goldfarb RJ, Richards JP (eds) Econ. Geol. 100 Anniversary Volume, 371–405.

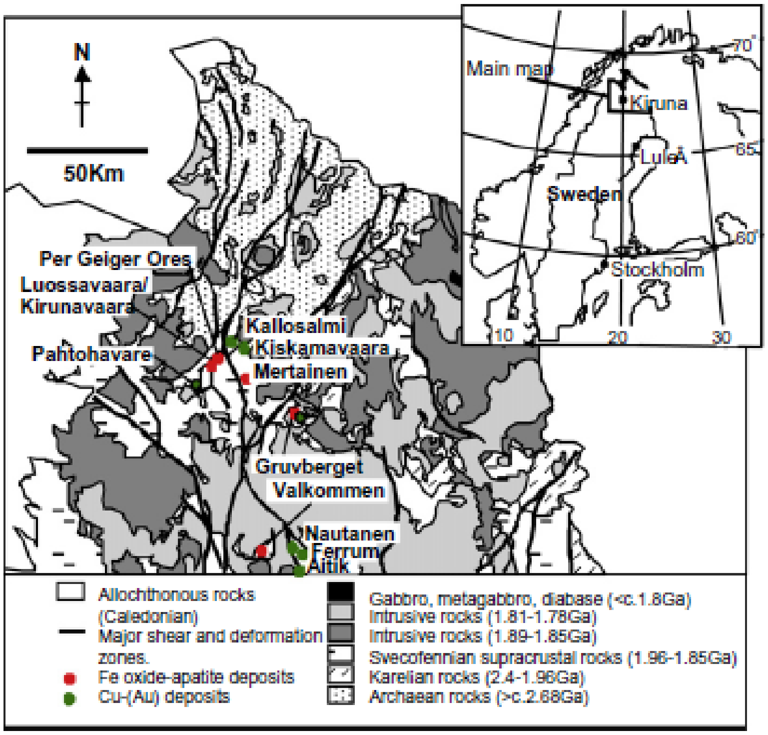

Figure 5-1 Location of the Norrbotten district, North Sweden.
Geology from Bergman et al. (2001).

Figure 5-2 Field context of scapolitisation, Norrbotten.
(A) Scapolite altered, greenschist facies metabasite, Torneälven River. Scapolite veins with actinolite selvedges cut the outcrop (RM). (B) Well preserved greenschist facies pillow breccia, Torneälven River. Matrix is intensely scapolite-albite altered. Pillows and clasts also pervasively altered with actinolite on margins (RM). (C) Scapolite-altered diorite, Nunasvaara (RM). (D) Scapolite-albite altered metasediment in breccia hosting. Sedimentary lamination is still preserved. Matrix is actinolite (RM). (E) Scapolite alteration in greenschist facies dolerite dyke rock, Pahtohavare (IOCG-M). (F) Magnetite-actinolite-calcite vein cutting intensely Na-altered metavolcanic rock. Gruvberget (IOCG-PS). Photos cortesy of M. Smith.

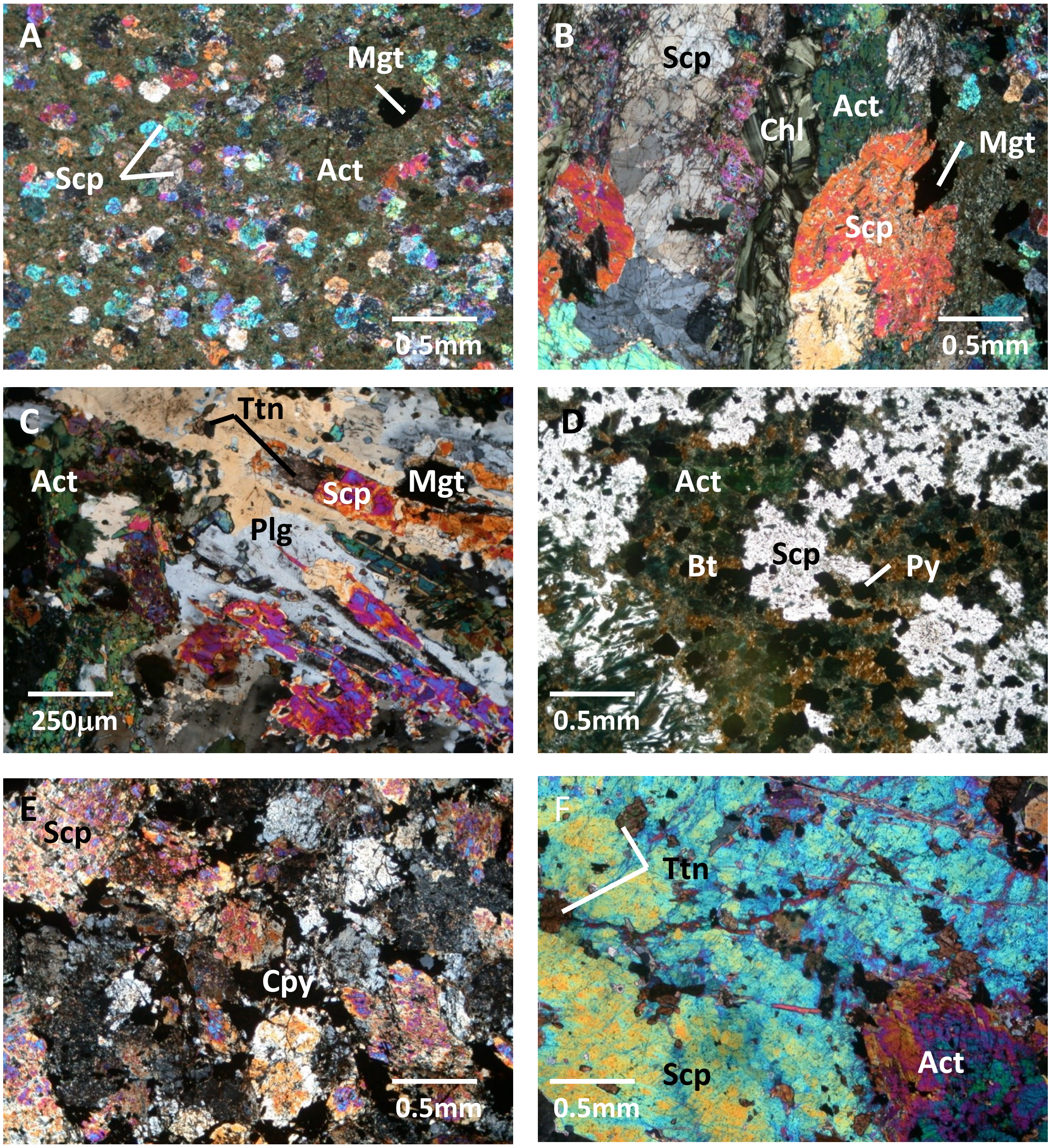

Figure 5-3 Representative textures in scapolite.
(A) 04Torn1 – Scapolite in greenschist facies pillow basalt (RM). (B) 04Torn1 – Scapolite-actinolite-chlorite vein in metabasalt. (C) N3.4D - Scapolite replacing plagioclase in meta-diorite (RM). (D) PAH88097 33.95m – Scapolite-actinolite-biotite alteration of dolerite dyke (IOCG-M). (E) PAH88093 19.35m – Scapolite metasomatite associated with chalcopyrite mineralisation (IOCG-PS). (F) SAR1 – Scapolite metasomatite ('Na-skarn') associated with chalcopyrite and molybdenite mineralisation (IOCG-PS). Act- actinolite; Scp – Scapolite; Ttn – Titanite; Plg – Plagioclase; Mgt – Magnetite; Chl – Chlorite; Bt – Biotite; Py – Pyrite; Cpy – Chalcopyrite.

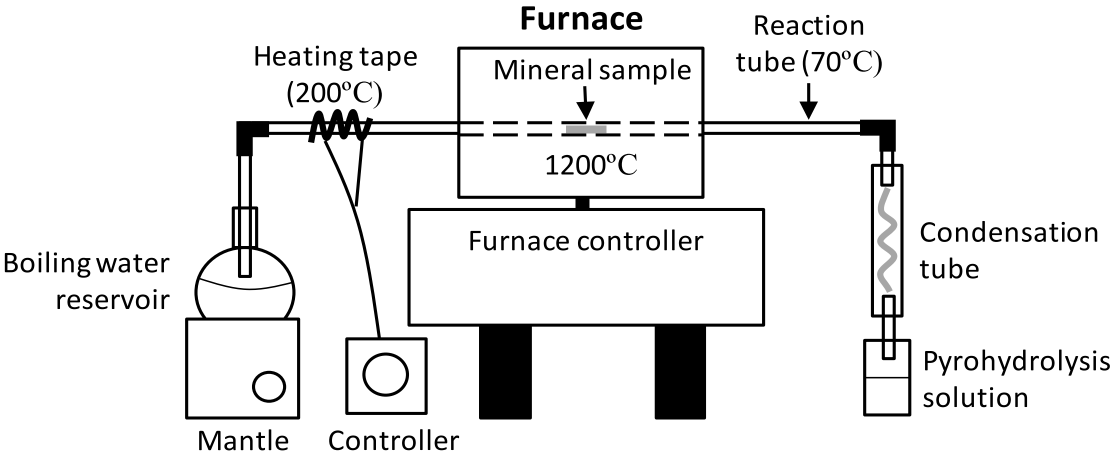

Figure 5-4 Schematics of the pyrohydrolysis apparatus used to extract Cl from scapolites.

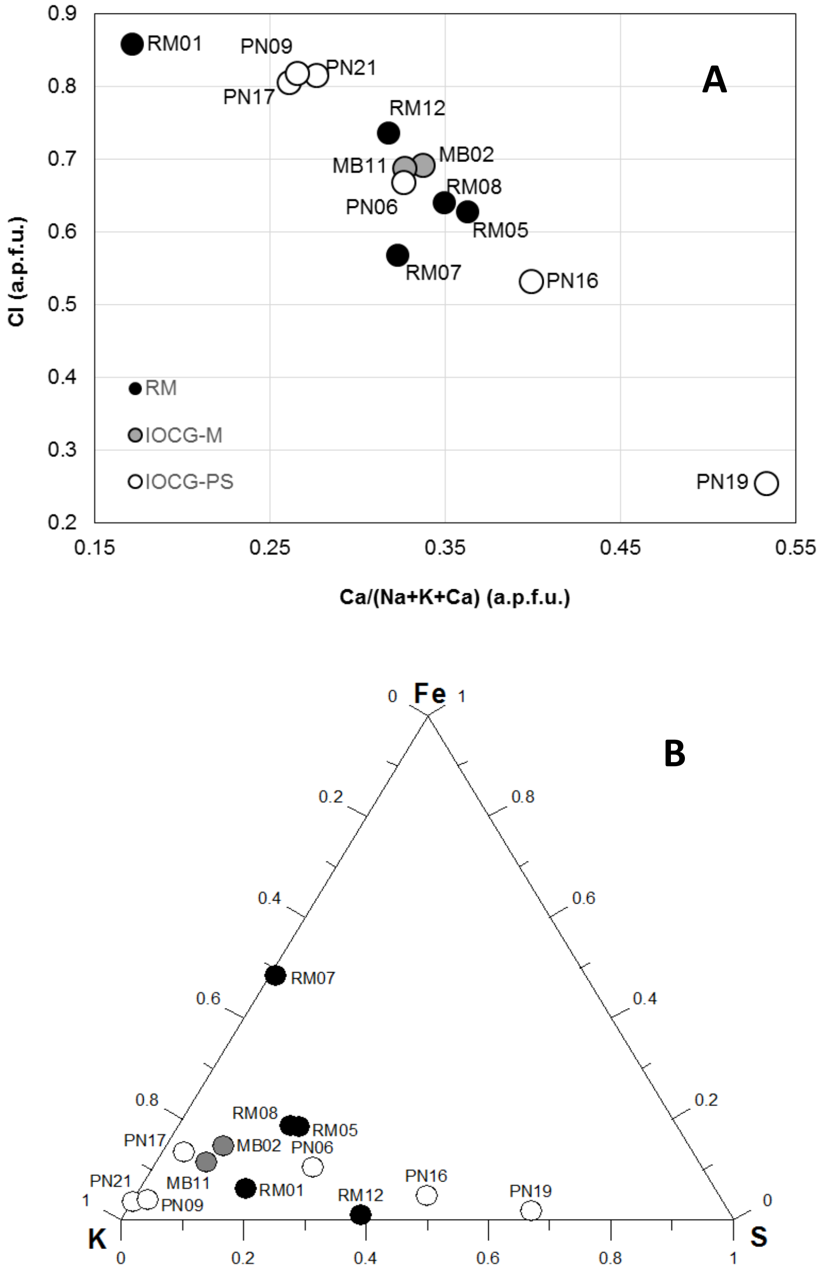

Figure 5-5 Distribution of major ions in scapolites.
A) Cl vs. Ca/(Na+K+Ca) (a.p.f.u.). B) Fe-S-K. Regional Na-Cl metasomatism (RM) alteration, IOCG-Scapolite altered metabasites (IOCG-M) and IOCG-Proximal Scapolite-rich alteration/Na-Skarn (IOCG-PS).

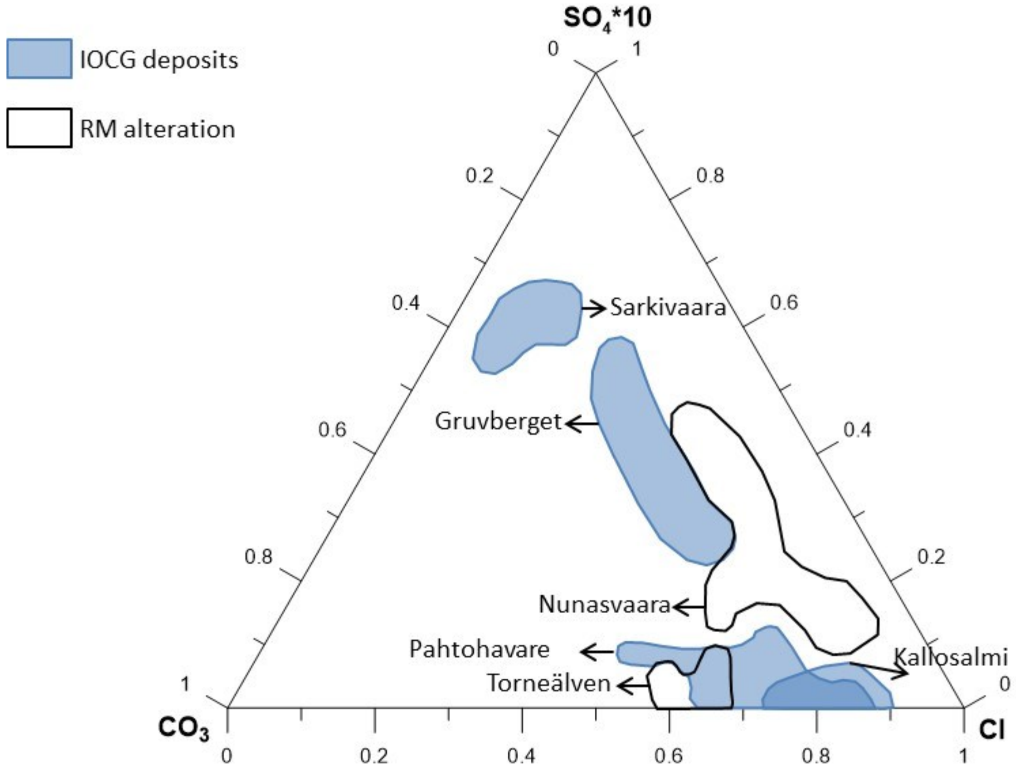

Figure 5-6 Ternary diagram SO_4-Cl-CO_3.

Relative anion contents of scapolites in atomic proportions from formulae calculated assuming 12 (Si, Al). Carbonate was calculated by difference assuming a full anion site occupancy. IOCG deposits: IOCG-PS and IOCG-M. Fields are made of individual EMPA points (Table 5.3).

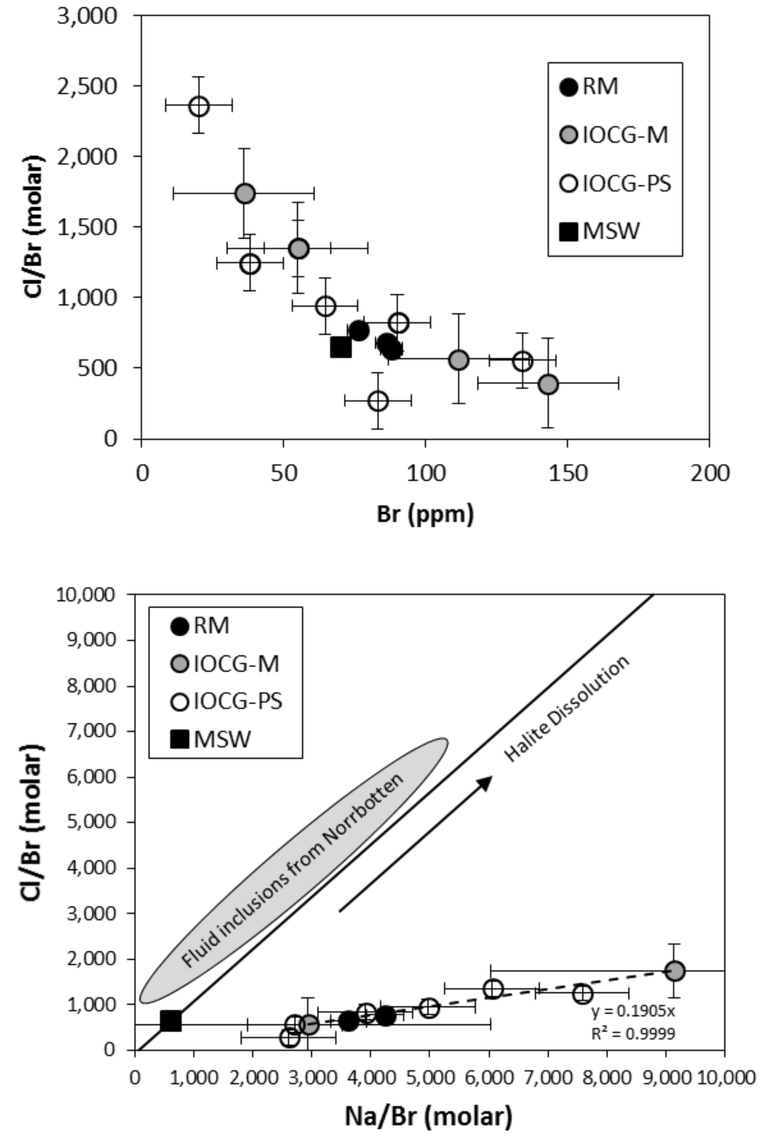

Figure 5-7 Halogen compositions and Na-Cl-Br systematic diagrams.

A) Cl/Br molar ratios vs Br concentrations and B) Na-Cl-Br systematic diagram. The samples with available Na data: two RM, two IOCG-M and nine IOCG-PS samples were plotted on this diagram (three of them overlapped due to their similar molar ratios). Regional Na-Cl Metasomatism alteration (RM), IOCG-scapolite altered metabasites (IOCG-M) and IOCG-proximal scapolite-rich alteration/Na-Skarn (IOCG-PS). Fluid inclusion data from Gleeson and Smith (2009) MSW: modern seawater.

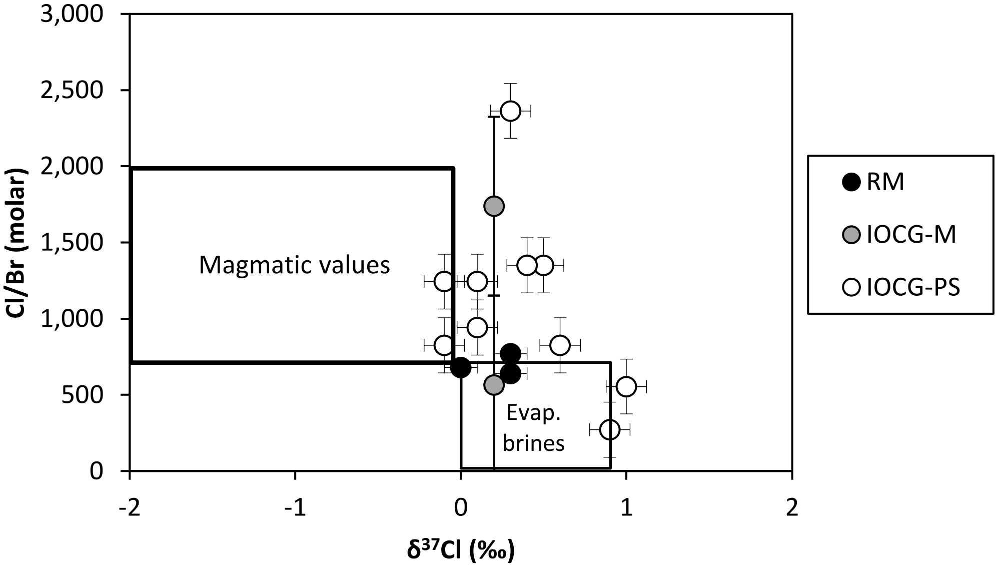

Figure 5-8 δ^{37}Cl values vs. Cl/Br molar ratios.

Data includes regional Na-Cl metasomatism (RM) alteration, IOCG-Scapolite altered metabasites (IOCG-M) and IOCG-Proximal Scapolite-rich alteration/Na-Skarn (IOCG-PS) samples. Cl/Br molar ratios and δ^{37}Cl values for magmatic sources from Jambon et al., (1995), Johnson et al., (2000), Sharp et al., (2007), Bonifacie et al. (2008), Layne et al. (2009) and Gleeson and Smith (2009). Evaporites values from Eastoe et al. (1999) and Eastoe et al. (2007).

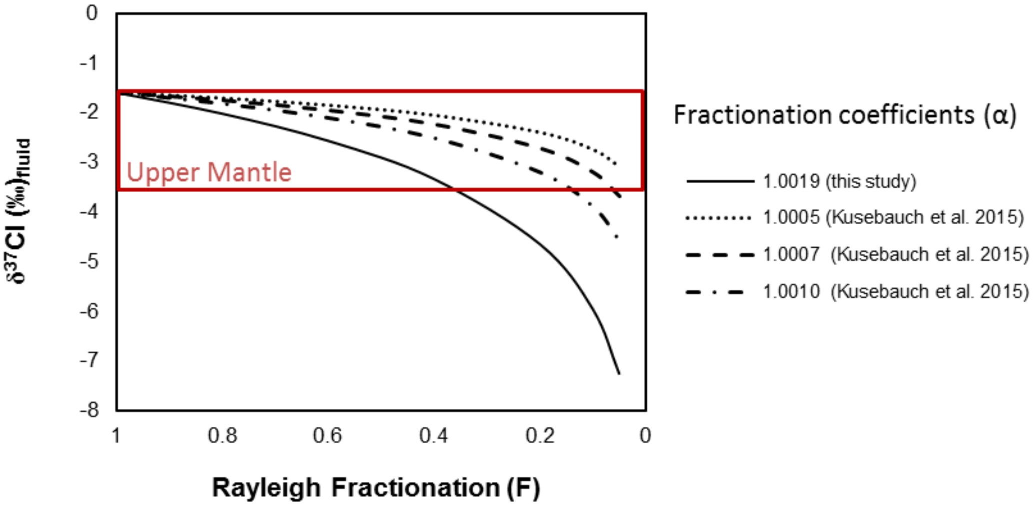

Figure 5-9 Rayleigh distillation curves.
Evolution of the fluid using the equation: $\delta^{37}Cl_{fluid}=(1000+\delta^{37}Cl_{o\text{-}fluid})*F^{(\alpha-1)}$ -1000 (adapted from Faure, 1986). Where, $\delta^{37}Cl_{o\text{-}fluid}$ and $\delta^{37}Cl_{fluid}$ are the initial and final isotopic compositions of the hydrothermal fluid, respectively; F is the fraction of Cl left in the hydrothermal fluid after isotope fractionation between the scapolite and the hydrothermal fluid, and α is the observed isotope fractionation factor at a given temperature. Using this equation starting with an initial upper mantle δ^{37}Cl value (Bonifacie et al. 2008), hydrothermal fluid values identified by Gleeson and Smith (2009) are reproduced.

Table 5-1 Pyrohydrolysis extraction results.
Sample size fraction, Cl concentrations by microprobe and ion chromatography, and pyrohydrolysis extraction yields in scapolites.
RM: samples from RM alteration; MB: samples from IOCG-M alteration; PN: samples from IOCG-PS alteration.

Sample	ID	Minerals by SEM	Mineralization	Sample size fraction (µm)	Sample weight (mg)	Microprobe		I.C.	Pyrohydrolysis			Scapolite grains %
						Cl (wt%)	Cl (mg)	Cl (ppm)	Solution (mL)	Cl (mg)	Yield %	
03NUN29	RM01	Scp, Alb and Ksp	RM	125-250	125	3.5	3.18	34.00	113	3.84	121	73
04TORN1veinwr	RM13	Scp	RM	100-125	98	2.5	2.45	18.00	100	1.80	73	100
04 TORN 1 vein	RM07	Scp	RM	250-500	150	2.6	3.90	20.92	134	2.80	72	100
04 TORN 1 vein	RM08	Scp	RM	100-250	153	2.6	3.98	21.50	130	2.80	70	100
04 TORN 2	RM05	Scp	RM	250-125	160	2.5	4.00	32.25	123	3.97	99	100
PAH 88217	MB02	Scp	IOCG-M	125-250	174	2.8	4.84	38.16	118	4.50	93	100
03PAH3	MB10	Scp	IOCG-M	125-250	122	2.8	3.42	32.00	90	2.88	84	100
KAL 90107 56.38m	PN09	Scp	IOCG-PS	125-250	130	3.3	4.29	24.00	161	3.86	90	100
KAL 90106 118.4m	PN21	Scp	IOCG-PS	100-125	146	3.3	4.82	9.32	124	1.16	24	100
KAL 90106	PN20	Scp	IOCG-PS	125-250	150	3.3	4.95	14.84	126	1.87	38	100
PAH 88093	PN17	Scp	IOCG-PS	100-125	152	3.3	5.02	40.21	103	4.14	83	100
PAH 88093	PN18	Scp	IOCG-PS	125-250	114	3.3	3.76	29.31	100	2.93	78	100
G1-1	PN16	(Alb+An), Qz, Scp, Ksp, Cal	IOCG-PS	100-125	160	2.1	1.14	9.47	108	1.02	90	34
G1-1	PN14	(Alb+An), Qz, Scp, Ksp, Cal	IOCG-PS	250-500	147	2.1	1.05	14.91	100	1.49	142	34
G1-1	PN15	(Alb+An), Qz, Scp, Ksp, Cal	IOCG-PS	125-250	157	2.1	1.12	11.70	107	1.25	112	34
G4-1	PN06	Scp	IOCG-PS	125-250	125	2.7	3.38	26.30	100	2.63	78	100
SAR1	PN19	Scp	IOCG-PS	125-250	226	1.0	2.26	18.44	111	2.05	91	100

Scp: scapolite
Alb: albite
Ksp: potassium feldspar
An: anorthite
Qz: quartz
Cal: calcite

Table 5-2 Efficiency of the pyrohydrolysis method using the internal biotite standard.

Sample	Cstd (ppm)	Mass Measured (g)	Cl expect	Cl by IC (ppm)	Vol Recov	Cl Recov	Yield %
Bt1	1900	0.1144	0.2174	1.56	124	0.1934	89
Bt2	1900	0.1009	0.1917	1.49	118	0.1758	92
Bt3	1900	0.1073	0.2039	1.68	115	0.1932	95

Table 5-3 Scapolite analysis results.

Cl, Br and Na composition of scapolite samples by microprobe and micro-XRF analysis, and stable Cl isotopes. RM: samples from RM alteration; MB: samples from IOCG-M alteration; PN: samples from IOCG-PS alteration.

Sample Name	Sample ID	Location	Mineralization	Mineralization	Cl (ppm) MXRF	Cl (ppm) M-probe	Br (ppm) MXRF	Na (ppm) EMPA	Cl/Br molar	Na/Br molar	δ^{37}Cl (‰) UT
03NUN29 125-250mm	RM01	Nunasvaara	Regional Alteration Na-Cl Metasomatisr	RM	35,000	35,020	n.m.	119,920	n.m.		-0.1
Nun3.4d	RM12	Nunasvaara	Regional Alteration Na-Cl Metasomatisr	RM	n.m.	30,730	n.m.	9,635	n.m.		n.m.
04 TORN 1 v. 250-500mm	RM07	Torneälven river	Regional Alteration Na-Cl Metasomatisr	RM	26,000	27,070	76	92,710	770	4,238	0.3
04 TORN 1 v. 100-250mm	RM08	Torneälven river	Regional Alteration Na-Cl Metasomatisr	RM	26,000	27,070	86	n.m.	680		0.0
04 TORN 2 250-125mm	RM05	Torneälven river	Regional Alteration Na-Cl Metasomatisr	RM	25,000	27,360	88	89,660	639	3,622	0.3
PAH 88217 125-250mm	MB02	Pahtohavare	IOCG-Sc altered Metabasic Rocks	IOCG-M	27,800	29,160	36	94,660	1,738	9,134	0.2
PAH 88217 100-125mm	MB03	Pahtohavare	IOCG-Sc altered Metabasic Rocks	IOCG-M	25,000	n.m.	143	n.m.	393		n.m.
03PAH3 125-250mm	MB10	Pahtohavare	IOCG-Sc altered Metabasic Rocks	IOCG-M	28,000	30,670	112	94,190	565	2,935	0.2
KAL 90106 125-250mm	PN20	Kallosalmi	IOCG-Sc altered Metabasic Rocks	IOCG-PS	33,000	n.m.	55	n.m.	1,350		0.5
KAL 90107 56.38m 125-250m	PN09	Kallosalmi	IOCG-Proximal sc-rich alt/Na Skarn	IOCG-PS	33,000	36,080	90	101,270	825	3,909	0.6
KAL 90106 118.4m 100-125m	PN21	Kallosalmi	IOCG-Proximal sc-rich alt/Na Skarn	IOCG-PS	33,000	30,880	55	95,920	1,350	6,059	0.4
PAH 88093 100-125mm	PN17	Pahtohavare	IOCG-Proximal sc-rich alt/Na Skarn	IOCG-PS	33,000	34,060	134	104,490	554	2,709	1.0
PAH 88093 125-250mm	PN18	Pahtohavare	IOCG-Proximal sc-rich alt/Na Skarn	IOCG-PS	33,000	n.m.	90	n.m.	825		-0.1
G1-1 100-125mm	PN16	Gruvberget	IOCG-Proximal sc-rich alt/Na Skarn	IOCG-PS	21,000	21,740	38	n.m.	1,244		0.1
G1-1 250-500mm	PN14	Gruvberget	IOCG-Proximal sc-rich alt/Na Skarn	IOCG-PS	21,000	n.m.	20	n.m.	2,363		0.3
G1-1 125-250mm	PN15	Gruvberget	IOCG-Proximal sc-rich alt/Na Skarn	IOCG-PS	21,000	n.m.	38	82,910	1,244	7,580	-0.1
G4-1 125-250 mm	PN06	Gruvberget	IOCG-Proximal sc-rich alt/Na Skarn	IOCG-PS	27,000	29,200	65	92,300	942	4,971	0.1
SAR 1 125-250mm	PN19	Sarkivaara	IOCG-Proximal sc-rich alt/Na Skarn	IOCG-PS	10,000	13,170	83	62,330	271	2,609	0.9
Modern Seawater	MSW								650	600	

n.m.; not measured

Table 5-4 Average major oxide compositions by microprobe in scapolite samples.
Formula calculations assuming 12 (Al, Si), carbonate calculated by difference assuming a full anion site occupancy.

Sample/analyte wt% oxide	RM12	RM01	RM08	RM07	RM05	MB02	MB11	PN17	PN21	PN09	PN06	PN16	PN19
F	n.d.	n.d.	n.d.	n.d.	n.d.	n.d.	n.d.	n.d.	n.d.	n.d.	n.d.	n.d.	n.d.
Na_2O	9.63	11.99	9.27	9.24	9.00	9.36	9.36	10.45	9.59	10.13	9.23	8.29	6.23
MgO	n.d.	n.d.	0.1	0.1	n.d.	0.1	0.3	n.d.	n.d.	n.d.	n.d.	n.d.	n.d.
Al_2O_3	23.3	21.1	23.4	23.2	23.4	23.2	23.1	21.9	21.8	21.9	22.6	23.0	24.6
SiO_2	55.1	59.1	54.6	55.6	54.4	54.6	55.1	56.8	56.3	56.7	55.6	53.2	50.3
SO_3	0.4	0.2	n.d.	n.d.	n.d.	n.d.	0.1	n.d.	n.d.	n.d.	0.4	0.7	1.0
Cl	3.0	3.6	2.6	2.3	2.5	2.8	2.8	3.3	3.3	3.3	2.7	2.1	1.0
CaO	8.35	4.59	9.15	9.06	9.43	8.83	8.53	6.91	7.23	6.99	8.52	10.43	13.55
K_2O	0.5	0.5	0.3	0.2	0.3	0.4	0.6	0.7	1.3	0.9	0.8	0.6	0.6
FeO*	n.d.	n.d.	0.2	0.3	0.2	0.3	0.5	0.1	0.1	n.d.	0.2	0.1	n.d.
Total	100.3	101.0	99.5	99.9	99.3	99.6	100.3	100.1	99.6	100.0	100.0	98.5	97.4
Cl = O	0.7	0.8	0.6	0.5	0.6	0.6	0.6	0.7	0.7	0.8	0.6	0.5	0.2
Corrected Total	99.6	100.2	99.0	99.4	98.7	99.0	99.6	99.3	98.9	99.3	99.4	98.0	97.1
Formula to 12 (Al, Si)													
F	n.d.	n.d.	n.d.	n.d.	n.d.	n.d.	n.d.	n.d.	n.d.	n.d.	n.d.	n.d.	n.d.
Na	2.7	3.3	2.6	2.9	2.6	2.7	2.6	2.9	2.7	2.9	2.6	2.4	1.8
Mg	n.d.	n.d.	n.d.	n.d.	n.d.	n.d.	0.1	n.d.	n.d.	n.d.	n.d.	n.d.	n.d.
Al	4.0	3.6	4.0	3.9	4.0	4.0	4.0	3.7	3.8	3.8	3.9	4.0	4.4
Si	8.0	8.4	8.0	8.1	8.0	8.0	8.0	8.3	8.2	8.2	8.1	8.0	7.6
S	n.d.	n.d.	n.d.	n.d.	n.d.	n.d.	n.d.	n.d.	n.d.	n.d.	n.d.	0.1	0.1
Cl	0.7	0.9	0.6	0.6	0.6	0.7	0.7	0.8	0.8	0.8	0.7	0.5	0.3
Ca	1.3	0.7	1.4	1.4	1.5	1.4	1.3	1.1	1.1	1.1	1.3	1.7	2.2
K	0.1	0.1	n.d.	n.d.	n.d.	0.1	0.1	0.1	0.3	0.2	0.1	0.1	0.1
Fe	n.d.	n.d.	n.d.	n.d.	n.d.	n.d.	0.1	n.d.	n.d.	n.d.	n.d.	n.d.	n.d.
CO_3	n.d.	0.1	0.4	0.4	0.4	0.3	0.3	0.2	0.2	0.2	0.3	0.4	0.6
Na+K+Ca	4.1	4.1	4.1	4.4	4.1	4.1	4.1	4.1	4.1	4.1	4.1	4.2	4.1

FeO : total iron*
n.d.: not detected

6 Conclusions

6.1 Analytical implications of the Cl extraction and the analysis of the stable Cl isotopes

The extraction of chlorine from fluid inclusion leachates, scapolites and geothermal fluids was a fundamental part of this research. The method proposed by Wassenaar and Koehler (2004) adapted to work with small size samples (100 μmol of Cl^-) was found to be the most suitable to work with a wide range of Cl concentrations, including the low concentrations of fluid inclusion leachates. Following the work by Eggenkamp et al., (1995), which demonstrated that both the mass of $AgNO_3$ added and the solubility of AgCl influence the amount of AgCl recovered, the general preparation procedure for AgCl precipitation was slightly modified to produce small AgCl crystals with high ionic strength (Taylor and Grimsrud, 1969). In addition, $AgNO_3$ was used in excess to increase the probability of AgCl formation. In the present study, this methodology was found to be effective to extract representative masses of Cl from aqueous solutions. Under the same conditions seawater standards bracketing the Cl concentrations of the actual samples were prepared in order to assure that comparable masses of AgCl were recovered for isotope analysis.

The amount of AgCl recovered from fluid inclusion leachates was too small to be weighted in a scientific scale and actual yields were not calculated. Nevertheless, the AgCl precipitate was observed in some samples during reaction and confirmed during the IRMS runs, as measurable signal peaks were observed in the chromatogram. This also confirmed the presence of CH_3Cl gas in these samples.

After assessing several methodologies to extract Cl from mineral samples, pyrohydrolysis was identified as the most suitable technique for the purpose of this research, after considering yields and minimization of possible fractionation effects (Bonifacie et al. 2007). The pyrohydrolysis apparatus built at the University of Alberta in order to extract the Cl contained in scapolite mineral separates, was based on a set up proposed by Bonifacie et al. (2007) and the apparatus used at the University of New Mexico. This new configuration assured a controlled melting process of the scapolite sample during uniform heating, preventing Cl mass loses and allowing the recovery of an aqueous sample without the use of a NaOH collecting solution. The pyrohydrolysis solution was found to be suitable for direct measurement of its Cl concentration by IC.

Two isotope laboratories were used to analyze the stable Cl isotopes, NWRI-EC, Saskatoon and the University of Texas. However, each laboratory has different sample preparation methodologies and MS analytical techniques. Therefore, it was necessary to assess if these differences had an effect on the δ^{37}Cl values of low Cl concentration samples. With this purpose, fluid inclusion leachate samples from the Butte PCD were sent to NWRI-EC and the University of Texas for comparison. It was concluded that the isotope values reported by the University of Texas tend to be higher than those reported by NWRI-EC. In contrast, the samples run at NWRI-EC were analyzed using seawater standards encompassing the range of Cl masses identified in actual samples, this allowed for a representative measurement of the Cl isotopes. It is possible, therefore, that the discrepancy may be due to the use of seawater standards with fixed Cl masses by the University of Texas. This practice masks variations in the isotopic composition of low Cl samples as concluded in the present work from δ^{37}Cl values measured in samples diluted to several concentrations from a single seawater standard. It was found that masses between 1.4 and 4.2 μmoles Cl, had delta values around 2.5‰ lower than seawater standard samples prepared with higher Cl masses.

6.2 Variations of the stable Cl isotopes and the halogen compositions of geothermal fluids evolving from the mantle to the surface.

Deep geothermal fluids representing 14 active geothermal systems in the TVZ, North Island New Zealand, were analyzed in this study to identify changes in the halogen (Cl and Br) and isotope compositions (δ^{37}Cl, δ^{7}Li, δ^{18}O and δD) of hydrothermal fluids associated with rhyolitic and andesitic magmas. The occurrence of these two types of active geothermal systems, the thin crust under the TVZ (~17 km) and the occurrence of an active subduction zone, make this area the ideal geologic setting to assess the influence of the mantle in the halogen and δ^{37}Cl composition of rhyolitic and andesitic magmas.

The $\delta^{18}O$, δD and $\delta^{7}Li$ values indicate that these geothermal fluids are meteoric waters which have interacted with their host rocks. According to low $\delta^{7}Li$ values, water-rock interactions are in the most part with rhyolitic rocks. Higher $\delta^{7}Li$ values were only detected in samples from the Kawerau geothermal system reflecting the low quartz content of the greywacke reservoir. Two different sources of Cl were identified in the geothermal waters, one related to andesitic magmas in the east and the other associated with predominantly rhyolitic magmatism in the west. The characteristic stable Cl isotope values of these waters reflect the isotopic signature of the source, a high-alumina basalt. The data indicate that chlorine stable isotopes are fractionated exclusively during magmatic segregation in the crust and to some extent by surface processes like evaporation and distillation in the hot spring systems. The data do not support stable Cl isotope fractionation during the transit of the geothermal fluids from the reservoir to the surface.

This work concludes that Cl/Br molar ratios and stable Cl isotopes have the potential to identify andesitic and rhyolitic magmatic sources of halogens in geothermal systems. Correlations with Cl and Br concentrations reported in MORB, MAR and EPR glass samples (Jambon et al. 1995; Kendrick et al. 2012), igneous standard rocks (Shinonaga et al. 1994; Michel and Villemant, 2003) and pyroclastic rocks (Bureau and Metrich, 2003), suggest an association with the halogen compositions of the geothermal fluids of the TVZ. The geothermal waters from the andesitic geothermal systems: Kawerau, Ohaki and Rotokawa are related to Cl and Br compositions identified in MORB samples from Macquarie Island (Kendrick et al. 2012). The geothermal samples related to rhyolitic magmatism: Mokai, Tokaanu, Wairakei, Tauhara and Ngatamariki are related to the acidic volcanic rocks (trachyte, pantellerite and rhyolite) analyzed by Bureau and Metrich (2003).

This study contributes the first data on the effect of magmatic segregation on the $\delta^{37}Cl$ composition of hydrothermal fluids, resulting in different and characteristic isotopic signatures for rhyolitic and andesitic sources. But it also supports the hypothesis that the $\delta^{37}Cl$ values of the upper mantle are negative.

6.3 The evolution of stable Cl isotopes and halogens in a deep hydrothermal fluid

The Butte PCD is characterized by the occurrence of pre-Main Stage and Main Stage (MS) mineralisation, both though to be generated by the evolution of a single hydrothermal fluid (Rusk et al. 2008). In the pre-Main Stage mineralisation, differences in the halogen distribution of vein minerals have been documented in fluid inclusion leachates, indicating that high Cl/Br molar ratios are characteristic of deep and moderate depth BQ/QMB veins. This contrasts with low Cl/Br molar ratios measured in the shallower PGS and GS veins. Several processes were considered to explain this variation: an external source of Br available to PGS and GS veins, distillation and phase separation during cooling and decompression of the hydrothermal fluid, and the retention of Cl or Br by a mineral phase.

It was concluded that the halogen compositions of deep and moderate depth BQ/QMB veins reflect the interaction between felsic and mafic magmas, which produced a range of high Cl/Br molar ratios. The lower Cl/Br molar ratios measured in PGS and GS veins were interpreted using experimental data (Berndt and Seyfried, 1990; Liebscher et al. 2006) and Cl/Br molar ratios measured in vapors and brines from three active geothermal fields in North Island, New Zealand, that were used as an empirical comparator. It was found that small concentrations of Cl and Br were partitioned from the brine to the vapor, and after phase separation the Cl/Br molar ratios were preserved in both phases with small variations detected. We conclude that the large range of Cl/Br molar ratios measured in this study (379 to 3550) are unlikely to be explained purely by unmixing of the hydrothermal fluid. Alternatively, the occurrence of Cl-bearing biotites in the upper veins, may control the low Cl/Br molar ratios, due to the preferential Cl uptake by this mineral.

The high δ^{37}Cl values measured in some moderate depth BQ/QMB, PGS and GS veins are explained by kinetic fractionation restricted to the Cl transferred from the brine to the vapor phase. The vapor phase was affected by a combination of several processes such as phase separation, brine condensation, vapor formation and remixing, occurring locally in cracks and fractures. However, most of the Cl, which remains in the brine, preserved its original isotopic signature.

The low δ^{37}Cl values measured in fluid inclusions of deep BQ/QMB veins and the younger, and economically important, MS veins (-0.8‰ and -0.7‰ respectively) are similar, which supports the hypothesis that the hydrothermal fluid at Butte has a single source which evolved to form all the alteration assemblages found in the deposit (Rusk et al. 2008a and Reed et al. 2013). These low δ^{37}Cl values also support a mantle-like signature of the hydrothermal fluid that was associated with the highest Cu grades in Butte PCD. Changes with depth in the halogen and isotope compositions detected in pre-Main Stage veins and the persistence of the magmatic source, lead to conclude that MS mineralization was generated as consequence of at least one last pulse of magmatic-hydrothermal fluid released from a deep porphyry intrusion. This hypothesis is in agreement with findings by Mercer and Reed (2013).

This study is relevant to the understanding of the evolution of hydrothermal fluids in PCDs as it contributes data regarding the effects of physico-chemical processes on the halogen and stable Cl isotopes composition of a single and persistent hydrothermal fluid in a closed system. It provides new data to support a single source of metals and halogens for pre-Main Stage and MS mineralization. This study concludes that stable Cl isotopes can fractionate at conditions of high pressure and temperature in the crust (up to 9 km depth and 650 °C, Rusk et al. 2008) if, following phase separation, small volumes of hydrothermal fluid in the vapor phase are isolated in fractures; however, overall the brine preserves the isotopic signature of the magma source. These characteristics can be applied to other PCDs in order to identify unmixing zones important for mineral precipitation and the isotopic characterization of parental magmas supplying metals to the hydrothermal system.

6.4 The use of halogen compositions and stable Cl isotopes to differentiate multiple sources of salinity

The IOCG-type deposits of the Norrbotten County, Sweden, were formed during the Paleoproterozoic. The halogen and stable Cl isotope composition of scapolites from RM, IOCG-M and IOCG-PS mineralisation record a complex interaction of sources due to regional metamorphism and subsequent magmatic intrusions. The scapolite samples studied are predominantly of marialitic composition.

However, some chemical differences were found: IOCG-PS alteration are more Ca and S enriched but Na and Cl depleted. In contrast, IOCG-M scapolites are more Cl and Fe rich, but depleted in Ca. The RM scapolites have intermediate compositions. The chemistry of these scapolites indicates that the RM alteration resulted from a hydrothermal fluid of homogeneous composition, owing to a more restricted availability of protoliths and fluids.

In addition, based on relative SO_4-Cl-CO_3 compositions and temporal correlations it is proposed that RM scapolites were incorporated or recycled into the later IOCG alteration. The halogen compositions of Kallosalmi, Gruvberget, Pahtohavare, Nunasvaara and Torneälven scapolites also supports the idea that RM alteration was recycled into these younger marialites. The Pahtohavare and Sarkivaara deposits contain scapolites with halogen compositions resembling evaporative brines; they have lower than seawater Cl/Br molar ratios. But most of the other scapolites had Cl/Br molar ratios related to seawater, magmatic or evaporitic sources or a mixture of these end-members.

Measured δ^{37}Cl values in fluid inclusions (Gleeson and Smith, 2009) and associated scapolite in one of the samples allowed for the calculation of an empirical isotope fractionation factor of +1.9‰ between the mineral and the fluid. This value contradicts numerical predictions for isotope fractionation between a silicate mineral such as scapolite and a monovalent hydrothermal fluid with high NaCl activities (Schauble et al. 2003). If the scapolite investigated in the present study and the hydrothermal fluid did not reach isotopic equilibrium, the low δ^{37}Cl values identified in fluid inclusions by Gleeson and Smith (2009) are perhaps explained by some other process. These may include water-rock interaction, kinetic isotope fractionation or an unknown source depleted in δ^{37}Cl. Our results suggest that experimental fractionation factors for the scapolite-hydrothermal fluid interaction are needed to test the theoretical predictions proposed by Schauble et al. (2003).

This research shows how the stable Cl isotopes and the halogen composition of minerals can be used to separate out different sources of salinity in a region characterized by a complex geologic history. However, the data had to be interpreted with caution as Cl/Br molar ratios and δ^{37}Cl values are decoupled owing to the presence of recycled Br in IOCG scapolites.

6.5 References

Berndt M. and Seyfried W., 1990. Boron, bromine, and other trace elements as clues to the fate of chlorine in mid-ocean ridge vent fluids. Geochim. Cosmochim. Acta. 54, 2235-2245.

Bonifacie M., Jendrzejewski N., Agrinier P., Coleman M., Pineau F. and Javoy M., 2007. Pyrohydrolysis-IRMS determination of silicate chlorine stable isotope compositions. Application to oceanic crust and meteorite samples. Chem. Geol. 242, 187-201.

Bureau H. and Métrich N., 2003. An experimental study of bromine behaviour in water-saturated silicic melts. Geochim. Cosmochim. Acta 67, 1689-1697.

Eggenkamp H. and Kreulen R., 1995. Chlorine stable isotope variations in volcanic gasses, volcanic springs and crater lakes from Indonesia. The geochemistry of chlorine isotopes. Doctoral, Universiteit Utrecht.

Gleeson, S.A., and Smith, M.P., 2009. The sources and evolution of mineralising fluids in Fe oxide-apatite and iron oxide-copper-gold systems, Norrbotten, Sweden: Constraints from stable Cl isotopes of fluid inclusion leachates. Geochim. Cosmochim. Acta 7, 5658-5672.

Jambon A., Deruelle B., Dreibus G. and Pineau F., 1995. Chlorine and bromine abundance in MORB: the contrasting behavior of the Middle-Atlantic ridge and East Pacific Rise and implications for chlorine geodynamic cycle. Chem. Geol. 126, 101 – 117.

Kendrick M. A., Kamenetsky V. S., Phillips D. and Honda M., 2012. Halogen systematics (Cl, Br, I) in Mid-Ocena Ridge Basalt: a Macquarie Island case study. Geochim. Cosmochim. Acta. 81, 82-93.

Liebscher A., Luders V., Heinrich W. and Schettler G., 2006. Br/Cl signature of hydrothermal fluids: liquid-vapour fractionation of bromine revised. Geofluids 6, 113-121.

Mercer C. N. and Reed M. H., 2013. Porphyry Cu-Mo stockwork formation by dynamic, transient hydrothermal pulses: mineralogic insights from the deposit at Butte, Montana. Econ. Geol. 108, 1347-1377.

Michel A. and Villemant B., 2003. Determintion of halogens (F, Cl, Br, I), sulfur and water in seventeen geological reference materials. Geostand. Newslet. 27, 163-171.

Reed M., Rusk B. and Palandri J., 2013. The Butte magmatic-hydrothermal system: One fluid yields all alteration and veins. Econ. Geol., 108, 1379-1396.

Rusk B.G., Miller, B.J., and Reed, M.H., 2008b. Fluid-inclusion evidence for the formation of Main stage polymetallic base-metal veins, Butte, Montana, USA, *in* Spencer, J.E., and Titley, S.R., eds., Ores and orogenesis: Circum-Pacific tectonics, geologic evolution, and ore deposits: Ariz. Geol. Soc. Dig. 22, 573-581.

Schauble E., Rossman G. and Taylor H., 2003. Theoretical estimates of equilibrium chlorine-isotope fractionations. Geochim. Cosmochim. Acta. 17, 3267-3281.

Shinonaga T., Ebihara M., Nakahara H., Tomura K. and Heumann K. G., 1994. Cl, Br and I in igneous standard rocks. Chem. Geol., 115, 213-225.

Smith M.P., Gleeson S.A., and Yardley B.W.D., 2012. Hydrothermal fluid evolution and metal transport in the \Kiruna District, Sweden: Constraining metal behaviour in aqueous and aqueous-carbonic brines. Geochim. Cosmochim. Acta. 102, 89-112.

Taylor J. W. and Grimsrud E. P., 1969. Chlorine isotopic ratios by negative ion mass spectrometry. Anal. Chem., 41, 805-810.

Wassenaar L. I. and Koehler G., 2004. On-Line technique for the determination of the δ^{37}Cl of inorganic and total organic in environmental samples. Analytical chemistry, 76, 6384 – 6388.